Doctor of Philosophy

DEVELOPMENT OF BIO-INSPIRED SUPERHYDROPHOBIC SURFACES AND THEIR ENVIRONMENTAL APPLICATIONS

The Graduate School of the University of Ulsan

Department of Civil and Environmental Engineering

TRAN THI VIET HA

DEVELOPMENT OF BIO-INSPIRED SUPERHYDROPHOBIC SURFACES AND THEIR ENVIRONMENTAL APPLICATIONS

Supervisor: Professor Byeong-Kyu Lee

A Dissertation

Submitted to
The Graduate School of the University of Ulsan
In partial Fulfillment of the Requirements
For the Degree of

Doctor of Philosophy

By

Tran Thi Viet Ha

Department of Civil and Environmental Engineering
University of Ulsan, Republic of Korea
December 2017

DEVELOPMENT OF BIO-INSPIRED SUPERHYDROPHOBIC SURFACES AND THEIR ENVIRONMENTAL APPLICATIONS

This certifies that the dissertation of

TRAN THI VIET HA is approved.

Committee Chairman:	Prof. Seok-Young Oh
Committee Member:	Prof. Hung-Suck Park
Committee Member:	Prof. Sung-Deuk Choi
Committee Member:	Prof. Eun-Woo Shin
Committee Member:	Prof. Byeong-Kyu Lee

Department of Civil and Evironmental Engineering

University of Ulsan, Ulsan
Republic of Korea

December, 2017

ACKNOWLEDGEMENTS

First and foremost, I would like to deeply thank and express my sincere gratitude my advisor, Professor Byeong-Kyu Lee, for his immense knowledge as well as his strong encouragement and supports. It is a great understatement to say that this work would not have been possible without his help.

I would like to acknowledge all of my committee members, Professor Hung-Suck Park, Professor Seok-Young Oh, Professor Sung-Deuk Choi, Professor Eun Woo Shin, for their comments and suggestions for my dissertation.

Furthermore, I would also like to take this opportunity to thank my lab members and faculty members as well as the technical and administrative staffs in Department of Civil and Environmental Engineering at University of Ulsan. I am also very grateful to be a member of the Air Environment and Energy Research Laboratory.

I also wish to thank my many friends and other colleagues who are too numerous to mention all by name.

Finally, I would like to thank my family for their continuous love and support of my desire to get a Ph.D. Mom and Dad, thanks for being the supportive parents for my study. My younger sister, thanks for being a great sister and taking care for our parents when I was busy with my study. And finally, to my boyfriend, absolutely none of this would have been possible without you.

Best regards,

Ulsan city, Republic of Korea

December, 2017

Tran Thi Viet Ha

CONTENTS

ABSTRACT

Recently, superhydrophobic materials with static water contact angle higher than 150^{o} and dynamic water contact angle less than 10^{o} have attracted the attention due to their unique properties and their potential for practical applications, such as self-cleaning, anti-wetting, anti-icing, anti-corrosion, etc.,. Superhydrophobic surfaces could help to minimizing the energy and water required for cleaning, reducing the utilization of pollution and waste caused by cleaning process and even can be applied for oil/water separation - one of the biggest issues in environmental field at this moment. This dissertation investigates the fabrication, characterization of various superhydrophobic surfaces and their diverse environmental applications.

The thesis is organized as follow: In Chapter I (Introduction), it includes: objective/goal of this research study, background of super-hydrophobicity and theoretical basis. Chapter II, III and IV describes about three different superhydrophobic materials developed on (i) the cotton fabric, (ii) polyurethane sponge and (iii) melamine sponge, respectively. Novel techniques for creating superhydrophobic surfaces on three different substrates are presented in this dissertation. Furthermore, several potential applications such as self-cleaning, anti-wetting, floating oil sorption and oil-water separation were proposed. Chapter V concluded the research and proposed the future work.

LIST OF TABLES

LIST OF FIGURES

LIST OF ABBREVIATIONS

WCA(s)	Water contact angle (s)
FESEM	Field emission scanning electron microscope
XRD	X-ray diffraction
XPS	X-ray photoelectron spectroscopy
FT-IR	Fourier-transform infrared spectroscopy
VSM	Vibrating sample magnetometer
CF	Cotton fabric
R_a	average roughness
PU	Polyurethane
SA	Stearic acid
FDTS	1H,1H,2H,2H-perfluorodecyltriethoxysilane
MS	Melamine sponge
DI	Deionized water

CHAPTER 1

CHAPTER 1 - INTRODUCTION OF SUPERHYDROPHOBIC SURFACE

Abstract

Nature is the creation of aesthetic functional systems, in which many natural materials have vagarious structures. The booming field of biomimetic allows one to mimic nature to develop nanomaterials, nanodevices, and processes which offer desirable properties. Biomimetics means mimicking biology or nature. Inspired from nature, researchers have recently developed and implemented biomimetic surfaces in a variety of smart and simple ways. Various thermo, physical, and chemical principles govern the surface properties of biosystems, which can be successfully mimicked in advanced manufacturing products.

Recently, superhydrophobic surfaces, which are mimicking from the nature phenomenon, have received increasing attention because of their potential applications in clean tech applications such as maintaining high building window glasses and automobile glasses clean, consumer applications such as waterproof textiles, protective coating for telecommunication antennas, anti-corrosion and anti-icing etc.,. This chapter will begin with an introduction of the fundamental background about (i) the basic wetting behaviours, (ii) superhydrophobic surfaces in the nature, (iii) comprehensive description of the various techniques used to fabricate the superhydrophobic surface, as well as (iv) the main objectives of this dissertation.

Keywords: wettability, superhydrophobic, nature, objectives

1.1. Wetting behavior of a solid surface

1.1.1. Basic wetting states

When a liquid droplet encounters a solid surface it may wet the surface to varying degrees. The contact angle (θ) is the quantitative measure of the wetting of a solid by a liquid. Contact angle meter is used to determine of wetting characteristics of solid materials. Traditionally the static contact angle has been use to quantify the wettability, adhesiveness, and solid surface free energy. Sliding angle, or roll-off angle, is defined as the minimum tilting angle before the droplet starts to slide off, this dynamic angle can also be used to characterize the wettability of a solid surface.

For a hydrophilic solid surface, water droplets will spread out and wet the surface resulting in a CA less than 90°; however, for hydrophobic surfaces a contact angle greater than 90° will be created which is characteristic of anti-wetting surfaces. In general there are different types of wetting on solid surfaces which are shown schematically in Fig.1.1 with their contact angles indicated. CA can range from 180° to 0° depending on the magnitude of the solid/vapor and solid/liquid interfaces. If a liquid creates a contact angle of 180° with a solid, a complete non-wetting condition is present and the droplet will only be in contact with the solid at one specific point. If the contact angle formed is above 150°, the surface is considered superhydrophobic. The majority of solid surfaces are classified as hydrophobic ($150° > CA \geq 90°$) or hydrophilic ($CA < 90°$). In the case of complete wetting liquid drops easily spread out over the entire surface forming a thin liquid layer on top of the solid. A contact angle of 0° is characteristic of this type of wetting condition.

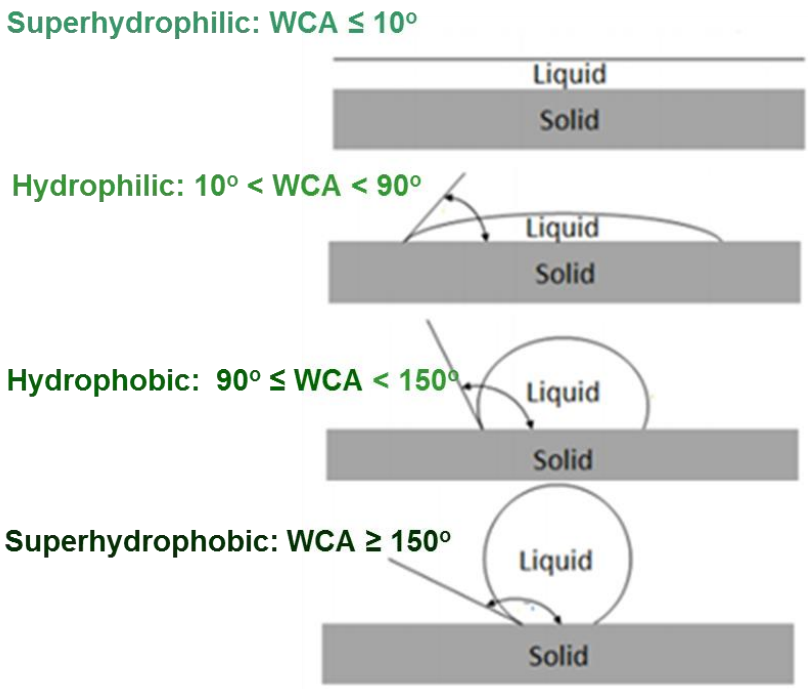

Fig.1.1. Different types of wetting on solid surface

1.1.2. Wetting of smooth surface

When a drop of liquid is deposited on a homogenous and flat solid surface, it forms a so-called contact angle (θ). The contact angle is the angle, conventionally measured through the liquid, where a liquid–vapor interface meets a solid surface. A contact angle less than 90° indicates that wetting of the surface is favorable, and the fluid will spread over a large area on the surface; while contact angles greater than 90° generally means that wetting of the surface is unfavorable so the fluid will minimize its contact with the surface and form a compact liquid droplet.

The theoretical liquid contact angle on the flat surface (θ) can be correlated to three interfacial free energies: the solid–gas interfacial energy (γ_{SG}), the solid–liquid interfacial energy (γ_{SL}) and the liquid–gas interfacial energy (γ_{LG}) (Fig.1.2). The equilibrium θ is determined by Young's equation (1.1) which is developed by Thomas Young in 1805:

$$\gamma_{LG} \cos \theta = \gamma_{SG} - \gamma_{SL} \qquad (1.1)$$

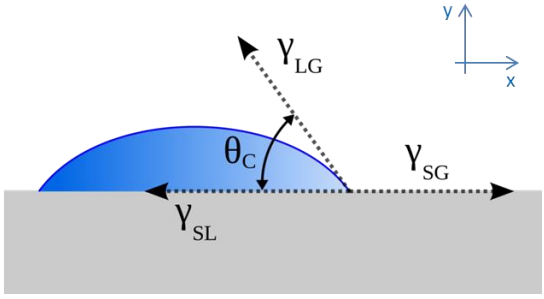

Fig.1.2. Schematic of a liquid drop showing the quantities in the Young equation

The Young's equation only works for flat surface, when the surface become rough, the Young's equation is not suitable anymore. When θ_{flat} is smaller than 90°, the solid surface is considered intrinsically hydrophilic; when θ_{flat} is greater than 90°, the solid surface is considered intrinsically hydrophobic. The reported lowest surface free energy of the solid-air interface is possessed by the trifluoromethyl group (CF_3)-terminated surface (~ 6 mN/m), with a θ_{flat} of approximate 120º, which is almost the highest water contact angle that can be obtained on a flat surface [1]. Further increase of the hydrophobicity requires manipulation of the surface topography.

1.1.3. Wetting on rough surface – Wenzel's and Cassie-Baxter's models

The effect of surface roughness on wettability was first discussed by Wenzel in 1936, and then by Cassie and Baxter in 1944.

Wenzel hypothesized that surface roughness plays an important role in increasing the contact angles by increasing the surface area, which is in turn affects both the surface wettability and the anti-wettability depending on the nature of the surface. Wenzel wettability theory is expressed by equation (1.2):

$$\cos \theta^* = r \cos \theta \qquad (1.2)$$

where θ^* is the apparent contact angle, r is surface roughness factor that is denoted by the ratio of total surface area to the projected area, and θ is the equilibrium contact angle on smooth surface

measured by Young's equation (1.1). According to Wenzel's assumption, the liquid entirely fills the protrusions of the rough surface when they become in contact (Fig.1.3 (a)).

On the other hand, Cassie-Baxter make an another theory, assuming that air pockets could be trapped by a water droplet which enables the droplet to roll off at relatively small angles due to reduction in solid-area fraction and correspondingly wetting area (Fig.1.3 (b)). The apparent contact angle proposed by Cassie-Baxter is given by equation (1.3):

$$\cos \theta_{CB} = f \cos\theta + (f - 1) \qquad (1.3)$$

where θ_{CB} is the Cassie-Baxter contact angle, f is the solid-area fraction, and θ is the contact angle on a smooth surface of the same material.

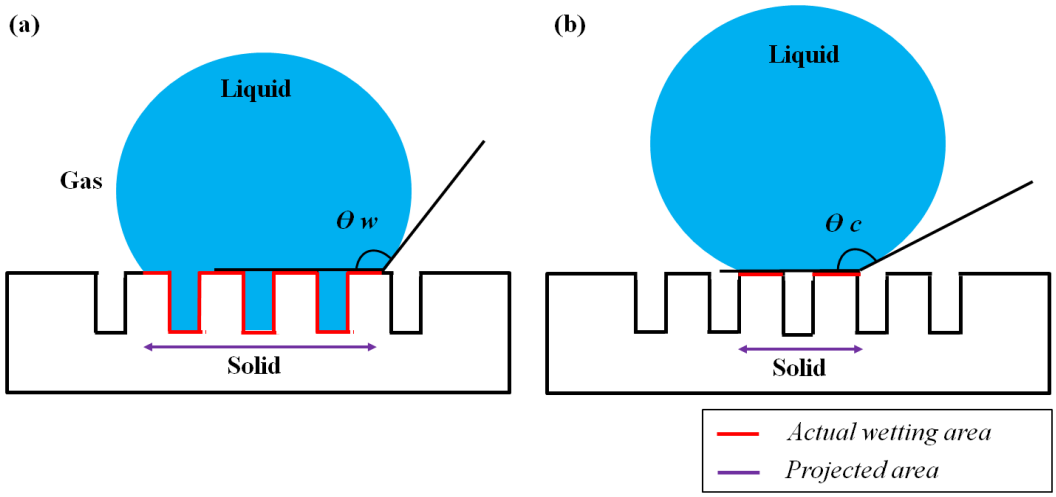

Fig.1.3. Wetting behavior of a droplet on solid substrates: (a) Wenzel state, (b) Cassie-Baxter state [2]

The difference between two models was the appearance of air gap between the liquid and the solid. Depending on the height and width of micro structure, the surface energy, the distance between the micro structures, and the shape of micro structure, the surface is followed Wenzel model or Cassie-Baxter model. Generally, superhydrophobicity is defined as follow: a water droplet has a static contact angle above 150° with the surface and a roll off angle of less than 10°.

A superhydrophobic surface is always in the Cassie's state, but a Cassie's state need not to be superhydrophobic.

1.2. Superhydrophobic surface in nature

The well-known and the most famous super water repellent surface is the lotus leaf. Water drops is directly roll-off from the lotus leaf surface by which all dirt and dust particles attached to lotus leaf could be carried away leaving the surface clean. The characteristics of self-cleaning and high water-repellency were discovered in 1977 by the Barthlott and Neihuis. By analyzing the structure, they discovered that the surface of the lotus leaves which showed a combination of nano- and micro-structures (Fig.1.4). A microstructure covered with nano-scale wax crystals is seen. The combination of the chemical property of wax and two different levels of roughness causes the self-cleaning phenomenon on the leaves of the Lotus with the contact angle often being higher than 150º. These waxes usually consist of a mixture of aliphatic hydrocarbons and/or their derivates, with the main components being primary and secondary alcohols, ketones, fatty acids and aldehydes. Long chain carbon molecules containing one or two hydroxyl groups account for the majority of the wax crystal chemistry. This observation has inspired a tremendous interest for both fundamental research and practical applications in order to understand and to identify the important role of the surface topography (hierarchical structure) as well as the surface chemistry and their influence on wetting behavior of the surface.

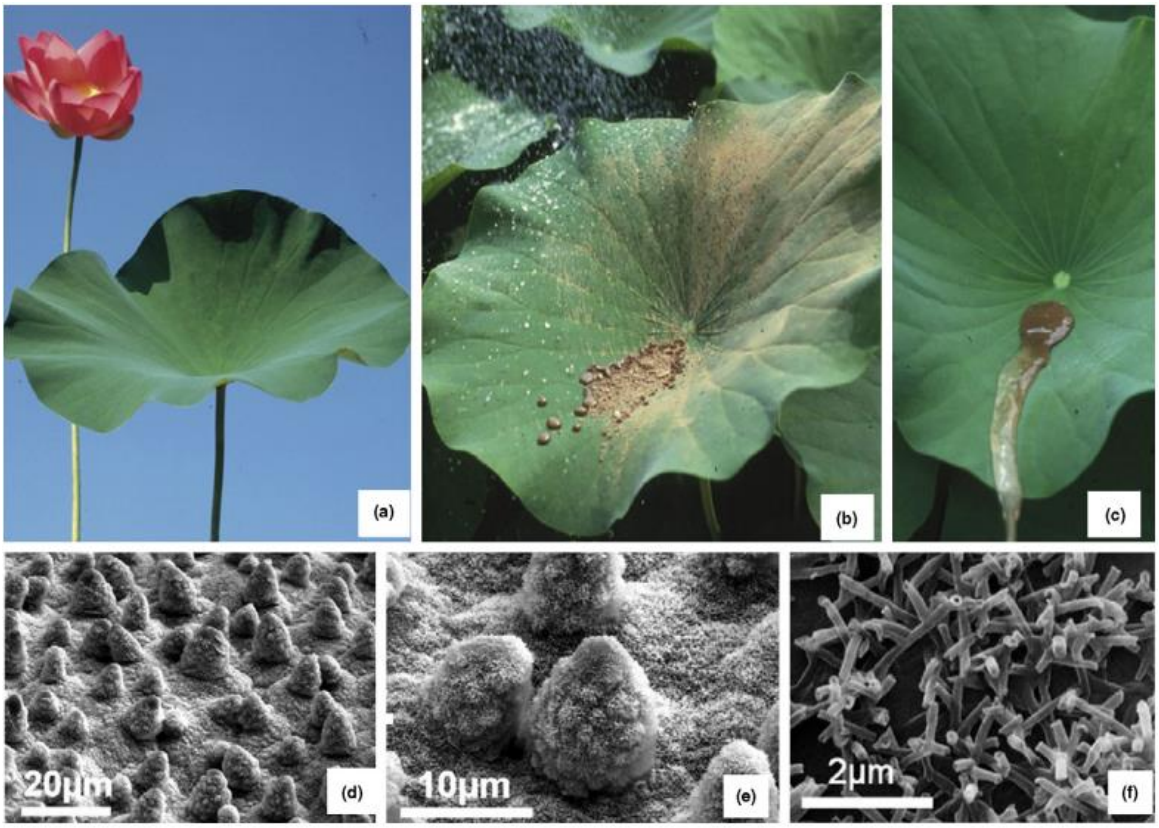

Fig.1.4.(a) Surface of lotus leaf, (b-c) self-cleaning effect, (d-e) microstructure and (f) nano-scale wax structure [3]

Another examples of superhydrophobic in nature are rice leaf with sinusoidal grooves covered with micropapilla and nanobumps, and butterfly wing with shingle-like scales with aligned microgrooves [2] (Fig.1.5). The feet of many insects are also superhydrophobic. Geckos are able to climb on vertical surfaces due to their feet having high solid–solid adhesion [4]. Many insects, such as water striders, are able to slide on the surface of water. The property to walk on water is in part due to the presence of hairs of 30 mm in length and about 1 mm in base diameter on theirs legs. Their hairs are tilted relative to the body surface, which increases the resistance to fluid impregnation and maximizes the propulsive thrust [4].

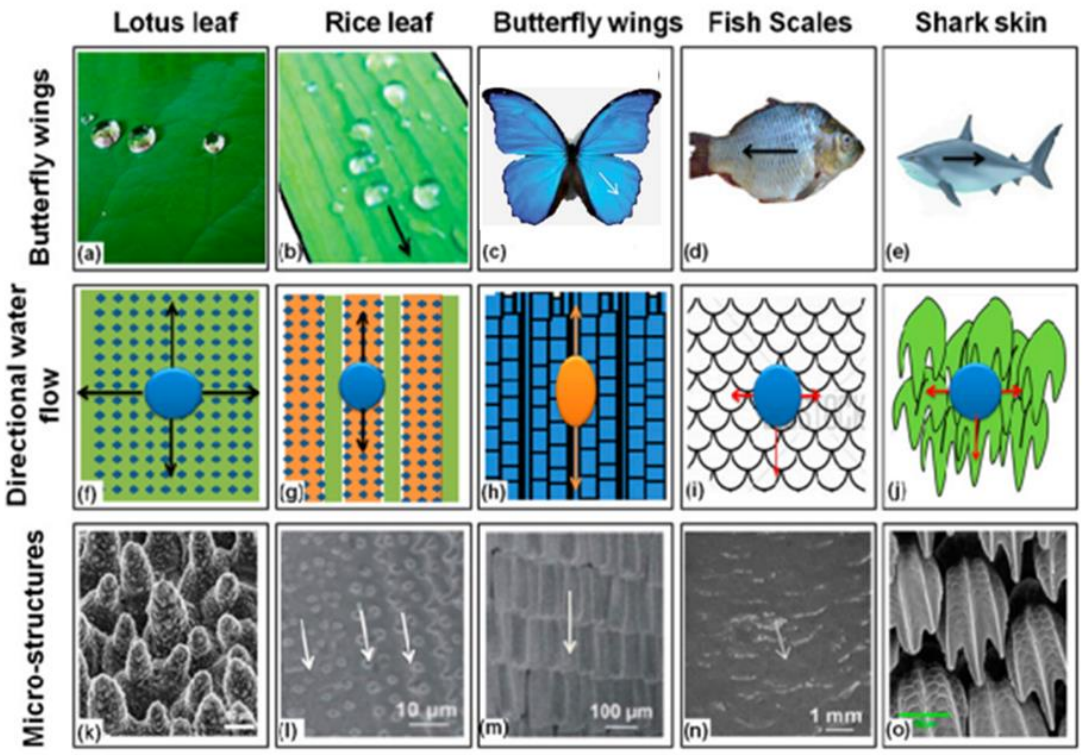

Fig.1.5. Schematic illustration of water flow on natural superhydrophobic surfaces: (a–e) the flow of water droplet on the natural surfaces of lotus, (f–j) the schematic microstructure of natural surfaces, and (k–o) micrographs of the natural surfaces [5].

1.3. Applications of superhydrophobic surfaces

Artificial superhydrophobic surface with its unique properties has broad practical applications and potential applications in daily life, industry, and agriculture such as self-cleaning, oil–water separation, anti-icing, open-air micro channel devices fluid mixing, fluid transport, and so on, as shown in Figure.1.6. Depending on inherent properties of each type of materials, they can be applied in the suitable applications.

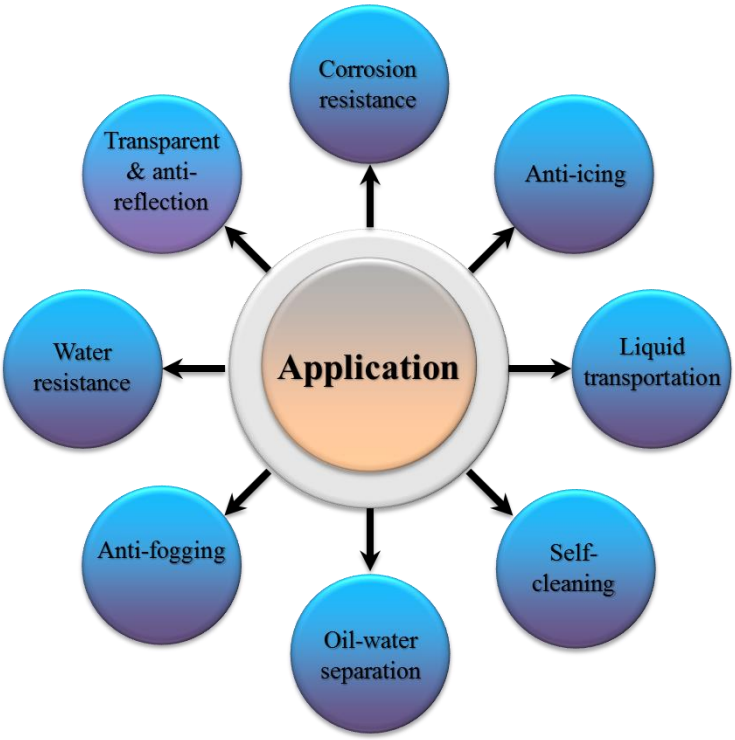

Fig.1.6. Applications of superhydrophobic surfaces

There are currently a handful of commercially available products that exhibit this type of non-wetting behavior, most of which are focused on keeping surfaces/textiles clean, stain-free and dry. For outdoor applications this results in surfaces degrading more slowly, therefore being replaced less often. A German paint company (Sto Corporation) has developed a fairly cost-effective (similar in cost to traditional paints) method to fabricate a superhydrophobic paint suitable for most exterior applications. Being inspired by the naturally occurring lotus leaf, they have named this product the StoCoat LotusanTM paint. Rain water does not wet the painted surface but instead rolls over it collecting dirt and contamination particles (Fig.1.7). The one drawback to this product is associated with its initial application. The company gives a very detailed curing procedure outlining a specific amount of UV light and water that must come into contact with freshly painted surfaces. This can create a difficult situation when there is a lack of environmental control (sun shine and precipitation) during the painting and curing of large exterior walls.

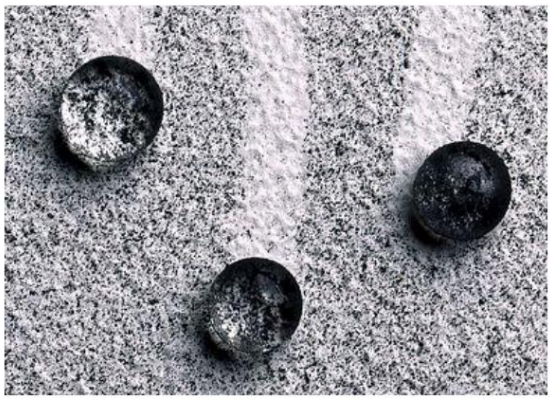

Fig.1.7. Superhydrophobic surface with StoCoat Lotusan™ paint [6]

Another effective superhydrophobic product has been developed an anti-adhesive spoon, based on the nonwetting mechanism that repels and allows very viscous liquids like honey to freely roll off its surface. Unfortunately, this product is currently not being produced in large quantities, most likely due to high production costs coupled with low prices of traditional spoons (Fig.1.8).

Fig.1.8. A spoon partially coated with a microstructure hydrophobic coating (right side) [7]

Another product with less practical importance, but interesting nonetheless has been created by Bandai™, the largest toy manufacturer in Japan. They have developed a maze-type game (Aqua Drop – Fig.1.9) that uses water droplets instead of metal ball bearings. The object is to get the droplets to gently rest in certain parts/depressions of the maze, or travel from one area to another. They do indicate that the base material of these mazes is polyethylene.

Fig.1.9. Four different versions of Bandai's Aqua Drop maze: courtesy of Bandai [8]

1.4. Fabrication of superhydrophobic surfaces

During the last few decades, many artificial self-cleaning surfaces were fabricated by different techniques. To date, a wide variety of physical and chemical methods have been explored to fabricate superhydrophobic surfaces through one of the following two approaches: (i) creating a rough surface on a hydrophobic material or (ii) modifying a rough surface with a hydrophobic coating. To fabricate superhydrophobic surfaces using a template-based approach there are two main requirements: 1) the surface must be sufficiently rough to allow for the formation of trapped air pockets underneath water droplets and 2) the surface should be a low surface energy material that is inherently hydrophobic.

1.4.1. Roughening a hydrophobic material

Methods to make superhydrophobic surfaces by roughening low surface energy materials are mostly one-step processes and have the advantage of simplicity. There are many ways to make rough surfaces, including laser/mechanical treatment [9], chemical etching [10, 11], lithography, sol–gel and hydrothermal processing [12, 13], layer-by-layer and colloidal assembling [14],

electrical/chemical deposition [15], electrospinning [16, 17],… For example, Jin et al. reported a laser etching method to make superhydrophobic polydimethylsiloxane (PDMS) surface, which contains micro-, submicro- and nano-composite structures [18]. Yan *et al.* fabricated superhydrophobic poly(alkylpyrrole) films by a electrochemical synthesis method. The film surface consists of thousands of ―needle‖-like microstructures in a perpendicular alignment [19].

As described by Cassie and Baxter, multi-level roughness enables trapping of air under the water droplet, enhancing the surface hydrophobicity. Microstructured pillar arrays fabricated by photolithography and soft lithography are often used to provide a predefined roughness. The major issues facing wide application of these techniques include high fabrication cost, limited applications to large scale coating, and reduced flexibility in modulation of surface morphologies. One of the low-cost alternatives is through surface deposition of nanoparticles. As silica nanoparticles are readily synthesized by a sol-gel process with uniform size, and as their surface chemistry is tunable via covalent modification, they are widely used in creating surfaces with desirable properties.

1.4.2. Modifying a rough surface with a hydrophobic coating

Generally, the wettability behavior of rough surfaces is governed by the interface chemistry. There are also several methods commonly used to modify the chemistry of a surface. Although it is a relatively simple and one-step process to make superhydrophobic surfaces by using intrinsically hydrophobic materials, unfortunately, many materials do not possess a low enough surface free energy to be intrinsically hydrophobic. In order to make superhydrophobic surfaces on these intrinsically hydrophilic materials, a two-step process is usually required, i.e., making a rough surface first and then modifying it with chemicals, such as alkanethiols, organic silanes, and fatty acids, which can offer a low surface free energy after linked to the surface. For example, Baldacchini et al reported a way to create micro/nanoscale roughness on silicon wafers by using a femtosecond laser to etch the silicon wafers [20]. Verplanck et al. made silicon nanowires on Si/SiO_2 substrates through a vapor-liquid-solid mechanism. The resulting rough surfaces were modified with a fluoropolymer C_4F_8, and exhibited superhydrophobicity [21].

1.5. Research objectives

The first objective of this dissertation is to investigate the different artificial superhydrophobic surfaces. As mentioned before, since in the meantime the mechanism of superhydrophobicity is well-understood, several methods have been developed to fabricate artificial superhydrophobic surface. This dissertation is mainly focused on the development of superhydrophobic artificial surfaces based on the fundamental understanding about controlling the wettability of the surface. The chosen fabrication method has some advantages:

- The technique is facile and economic
- The fabrication time is much shorter as compared to other current laboratory techniques
- No specific apparatuses are required
- Selection of environmental friendly coating materials

The second objective of the study is to understand the influence of topography and surface on the wettability of fabricated superhydrophobic surfaces. The surface morphology is characterized by various techniques such as FE-SEM, XRD, XPS, FT-IR, etc.. Surface wettability is characterized by measuring the static WCA and dynamic WCA (sliding and shedding angles) on those fabricated surfaces. The mechanism of wettability change was also explained.

Based on the study on the characteristics, the third objective of the study is to simulate the various applications of the fabricated superhydrophobic surfaces. It was found that the fabricated superhydrophobic surfaces can become the good candidate for anti-wetting, self-cleaning materials. Furthermore, the fabricated materials can be applied for oil/organic solvents-water separation with very high separation capacity for several cycles.

However, many challenges still exist, such as fabricating, robust superhydrophobic surfaces that can resist moisture, temperature, and abrasions, which may require more research efforts. Thus, further investigation for improving mechanical robustness is very necessary. The fourth objective of this dissertation is to test the stability of fabricated materials – which is very important in practical applications.

This research can provide a useful guideline for other researchers as well as industrial/manufacturing engineers to choose an efficient and environmental friendly method to fabricate superhydrophobic surfaces with various substrates. This research is also extremely meaningful since the environment issues caused by oil or organic pollutants are rising rapidly.

CHAPTER 2

CHAPTER 2 - SUPERHYDROPHOBIC COTTON FABRIC

Abstract

A composite of ZnO and cotton fabric (ZnO–CF) with a superhydrophobic surface was successfully synthesized with Teflon-lined stainless steel autoclave at low temperature 100 °C. X-ray diffraction (XRD) results indicated that the fabricated ZnO–CF had a uniform stacked hexagonal slice structure without any impurities. The fabric surface firmly bonded with ZnO through chemical bonding and possessed superhydrophobicity with a surface water contact angle (WCA) greater than 150°. The rough structure of ZnO and the enhancement of nonpolar functional groups on the composite surface gave ZnO–CF its superhydrophobicity. ZnO–CF showed a stable and robust self-cleaning property. When applied to separate a mixture of water (dyed with methylene orange) and organic solvent (hexane), ZnO–CF achieved a separation efficiency of over 99% that decreased only insignificantly even after several cycles. Therefore, this outstanding separation performance demonstrates the strong potential of ZnO–CF for practical applications such as wastewater treatment and water purification.

Keywords: cotton fabric; ZnO; superhydrophobic; self-cleaning; separation

2.1. Introduction

Selective separation technologies for organic solvents and aqueous solution containing organics have become global concerns along with the huge increases in wastewater volume requiring proper treatment. Conventional separation methods, such as oil skimming [22], centrifuging [23], and flotation [24], are limited by numerous disadvantages, such as low separation efficiencies, high costs and complicated equipment requirements [25]. There are several publications reported on the organic solvents and aqueous solution separation with outstanding methods [26-28]. Recently, superhydrophobic filters are promising candidates for organic solvents/water separation if they have high efficiency, low cost and environmentally friendly properties. The superhydrophobic filters with water contact angle (WCA) higher than 150^{o} and organic solvent contact angle less than 5^{o} [29-33] could become the potential candidates for the selective separation of organic solvent/water because they can absorb organic solvent only while repelling water.

Inspired by the water repellency ability of lotus or taro leaves, various superhydrophobic materials have been developed for organic solvent/water separation. For instance, the PMIA/SiO_2 membrane with a dense silicone nanofilament layer was prepared to separate water from light oil (canola oil) and heavy oil (carbon tetrachloride, CCl_4) [34]. A fabrication method of the superhydrophobic filter paper was also developed via colloidal deposition [35]. Superhydrophobic copper mesh filters were fabricated via a hydrothermal method to separate diesel from water [36]. However, only a few studies have reported the utilizations of cotton fabric to make the superhydrophobic filter.

Cotton fabric is well known as a porous, rough, flexible and hydrophilic surface with extremely high water absorption ability. As a result, cotton fabrics cannot be used for organic solvents - water separation in their original form because they strongly absorb water and other organic solvents. Thus, prudent chemical modifications are required to control the selectivity and wettability of cotton textiles. Also, maintaining good stability of the cotton fabric-based material and coating with non-toxic chemicals are essential for large-scale practical application.

In this study, we attempted to fabricate superhydrophobic surfaces that can exhibit the

superhydrophobicity by the ZnO particles deposition on the cotton fabric surfaces via a very simple hydrothermal method at low temperature. ZnO was selected as the functional material due to its superior biochemical abilities: ZnO is biocompatible, biodegradable and bio safe for environmental applications [37, 38]. Furthermore, ZnO is expected to exhibit more advanced controllable wettability due to the ease with which the surface structure can be developed [39, 40]. ZnO has abundant structures: hexagonal, wurtzite, rod, pillar, wire, belt, flake, and flower-like [41-44]. The WCA can be enhanced by using ZnO's microstructure or nanostructure to change in the surface roughness of the cotton fabric. The goal of the present study is to fabricate a ZnO coating on a cotton fabric surface (ZnO-CF) capable of satisfying the criteria for water superhydrophobicity. The properties of fabricated ZnO-CF were sufficiently studied and the results showed that ZnO-CF have excellent superhydrophobicity, mechanical stability and reusability. After that, it was used to selectively absorb hexane while repelling water completely. The relationship between the surface properties and the wettability of the fabrics was also discussed in detail.

2.2. Materials and experiments

2.2.1. Materials

Zinc acetate dihydrate ($Zn(CH_3COO)_2.2H_2O$), zinc nitrate hexahydrate ($Zn(NO_3)_2.6H_2O$), ammonium hydroxide (NH_4OH) and hexamethylenetetramine (HMTA, $C_6H_{12}N_4$) were all purchased from Samchun Pure Chemical Co., Ltd, Korea. All chemicals were reagent grades and used as received without further purification. Deionized water was used for all experiments.

Cotton fabric (CF) was purchased from a local store in Ulsan, Korea. The CF was cut into 10 × 10 cm pieces, cleaned in an ultrasonic bath for 2 h with a mixture of methanol and water, were washed several times with deionized water and dried in an air oven at 50 ^oC for 24 h.

2.2.2. Fabrication of superhydrophobic cotton fabric

- Preparation of ZnO crystal nucleus

In a typical process to prepare the cotton fabric loaded with Zn^{2+}, as an initial step,

$Zn(CH_3COO)_2.2H_2O$ was dissolved in water at a concentration of 0.03 M. A piece of CF was then immersed into the prepared zinc acetate solution. NH_4OH was then slowly added into the solution with stirring maintained for 3 h at 50 ^oC. Cotton fabric with Zn^{2+} nucleus was dried in an air oven at 50 ^oC for 12 h.

- Preparation of ZnO-coated cotton fabric (ZnO-CF)

A 1:1 molar ratio mixture of 0.025 M $Zn(NO_3)_2.6H_2O$ and 0.025 M HMTA was prepared with constant stirring for 3 h. A piece of CF loaded with Zn^{2+} nucleus was immersed in this transparent mixture in a 200 mL Teflon-lined stainless steel autoclave. The autoclave was heated in a laboratory oven at a constant temperature of 100 ^oC for 6 h. After that, the autoclave was taken out from the oven and cooled down at room temperature. The fabric was cleaned several times with deionized water and dried in an air oven at 50 ^oC for 24 h.

2.2.3. Characterization methods

The surface morphology and chemical composition of the original CF and ZnO-CF were characterized by using field emission - scanning electron microscopy (FE-SEM, JEOL 6500), X-ray diffraction (XRD, AXS D8 ADVANCE) and X-ray photoelectron spectroscopy (XPS, ThermoFisher Scientific K-Alpha).

The surface roughness was evaluated by confocal fluorescence microscopy (Keyence VK-X200) with a sample magnification of 50 times. The static WCA was measured using a Smart drop contact angle system maintained by a computer-controlled device with the 5 µL droplet. The fabric samples were enclosed on glass slides with double-side tape before the confocal and WCA analysis. The WCA test was conducted at least five times at different areas on each sample.

The dynamic WCA measurements including sliding WCA and shedding WCA were also carried out in order to confirm the superhydrophobicity of the surface (Fig.2.1). All the equipment was placed on a balance table under ambient condition in order to minimize the experimental error. The sliding WCAs at 1^o to 10^o at intervals of 1^o were also measured using the experimental unit shown in Fig. 2.1 (a). For the shedding WCA measurement (Fig.2.1(b)), the fabric sample was placed on a tilting base and the measurements were started at an inclination angle of 50^o. The

syringe was kept at 2 cm far away from the sample surface and the volume of the drop was controlled at 5 µL. If all droplets run off from the fabric surface, the angle was reduced by 1^{o} and the experiment finish until the drop cannot completely run off the surface. The lowest angle at which all the drops completely come out from the fabric surface was noted as the shedding WCA.

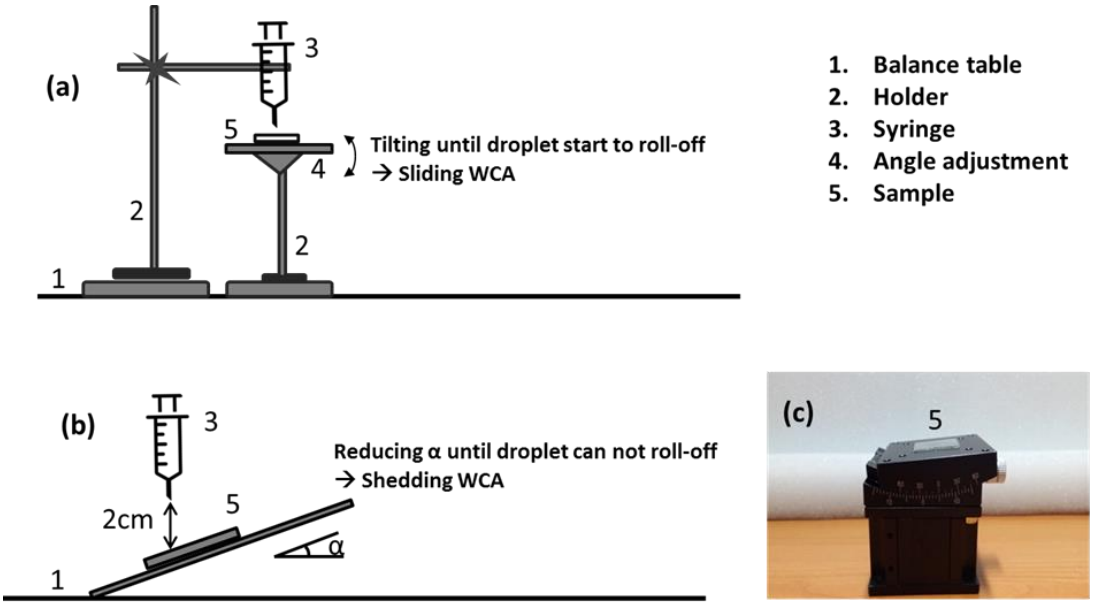

Fig.2.1. Design experiment for (a) sliding WCA, (b) shedding WCA and (c) tilting base for shedding WCA

2.2.4. Separation tests

In the separation test, 20 mL of water (dyed with methylene orange) and 20 mL of hexane taken by a mess cylinder were mixed vigorously. After that, the hexane-water mixture was poured onto the fabrics. The separation of hexane from water was performed as shown in Fig. 2.2. The same experiment process was also carried out with other types of oil (including toluene, octane, chlorobenzene, kerosene and diesel) in order to check the oil-water separation ability of fabricated ZnO-CF.

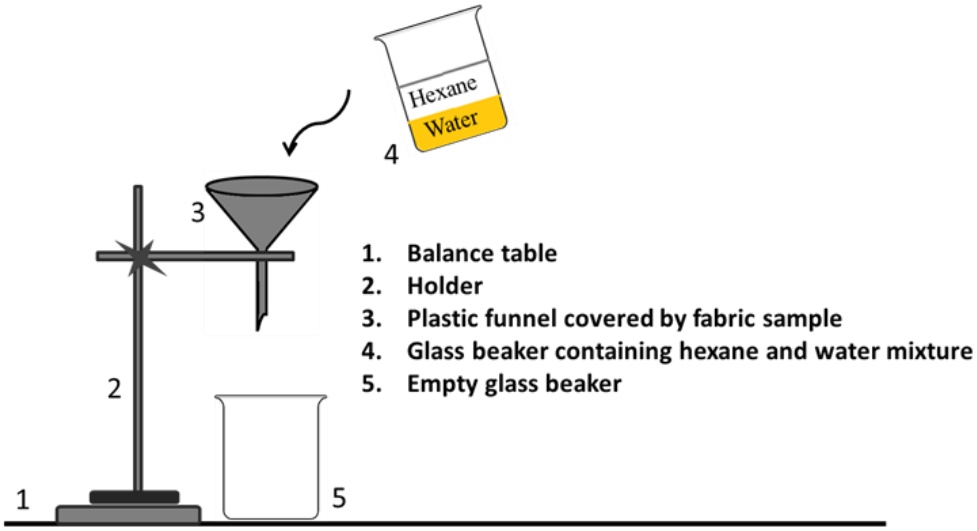

Fig.2.2. Experimental design of hexane-water separation test

In this experiment, the effect of the hexane mass on the separation efficiency was not evaluated due to its penetration into the fabric and its ease of in evaporation. The separation capacity of cotton fabric was calculated depending on the mass of water according to equation (2.1):

$$\text{Separation capacity} = \frac{M}{M_0} \times 100\ \% \qquad (2.1)$$

where M_0 and M are the weights of water before and after separation, respectively. The value of M_0 was measured before water was mixed with hexane and the value of M was measured immediately after the separation process. The average value of 10 separation experiments was used. Some procedural and instrumental errors could be involved in the transfer process of the liquid mixture into different apparatuses, the subjective view in the mess cylinder and the balancing process. However, the total measurement error was less than 3 %, thus the accuracy of the data is acceptable. UV-Vis spectrometry (UV-Vis, USA Model GENESYSTM 10S) with a quartz cuvette was used to confirm the purity of the water after the separation process. The scan range was 200 to 800 nm, using baseline correction with a medium scan rate and a data point interval of 1 nm.

The flow separation flux (J) was determined by calculating as the following equation:

$$J = \frac{V}{A \times T} \qquad (2.2)$$

where V is the volume of the permeated solution, A is the separation area and T is permeated time.

2.2.5. Stability and reusability tests

The durability or mechanical stability and the reusability of a material are very important for practical applications. To the best of our knowledge, most recent research has focused on hard substrates such as copper and stainless steel meshes [45, 46]. The ZnO-CF developed in this study is soft and flexible, thus they may be own a weaker stability in the separation process as compared with the harder substrates. Therefore, a set of experiments was conducted to check the stability and reusability of the as-prepared ZnO-CF.

The mechanical stability of the ZnO-CF was tested using different qualitative methods according to previous reported methods [25, 47-49], including abrasion test with 1000 mesh sandpaper (1500 gr load and 5 times of abrasion) (M.T.#1), adhesion with tape (M.T.#2), finger press test (M.T.#3) and twisting by hands test (M.T.#4) (Fig.2.3). The ZnO-CF also was put in the room condition for 7 days (M.T.#5) The chemical stabiltity of as-prepared ZnO-CF was evaluated by soaking it into alkaline (pH = 10) (C.T.#1) and acidic (pH = 3) (C.T.#2) solutions. After these tests, the static WCA and advanced WCA of the fabric samples were evaluated and compared with initial values before the tests.

The reusability of ZnO-ACF after several separation processes was tested via a simple method as follows. After each separation process, ZnO-CF was dried in oven for 6 h at 30 ^{o}C and then it was applied for subsequent separation process. The quality of separated solution was checked by UV-Vis spectrometry (UV-Vis, USA Model GENESYSTM 10S).

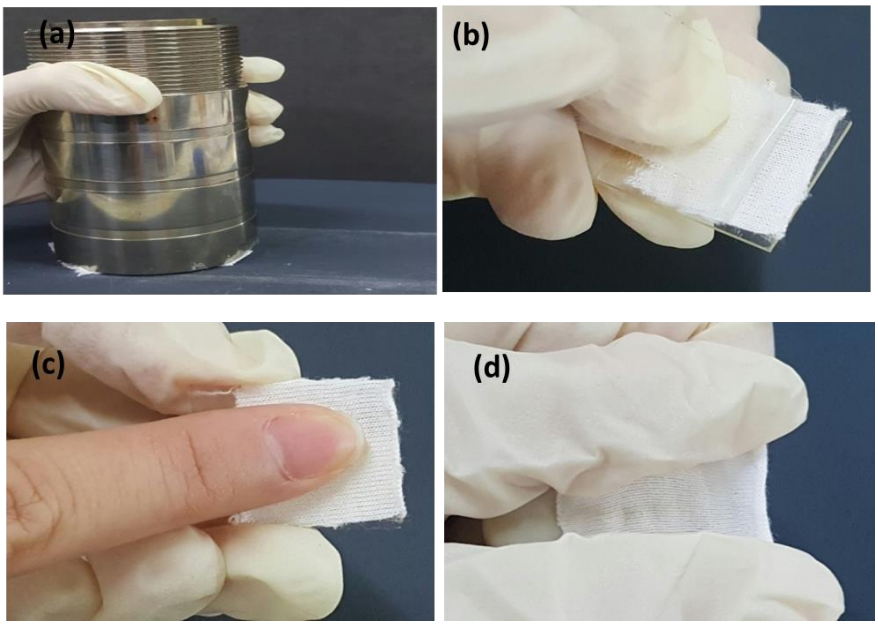

Fig.2.3. Mechanical stability test via (a) abrasion test with 1000 mesh sandpaper, (b) adhesion with tape, (c) finger press and (d) twisting by hands

2.3. Characterization of fabricated fabric

2.3.1. Surface morphology

Fig.2.4 presents the morphologies of the original fabric and ZnO-CF, which were recorded using FE-SEM. The original cotton fabric has a smooth surface, as clearly shown in Fig. 2.4 (a). Fig. 2 (b-d) showed the well-defined morphology of ZnO with stacked hexagonal slices or very thin plate-like structures with an average diameter of 0.8 – 1.0 µm. The uniformity of the Zn^{2+} nuclei and ZnO loading was confirmed in the mapping analysis result (Fig. 2.4 (e)). The relative intensity of C elements was decreased as the intensity of Zn was enhanced due to the loading of the ZnO layer onto the fabric surface.

An alkaline condition is essential for the formation of ZnO in solution. Alkaline reagents that have been used to provide OH^- during the ZnO formation process include NaOH, KOH [50, 51], ammonia [52, 53] and HMTA [54, 55]. In this research, the ZnO crystalline structure was formed by the hydrolysis of zinc nitrate in water in the presence of HMTA. The ZnO synthesis process involves the following chemical reactions (Eq. (2.3) to Eq. (2.9)). The detail role of HMTA remains

unclear but HMTA offers undoubted advantages over other alkaline reagents. The first advantage is that the synthesis process can be carried out at lower temperature by using HMTA [37]. In most cases, the synthesis temperature of ZnO is over 400 ^{o}C [56, 57]. However, in this research ZnO synthesis was achieved with a reaction temperature of only 100 ^{o}C. Secondly, as a non-ionic cyclic tertiary amine, HMTA is decomposed upon heating and can act as a Lewis base with metal ions (Eq. (2.3)-(2.5)). Third, HMTA not only acts as a OH^- supplier but also as a pH buffer to slowly release OH^- ions when heat is provided [37, 58, 59], thus stabilizing the solution pH as well as ensuring the uniformity of the grown structure .

$$(CH_2)_6N_4 + 6\ H_2O \rightarrow 6\ HCHO + 4\ NH_3 \quad (2.3)$$

$$NH_3 + H_2O \leftrightarrow NH_4^+ + OH^- \quad (2.4)$$

$$Zn^{2+} + 4\ NH_3 \rightarrow Zn(NH_3)_4^{2+} \quad (2.5)$$

$$Zn^{2+} + 4\ OH^- \rightarrow Zn(OH)_4^{2-} \quad (2.6)$$

$$Zn(NH_3)_4^{2+} + 2\ OH^- \rightarrow Zn(OH)_2 + 4\ NH_3 \quad (2.7)$$

$$Zn(OH)_4^{2-} \rightarrow ZnO + H_2O + 2\ OH^- \quad (2.8)$$

$$Zn(OH)_2 \rightarrow ZnO + H_2O \quad (2.9)$$

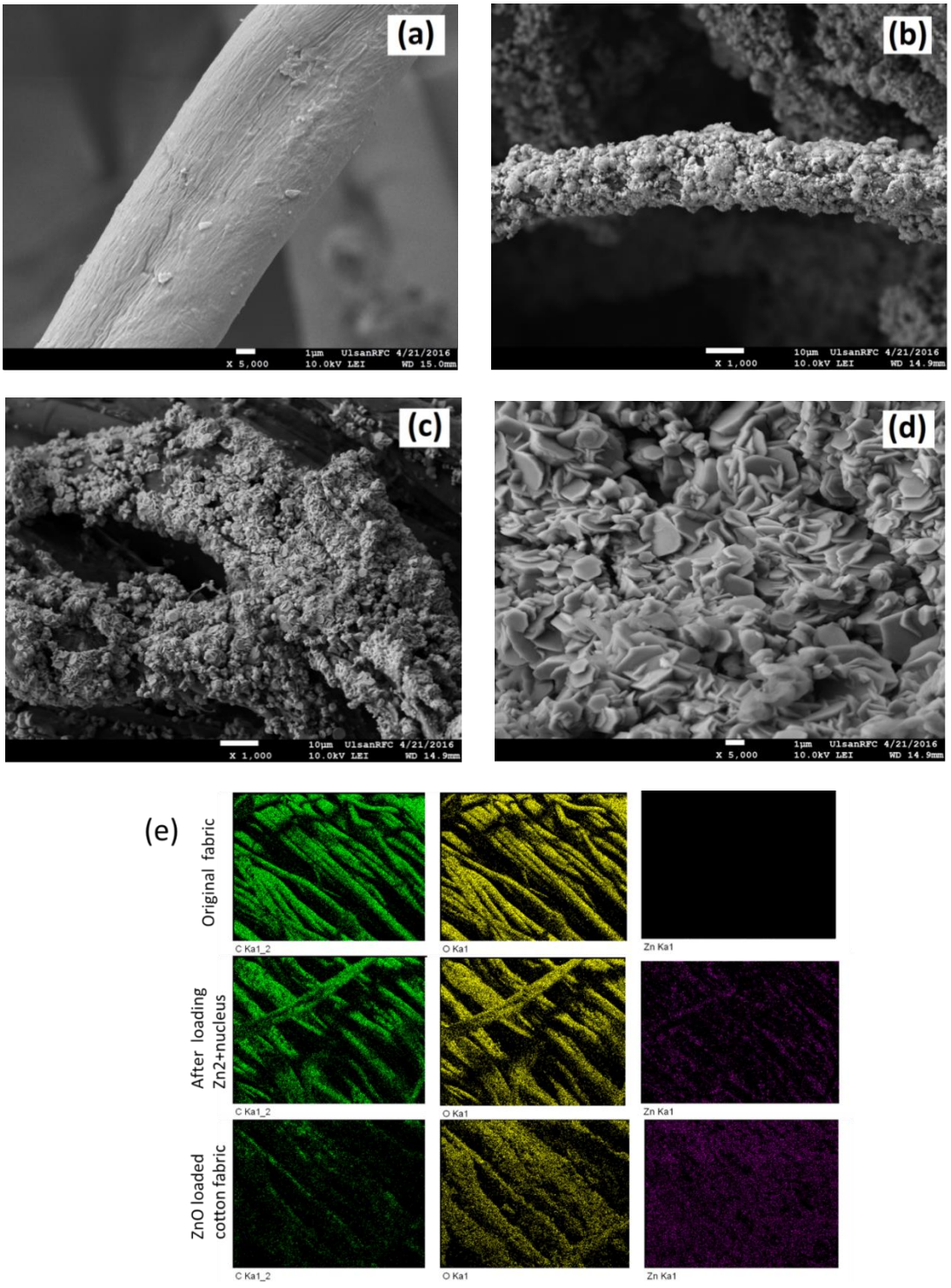

Fig.2.4. SEM images of (a) original cotton fabric, (b, c, d) ZnO-CF; and (e) mapping analysis data of original cotton fabirc, Zn^{2+} nucleus and ZnO-CF

2.3.2. Crystalline structure

The XRD pattern of the original cotton fabric and ZnO-CF are shown in Fig.2.5. The peaks at 2θ = 14.98°, 16.89° and 22.86° observed in both samples correspond to the characteristic peaks of cellulose, the main ingredient of the cotton fabric. The remaining relative peaks were compared to the ZnO structure in JCPDS standard (Jointed Committee of Powder Diffraction Standard - card number 36-1451). The crystals were observed to be randomly arranged. All obtained peaks corresponded to the hexagonal structure of ZnO. The detected peaks at 2θ = 32.09°, 34.63°, 36.44°, 47.60°, 56.76°, 63.18°, 66.44°, 68.20°, 69.18°, 72.83° and 76.91° correspond to the lattice planes (1 0 0), (0 0 2), (1 0 1), (1 0 2), (1 1 0), (1 0 3), (2 0 0), (1 1 2), (2 0 1), (0 0 4) and (2 0 2), respectively. Furthermore, no impurities were found in the XRD patterns, which provide strong evidence for the high purity of the ZnO crystal phase synthesized on the cotton fabric surface.

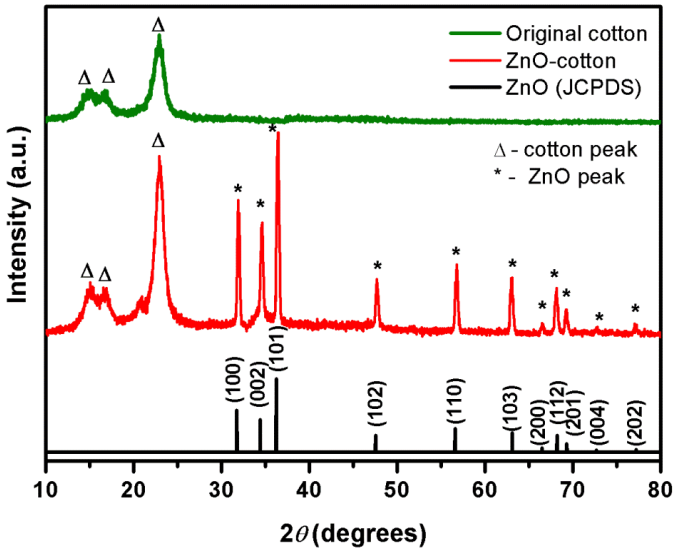

Fig.2.5. X-ray patterns of original cotton fabric and fabricated ZnO-CF

2.3.3. Elemental composition

XPS analysis was used to obtain useful information about the surface elemental composition (Fig.2.6 and Table 2.1). It should be mentioned that XPS analysis result is important evidence for

the change in the surface energy, which can contribute to creating the superhydrophobic fabric surface. XPS measurement survey analysis confirmed the presence of carbon and oxygen in the original cotton fabric sample. After the coating process, the ZnO-CF surface exhibited Zn peaks that were not observed from the original cotton fabric (Fig.2.6 (a)). In order to gain better insight into the chemical composition, a high-resolution scan was performed in the Zn 2p, O 1s and C 1s regions for ZnO-CF (Fig.2.6 (b-d)). In Fig.2.6 (b), two peaks, namely Zn $2p_{1/2}$ and Zn $2p_{3/2}$ peaks, were observed at 1025 eV and 1046 eV, respectively. Fig.2.6 (c) shows the O 1s spectra, including the peaks shown at around 537 eV (O-H bonds), 535 eV (O-C bonds), 534 eV (O=C bonds). The peak observed in the spectra of ZnO-CF at 532 eV was assigned to O-Zn bonds and probably indicates that ZnO structures not only existed on the fabric surface, but were also grafted onto the fibers through the strong adhesion via O-Zn bonding. Fig.2.6 (d) shows the carbon C 1s composition of the original fabric and ZnO-CF. The peaks seen around 290, 287 and 284 eV can be assigned to the C=O, C-O and C-C/C-H bonds. Interestingly, this figure shows the change in the intensity of the bonding types. The C-C/C-H bonds had the lowest intensity in the original cotton fabric sample, whereas the peak intensities of C-O and C-C/C-H were much improved in ZnO-CF (Table 2.1). This remarkable observation in the C 1s data could be used to explain the separation mechanism discussed in later section.

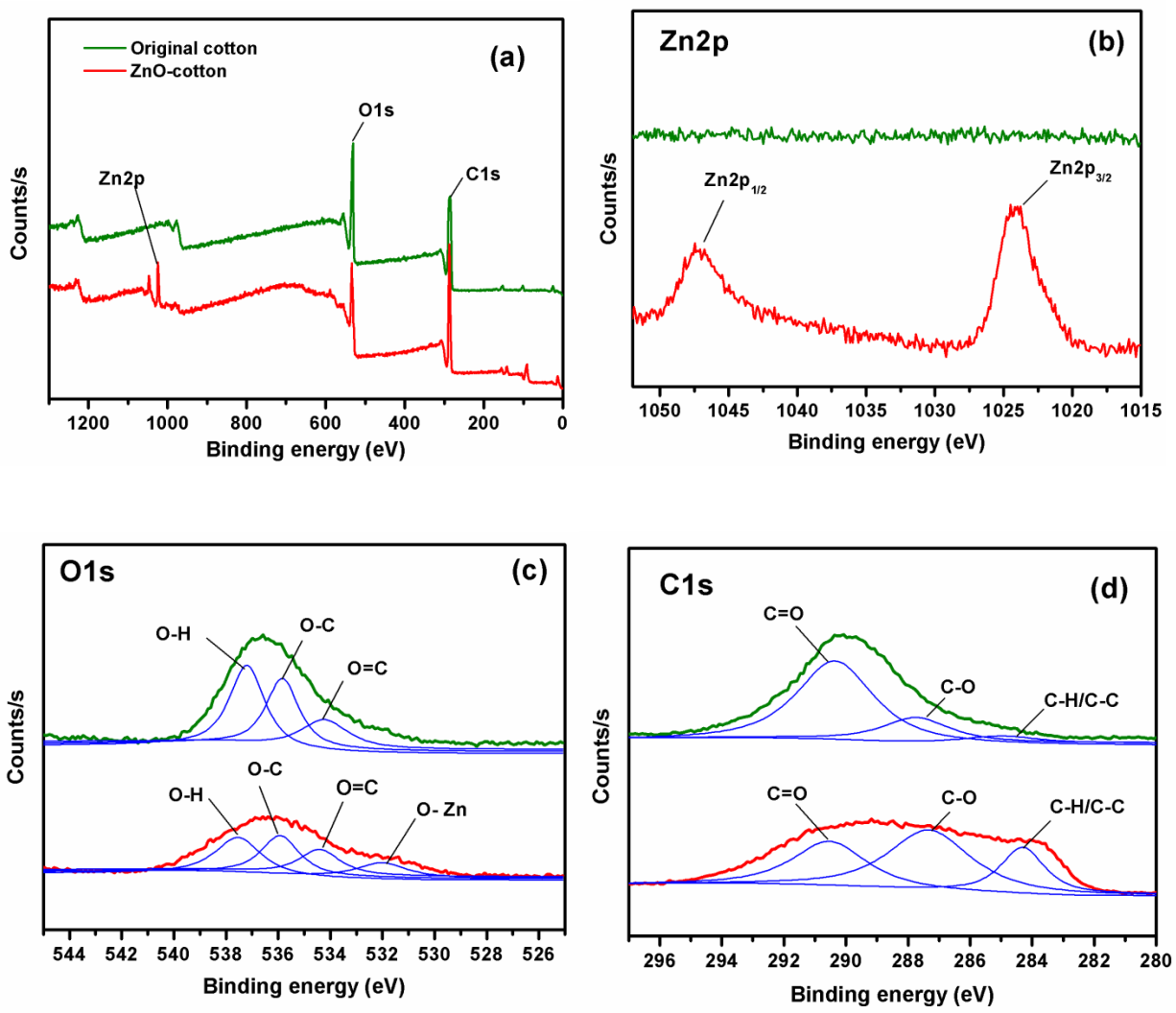

Fig.2.6. XPS spectra (a) survey spectra of original cotton fabric and modified cotton fabric, (b) Zn 2p, (c) O 1s, (d) C 1s

Table 2.1. Position and relative peak area ratio of O 1s and C 1s in original cotton fabric and modified ZnO-CF samples

Element	Type of bonding	Binding energy (eV)		Peak area (%)	
		Original	Modified	Original	Modified
O1s	O-H	537.2	537.6	45.5	35.9
	O-C	535.8	535.9	35.3	30.0
	O=C	534.2	534.4	19.2	20.1
	O-Zn	Not detected	532.0	0	14.0
C1s	C=O	290.4	290.6	74.7	40.4
	C-O	287.7	287.4	19.6	38.7
	C-H/C-C	284.5	284.3	5.7	20.9

2.3.4. Surface roughness and wettability

As cotton fabric has good water absorption and hydrophilic ability (Fig. 2.7 (a)), the WCA could not be recorded in the original fabric sample because the water was rapidly absorbed into the fabric in a few seconds. However, after the ZnO coating process, the static WCA was significantly enhanced (Fig.2.7 (b)). Theoretically, a surface with static WCA greater than 150^o and dynamic WCA lower than 10^o can be termed superhydrophobic. The reliability of the WCA measurement for the cotton fabric was difficult to determine due to the weave structure with numerous protruding fibers. Thus, the reported WCA is the average of at least five WCA measurements. After the coating process, ZnO-CF exhibited superhydrophobicity with extremely high static WCA (static WCA = $151^o \pm 3^o$) and low dynamic WCA (sliding WCA = $9^o \pm 1^o$ and shedding WCA = $8^o \pm 1^o$) (Table 2.2).

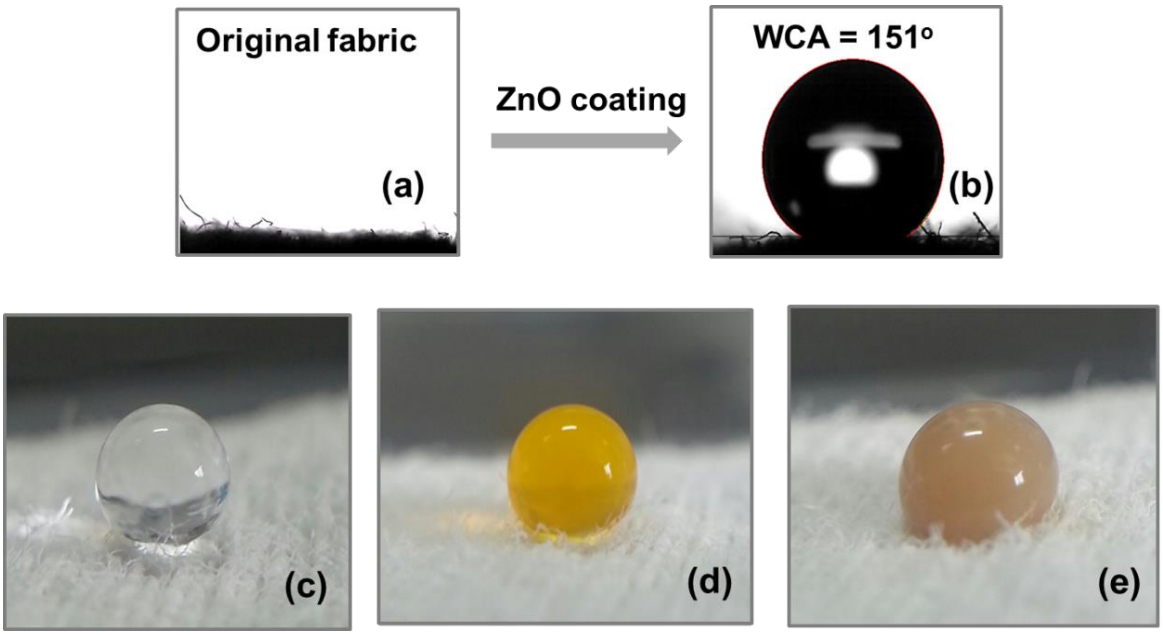

Fig.2.7. (a) WCA of (a) original and (b) ZnO-coated cotton fabric, (c)(d)(e) water, water dyed with methylene orange, coffee drop on the ZnO-CF

Table 2.2. Water contact angle data for original cotton fabric and ZnO-CF

Name of sample	Static WCA (°)	Dynamic WCA (°)	
		Sliding WCA	Shedding WCA
Original cotton fabric	Not detected	Not detected	Not detected
Prepared ZnO-coated cotton fabric	151 ± 3	9 ± 1	8 ± 1

The confocal analysis was carried out for further confirmation of the changes in surface roughness after ZnO coating (Fig.2.8). The surface of the original cotton fabric was even and flat with an average roughness (R_a) of 0.85 and a surface thickness of 91.1 µm. In contrast, after coating, the thickness of ZnO-CF was increased up to 105.4 µm due to the coated material layer. The ZnO-CF surface after ZnO coating also became rougher with R_a = 2.42.

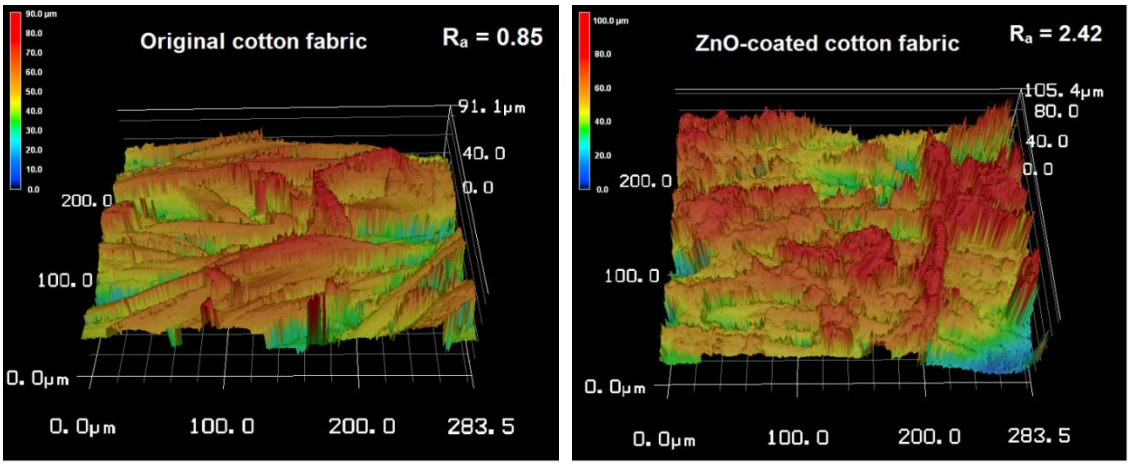

Fig.2.8. Confocal analysis data of orginal and ZnO-CF

As aforementioned, the hydrophilic state of the original cotton fabric was changed to superhydrophobic state after the ZnO coating. The changes in the two main factors, the chemical composition (surface energy) and geometrical structure (micro- or nano-scale roughness), explained this interesting phenomenon. Altering one or both of these two factors changes the surface wettability state.

Presented XPS analysis data are solid evidence of the change in the surface energy of ZnO-CF derived after the ZnO coating process. The O 1s spectra revealed that the area ratio of the O-H group was decreased after the coating process from 45.5 % to 35.9 % (Table 2.1), thus confirming the higher hydrophobicity. In the C 1s spectra, the area ratio of the C-H/C-C bond was increased from 5.7% to 20.9 % after the ZnO coating process. In terms of electronegativity, the C-H/C-C bond is non-polar, while C=O and C-O bonds are polar. The water repulsion of the ZnO-CF surface and hence its impermeability to water can be attributed to the enhanced C-H/C-C bonding and the decrease in C=O and C-O bonding. The modified ZnO-CF surface seems to prefer the penetration of nonpolar solutions such as hexane, toluene and chloroform, which enables the fabricated ZnO-CF to be used in the separation of a mixture of nonpolar organic solvents and water.

The wettability of ZnO-CF can be also considered, based on the change in the surface roughness according to the theoretical application of the Wenzel or Cassie-Baxter models. Wenzel found that the liquid completely fills the grooves of the rough surface where they contact. Thus, the water

drop cannot roll off from the surface by itself in the Wenzel model. The Cassie-Baxter model postulates the presence of vapor pockets trapped underneath the liquid, which minimizes the contact area between the water drop and the surface so that the WCA is greatly improved. Thus, the “microabobinary structures”, which have some roughness on both micro- and nano-scales, are promising candidates for high hydrophobic surfaces. As seen in the SEM images (and the confocal analysis, the layer coated with ZnO changed the surface roughness of the original cotton fabric. Based on the Cassie-Baxter model, the adhesion between the fabric surface and water was very small due to the air trapped between the rough structures. Thus the interface between the water drop and fabric was easily separated and the water drop rolled off.

2.4. Applications of fabricated fabric

2.4.1. Anti-wetting and self-cleaning

Superhydrophobic surfaces have many applicale features such as self-cleaning, anti-icing and anti-corrosion. In this research, the fabricated ZnO-CF demonstrated excellent anti-wetting and self-cleaning properties. In the first experiment, pieces of the original CF and of ZnO-CF were soaked several times in the water (dyed with methylene orange) (Fig. 2.9 (a)). The original fabric rapidly became wetted and colored, whereas ZnO-CF remained completely dry even after being dipped into and taken out of the dye solution. In the second experiment to demonstrate the self-cleaning ability (Fig.2.9 (b)), the dusts powder was placed on the original CF and ZnO-CF. The water was rapidly absorbed and left the original CF surface dirty. In contrast, water droplets were immediately formed on ZnO-CF and the dust powder was taken out and to leave a clean surface.

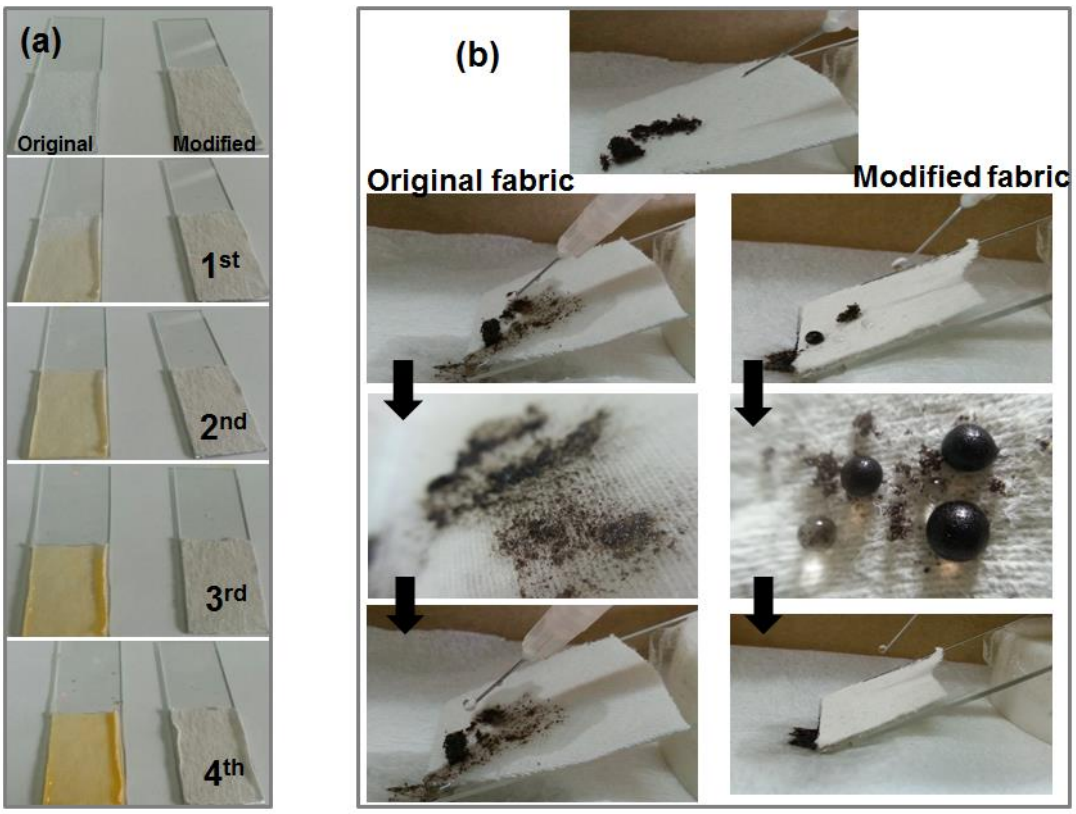

Fig.2.9. Anti-wetting and self-cleaning activity of ZnO-CF

2.4.2. Organic solvent-water separation

Superhydrophobic fabrics with soft and flexible properties are good candidates for efficient separation of organic solvent-water mixtures. Fig.2.10 shows the separation experiment of the mixture of 20 mL water (dyed with methylene orange) and 20 mL hexane using the original cotton fabric and ZnO-CF as the filters. The original cotton fabric was unable to selectively separate hexane from water. However, with the utilizing of fabricated ZnO-CF, hexane was quickly penetrated through ZnO-CF while water was still retained above the fabric. Separation efficiency after the first cycle of over 99 % was attained when no external pressure or outside force, accept atmosphere pressure, was applied for the separation.

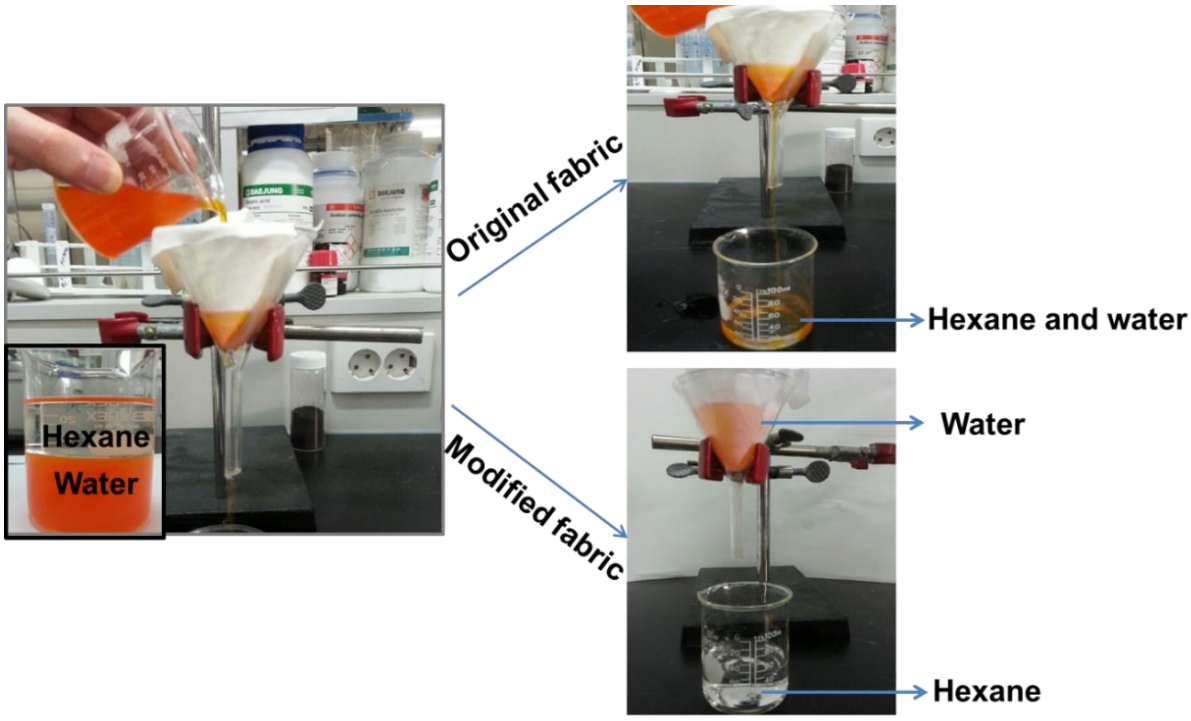

Fig.2.10. Hexane – water separation experiments with original CF and ZnO-CF

From the UV-Vis analysis results (Fig.2.10 (a)), no new peaks of impurity appeared and the intensity of the water's peaks (dyed with methylene orange) was not greatly changed after several separation cycles. This demonstrated the ability of ZnO-CF to selectively separate the hexane and water mixture into extremely high purity water after the separation process. In the other hand, the separation capacity of other oil-water mixtures also reached over 90 % (Fig.2.10 (b)). These results indicated the useful of ZnO-CF in separation of various kinds of oil with water. According to the separation results, the flow flux rate could be estimated and demonstrated in Fig.2.10 (c). The fabricated ZnO-CF filter allowed flow flux rate for the first cycle of 1203, 1192, 1028, 1033, 1001 and 987 $L/m^{-2}.h^{-1}$ for hexane/water, toluene/water, octane/water, chlorobenzene/water, kerosene/water and diesel/water, respectively. It is relatively high and promising value for the fabric filter, which are comparable to polymeric or ceramic membranes for oil-water separation. For the next ten cycles the allowed flow fluxes decreased, however the decrease rate were not significant.

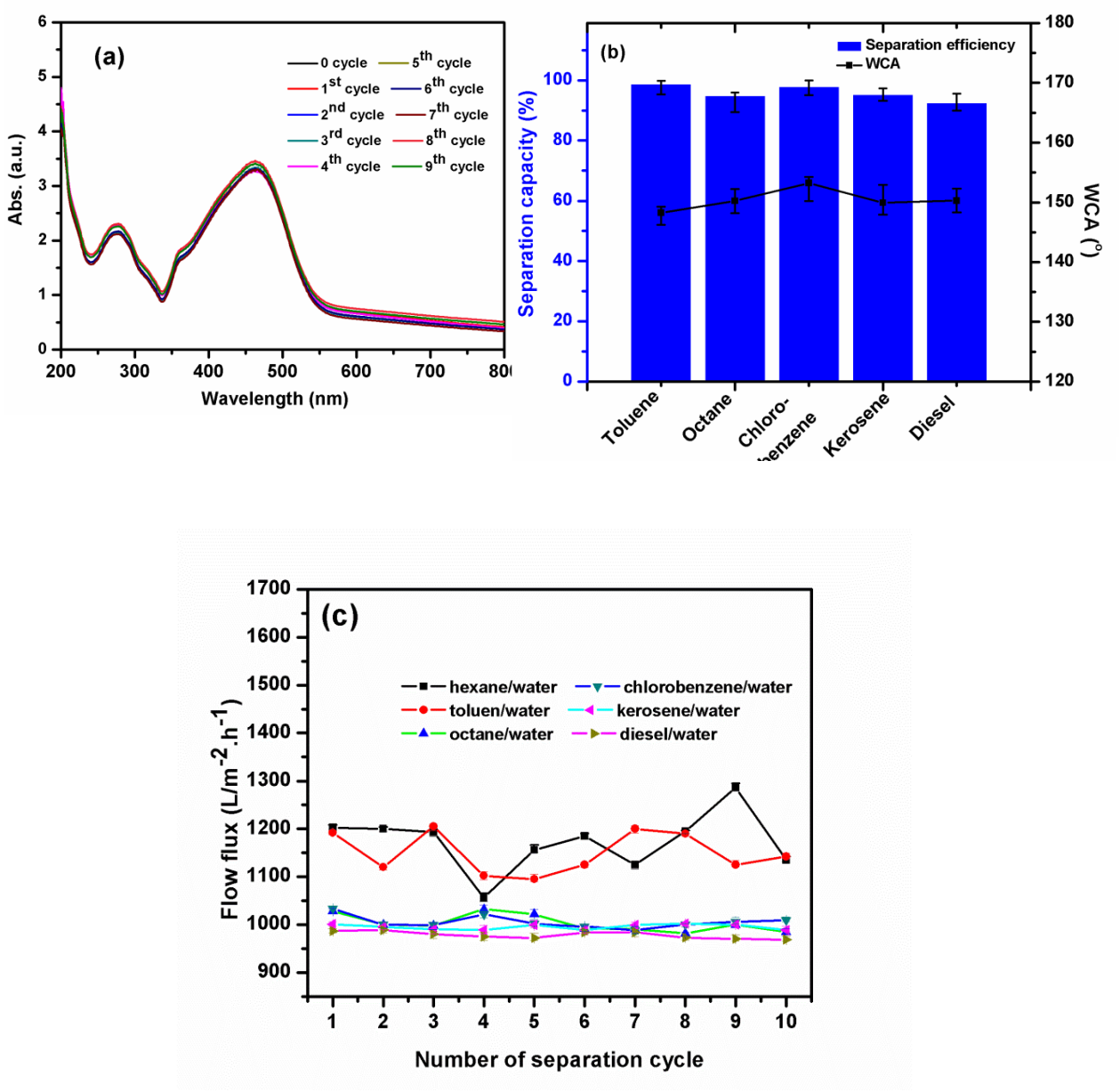

Fig.2.10. (a) Purity of water after separation process, (b) separation efficiency of as-prepared ZnO-CF for various types of oil/water mixtures and (c) flow flux for several cycles

2.5. Stability and reusability of fabricated fabric

After the mechanical and chemical stability tests, the as-prepared ZnO-CF return to its original shape without any changes or cracks, which firstly confirm its good stability as well as good

flexibility. Secondly, the good stability and reuseability of ZnO-CF was proved via the stable in the WCAs. After the mechanical and chemical stability tests, the static WCAs as well as advanced WCAs of treated ZnO-CF samples were not much changed as compared with the initial ZnO-CF sample (Fig.2.11 (a)). The ZnO-CF also was put in the room condition for 7 days and it was observed that it was resistant to outdoor affects. In addition, as shown in the inset of Fig.2.11 (b), the separation efficiency of ZnO-CF was only slightly decreased after several repeated cycles, indicating that it retained good reusability. The excellent stability of ZnO-CF provides more opportunities for numerous practical applications, such as waste water treatment and purification, and garment manufacturing for medical and military uses.

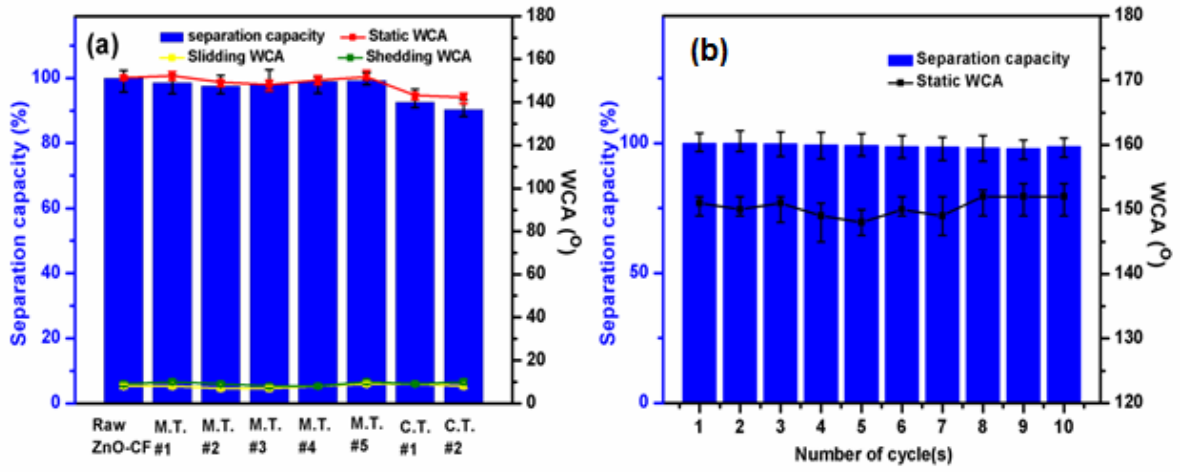

Fig.2.11. (a) Mechanical and chemical stability and (b) reusability of fabricated fabric

2.6. Summary

A stable and robust superhydrophobic composite of ZnO and commercial cotton fabric was successfully fabricated with a simple approach. During the coating process, ZnO of high purity and uniform structure was grown on the cotton fabric surface. Superhydrophobicity was achieved with a WCA up to 151 ± 3^{o} because the ZnO coating on the original cotton fabric changed the surface roughness and surface energy. The surface of the original cotton fabric was even and flat with Ra = 0.85, whereas the ZnO-CF surface was much rougher with R_a = 2.42. The enhanced C-H/C-C bonding and the decrease in C=O and C-O bonding also increased the water repulsion of

ZnO-CF. ZnO-CF with soft and flexible properties exhibited an excellent hexane-water separation capacity and good stability in repeated applications. Therefore, ZnO-CF can be utilized for the selective separation of hexane and water in applications requiring self-cleaning ability.

CHAPTER 3

CHAPTER 3 - SUPERHYDROPHOBIC POLYURETHANE SPONGE

Abstract

We report a novel superhydrophobic material based on commercially available polyurethane (PU) sponge with high porosity, low density and good elasticity. The fabrication of a superhydrophobic sponge capable of efficiently separating oil from water was achieved by imitating or mimicking nature's designs. The original PU sponge was coated with zinc oxide (ZnO), stearic acid (SA) and iron oxide particles (Fe_3O_4) via a facile and environmentally friendly method. After each treatment, the properties of the modified sponge were characterized, and the changes in wettability were examined. Water contact angle (WCA) measurements confirmed the excellent superhydrophobicity of the material withhigh static WCA of 161° andlow dynamic WCA (sliding WCA of 7° and shedding WCA of 8°). The fabricated sponge showed high efficiency in separation (over 99 %) of different oils from water. Additionally, the fabricated PU@ZnO@Fe_3O_4@SA sponge could be magnetically guided to quickly absorb oil floating on the water surface. Moreover, the fabricated sponge showed excellent stability and reusability in terms of superhydrophobicity and oil absorption capacity. The durable, magnetic and superhydrophobic properties of the fabricated sponge render it applicable to the cleanup of marine oil spills and other oil-water separation issues, with eco-friendly recovery of the oil by simple squeezing process.

Keywords: polyurethane sponge, ZnO, stearic acid, magnetic, superhydrophobic, separation

3.1. Introduction

With the increasing use of fossil fuel and the global population growth, oil spill accidents occurring during oil utilization and transport processes have adversely impacted the environment. For example, the Deep-water Horizon oil spill (2010) in Mexico was considered the world's largest accidental release of oil into marine water in history, causing significant environmental damage associated with the discharge of nearly five million barrels of oil and the death of eleven people [60]. More recently, a pipeline spill (2016) in North Dakota, USA, leaked 4200 barrels of oil, and up to 5.4 miles of a creek was heavily polluted [61]. Therefore, the separation of oil from water has received great attention from scientists and engineers because of the increase in oil pollution events worldwide. However, it is very difficult to collect or separate spilled oil from bodies of water. Thus, oil companies have spent large sums to clean up oil spills. Many remediation processes, such as electrochemical methods [62, 63], controlled burning [64, 65], membrane filtration [66, 67], chemical dispersants and biological agents [68, 69], have been developed to clean up oil pollution. However, most of these methods suffer from high operation costs, low efficiency and, in some cases, the creation of secondary pollutants.

Consequently, the developments of advanced materials capable of selectively separating oil from bodies of water in oil spill areas are highly desirable. Currently, superhydrophobic materials with a static water contact angle (WCA) higher than 150° and a dynamic WCA less than 10° have attracted attention due to their unique super-antiwetting, self-cleaning properties and their potential for use in practical applications [4, 70-72], including oil-water separation. Our relevant literature survey revealed that an increasing number of studies with the topics of "oil-water separation" and "superhydrophobic surface" were published from 2007 to 2016 (Fig.3.1). This clearly demonstrates the focus of investigations on durable superhydrophobic materials for application to the proper separation of oil and water and the clean-up of spilled oils.

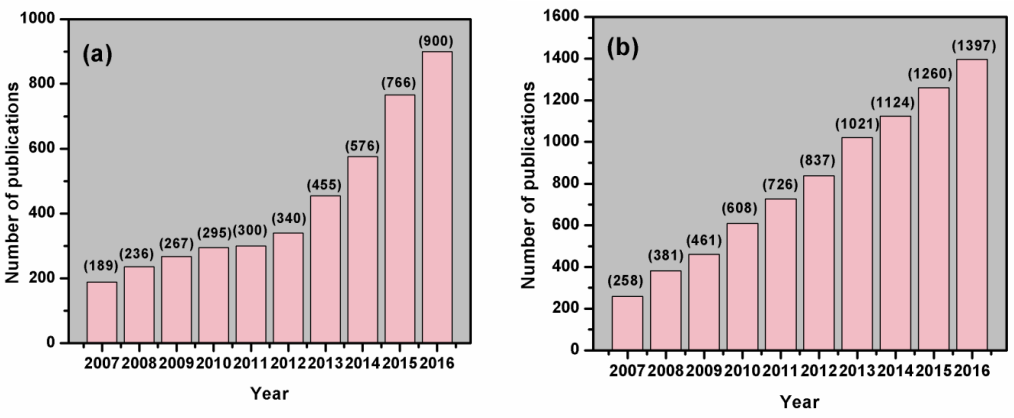

Fig.3.1. Number of paper published from 2007-2016 under the topic (a) oil-water separation and (b) superhydrophobic/superhydrophobicity (Source: ISI Web of Science)

In nature, water repellence and superhydrophobic phenomena are frequently observed, for example, lotus leaves (*Nelumbo buciferea*) with nano/micro structures, Ramee leaves (*Boehmeria nivea*) and Chinese watermelon (*Citrullus lanatus*) with microstructures on their surfaces all exhibit hydrophobic properties. The term biomimetic is defined as actions to imitate or mimic nature. The rapidly increasing interest in the biomimetic field is creating a new current trend in research, which includes mimicking natural surface structures to develop desirable materials, devices and processes. Artificial superhydrophobic surfaces are developed based on mimicking natural superhydrophobic phenomena by employing two approaches: (i) utilization of micron- or nanometer-scale surface roughness and (ii) application of chemical hydrophobicity. While the initial surface is hydrophilic, proper control of the roughness and a surface treatment or coating are required to switch from a hydrophilic state to a superhydrophobic state. Generally, superhydrophobic surfaces have been developed in the form of fabrics [29, 73], meshes [74], films [75] and 3D porous materials [76]. Among these materials, commercially available polyurethane (PU) sponge, which has a high porosity, light weight and good elasticity, is a promising substrate for the preparation of a superhydrophobic material for oil-water separation and oil absorption. However, the PU sponge is hydrophilic and can easily absorb both oil and water. Therefore, researchers have tried various methods to change the wettability of the original PU sponge by increasing the surface roughness with SiO_2/graphene oxide nanohybrids [77] or changing the chemical functional groups with carbon nanotubes/poly(dimethylsiloxane) [78] or

SiO_2/poly(tetrafluoroethylene) [79]. However, these materials are very expensive, non-biodegradable and harmful to the environment. Furthermore, most researchers have focused on only one approach for fabricating superhydrophobic PU and, no studies have combined both approaches for attaining superhydrophobicity.

In this study, we report the preparation of a novel, magnetic, durable and superhydrophobic composite material based on a commercial PU sponge via a facile method. The surface of the fabricated material clearly mimics natural superhydrophobic phenomena. The hydrophobicity was first derived from the microstructure, which was grown on the initial surface and was similar to that observed on the natural surface of Ramee leaves or Chinese watermelon. For this first approach towards engineering a suitable surface roughness, a zinc oxide (ZnO) coating layer was selected due to its superior abilities, which include easily controlled of structure growth, low cost and environmental non-toxicity [73, 80]. After a facile ZnO coating step performed with a commercial microwave, the wettability of the PU sponge was transformed from a hydrophilic state to a hydrophobic state. In the second step of engineering, to achieve the surface chemical hydrophobicity observed for the wax surface of the lotus leaf, stearic acid (SA) (Fig. 3.2) - a long-chain fatty acid - was used as a modifier to tune the surface wettability from hydrophobic to superhydrophobic. The functionalized sponge should also exhibit magnetic responsivity for the treatment of oil floating on the composite surface due to the addition of Fe_3O_4 particles to the surface. The fabricated PU@ZnO@SA@Fe_3O_4 sponge was then tested in two experiments: (i) selective absorption of oil floating on water and (ii) separation of oil from a mixture with water. The oil sorption capacity and separation efficiency of the sponge were investigated for hexane, toluene, dichloromethane, gasoline, soybean oil, diesel engine oil and vacuum pump oil. The durability and reusability of the fabricated sponge were also tested. Because of its robust superhydrophobicity and good mechanical stability, the as-prepared PU@ZnO@Fe_3O_4@SA sponge ranks as a promising material for practical application to the sorption and recovery of oil from water.

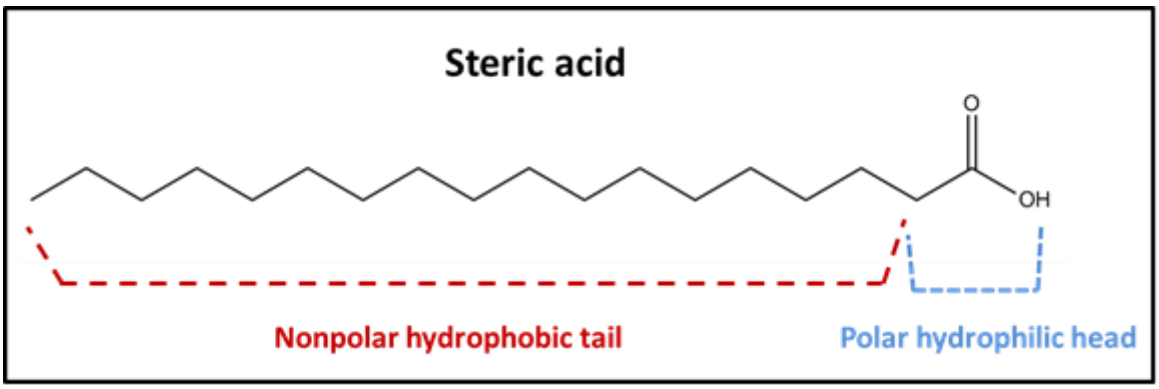

Fig.3.2. Chemical structure of stearic acid

3.2. Materials and experiments

3.2.1. Materials

Commercial PU sponges - a product of Clean Life Co., Ltd., Korea (product No. 48475) - were purchased from a local store in Ulsan, Korea. Zinc acetate ($Zn(CH_3COO)_2$), ammonia solution (NH_4OH), iron (II) chloride tetrahydrate ($FeCl_2.4H_2O$), anhydrous iron (III) chloride ($FeCl_3$) and SA ($C_{18}H_{36}O_2$) were purchased from Daejung Chemicals & Metals Co., Ltd., Korea. Extra-pure grade ethanol and acetone were purchased from Samchun Chemical Co., Ltd., Korea. N-hexane, vacuum pump oil, diesel engine oil, soybean oil, toluene, dichloromethane and gasoline were used to test the oil absorption capacity of the fabricated sponge samples. Characteristic information about the oils and organic solvents was taken from the catalog published by the manufacturers and is summarized in Table 3.1.

Table 3.1. List of the oils and organic solvents used

Type	Manufacturer	Specification	Density (kg/L, 15 °C)	Viscosity (mm^2/s, 40 °C))
Hexane	Samchun Chemical (Korea)	Pure 99.99 %	0.66	13.10
Vacuum pump oil	Moresco Corporation (Japan)	NEOVAC MR-200	0.89	71.0
Diesel engine oil	GS Oil (Korea)	KIXX HD1 Cl-4/SL 15W-40	0.87	103.90
Soybean oil	Ottogi Ltd. (Korea)	Soybean oil extract	0.73	56.3
Toluene (methylbenzene)	Daejung Chemicals and Metals	Above 99.5 %	0.8667	0.59
Dichloromethane	Daejung Chemicals and Metals	Above 99.5 %	1.318	0.43
Gasoline	SK energy	Commercial product	0.77	0.673

3.2.2. Fabrication of superhydrophobic PU sponge

The PU@ZnO@Fe_3O_4@SA sponge was prepared as shown in Fig.3.3.

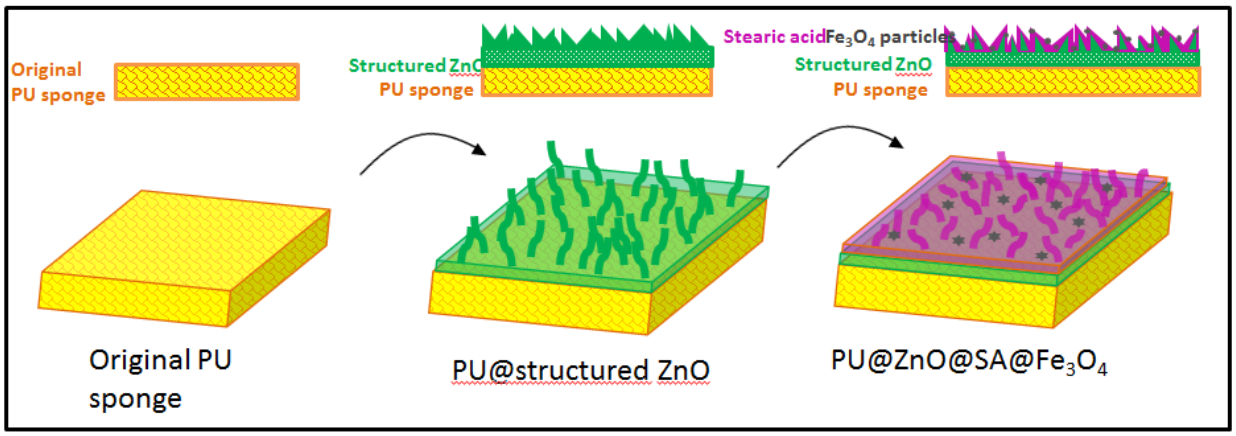

Fig.3.3. Illustration of the fabrication process of PU@ZnO@Fe_3O_4@SA

PU sponge pretreatment: The original PU sponge was cut into cubes of the desired size (3 × 3 ×

3 cm^3) and cleaned with deionized (DI) water and ethanol several times to remove impurities that could cause unwanted reactions on the PU surface. The cleaned PU sponges were oven dried at 50 °C for 6 h, and this drying process did not affect the structure or the properties of the PU sponge. After the pretreatment, the coating steps were carried out according to the two fabrication processes described below.

Fabrication of ZnO flakes on the PU sponge surface: ZnO flakes were grown on the PU surface by a rapid microwave method [81]. A seeding solution of Zn^{2+} was prepared by dropwise addition of 25 % NH_4OH into 100 ml of 0.1 M zinc acetate, and a white precipitate was observed in the solution within a few seconds. Ammonia was added dropwise to the zinc acetate solution until the solution became transparent and reached a pH of pH 10-11. After that, the cubic PU sponges were immersed in a reaction flask containing the seeding solution with slight stirring. After 6 h, the reaction flask was heated in a commercial microwave oven (Daewoo KR-G20EW, 1120 W, 2450 MHz) in three steps, each consisting of 30 s of heating followed by 30 s of standing. Subsequently, the reaction flask was cooled to room temperature (approximately 20 °C) for 5 min. The PU sponges with a ZnO coating layer (PU@ZnO sponge) were taken out, rinsed with distilled water several times, and oven dried at 50 °C for 6 h.

Fabrication of PU@ZnO@Fe_3O_4@SA: Fe_3O_4 was synthesized by a co-precipitation method. After 100 ml of 0.1 M $FeCl_3$ was added into 50 ml of 0.1 M $FeCl_2$, chemical precipitation was achieved by adding an NH_4OH solution under vigorous stirring. The reaction system was kept at 80 °C and a solution pH of 11-12 for 3 h. After the reaction system was cooled, the precipitates were separated by filtration and further washed with water and acetone until a neutral pH was reached. After that, the Fe_3O_4 product was oven dried at 60 °C for 12 h and milled to a powder using a manual grinder.

After 0.1 g of the prepared Fe_3O_4 powder was diluted in 100 ml of ethanol, the mixture was sonicated for 1 h at 30 °C. Then, the PU@ZnO sponge was soaked in the Fe_3O_4-ethanol solution for 60 min to obtain PU@ZnO@Fe_3O_4. The PU@ZnO sponge was uniformly coated with Fe_3O_4 particles. However, it was found that the interaction between the sponge and the Fe_3O_4 particles was weak. Finally, SA was coated on the sponge surface by immersing the PU@ZnO@Fe_3O_4 sponge in 50 ml of 10 mmol/L SA dissolved in ethanol for 3 h. This SA layer was used as the top

coating layer to decrease the loss of Fe_3O_4 particles and thus maintain the stability of the material as well as provide the necessary chemical bonding for promoting superhydrophobicity. The PU@ZnO@Fe_3O_4@SA samples were finally washed with ethanol and distilled water to remove any excess reactants and then oven dried at 50 °C for 6 h.

3.2.3. Characterization methods

Scanning electron microscopy (SEM) analysis was performed on an FE-SEM JEOL 6500 instrument to observe the morphology of the fabricated materials. A mapping technique combined with SEM analysis was used for elemental distribution analysis. The crystalline phases in the samples were determined by using an X-ray diffractometer (XRD, Bruker, Model AXS D8 ADVANCE). The XRD data were collected using Cu-Kα (λ = 0.154060 nm) radiation (step size, 0.02°; 2θ angular range = 10°-80°). The chemical composition and functional groups on the material surface were determined by X-ray photoelectron spectroscopy (XPS, Thermo Fisher Scientific, Model ESCALAB 250 XI XPS) and Fourier transform infrared spectroscopy (FT-IR, Varian 670/620). The magnetic properties of the materials were measured using a vibrating sample magnetometer (VSM PPMS Quantum Design, Inc.).

The WCA was measured using a contact angle meter (SmartDrop, Femtofab Co. Ltd., Korea) maintained by a computer-controlled device on an anti-vibration table and cabinet for reliable measurement. The volumes of the droplets used for static WCA and dynamic WCA measurements were 5 and 10 µl, respectively. In addition, the WCA tests were conducted at least five times at different positions on each sample. The sliding WCAs and shedding WCAs at intervals of 1° were also measured using a previously reported experimental unit in Chapter 2.

3.2.4. Oil-water separation experiments

To demonstrate the oil absorption ability of the fabricated sponges, seven organic solvents and oils (including hexane, toluene, dichloromethane, gasoline, soybean oil, diesel engine oil and vacuum pump oil, which were dyed with oil red O dye) were used as sorbates. PU@ZnO@Fe_3O_4@SA sponges were applied in two experiments: (i) selective absorption of floating oil/organic solvent on water, (ii) separation of oil/organic solvent in a mixture with water and separation of emulsified oil in water.

The first experiment was carried out as shown in Fig.3.4. After 10 ml of DI water was placed in a Petri dish, several drops of vacuum oil were added by a pipette, and the oil drops floated on the water surface. A cube of fabricated sponge ($1 \times 0.5 \times 0.5$ cm^3) was placed in the Petri dish, and a magnet was used to guide the sponge to the locations of the oil drops. The resulting phenomenon was recorded by a digital camera. The sponge was then removed from the disk, and the purity of the remaining solution after oil absorption by the fabricated sponge was checked by UV-Vis spectroscopy.

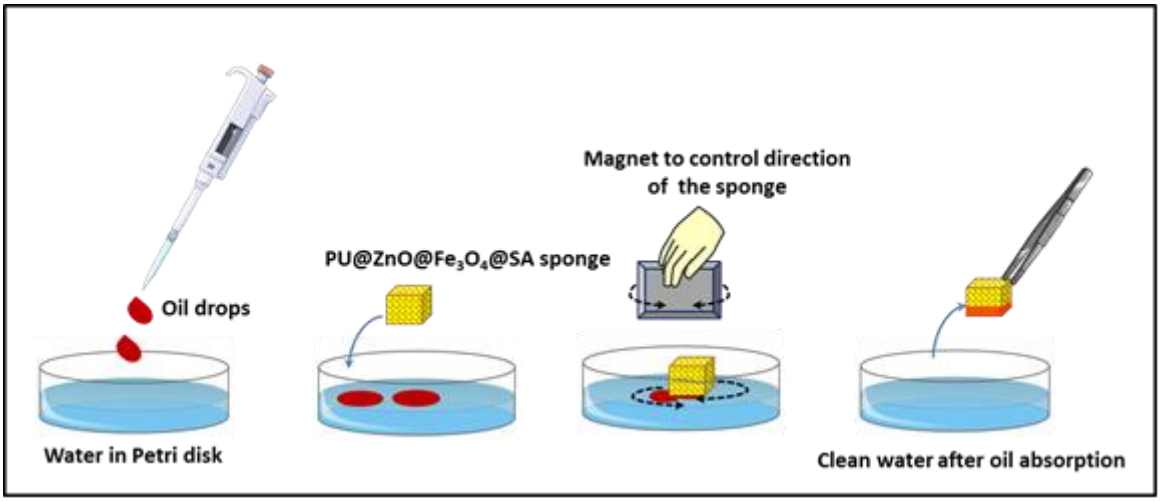

Fig.3.4. Experiment set up for floating oil absorption with a magnet

The second experiment consisted of two different tests: determination of the maximum oil absorption capacity (Fig.3.5) and the oil-water separation efficiency (Fig.3.6). Stainless-steel mesh - as a sponge holder - was fixed on a homemade tube, and then a piece of PU@ZnO@Fe_3O_4@SA sponge (diameter of 7 cm and height of 2 cm) was placed on the mesh in the tube. An immiscible oil-water mixture and a toluene-in-water emulsion were used for the separation process. The toluene-in-water emulsion was prepared with a volume ratio between oil and water of 5 % via the addition of 3 mg/mL of surfactant Tween80. The emulsion was stirred for 3 h and kept stable at room temperature for 7 days. For the maximum absorption capacity analysis (Fig. S6), oil drops were slowly dropped onto the sponge, and the oil was absorbed into the sponge until it was saturated with oil. The oil-saturated sorption state of the sponge was obtained when the sponge was completely covered with oil and no oil droplets fell onto the collecting disk underneath. The

maximum oil absorption capacity (k) of the sponge was calculated by the weight-gain ratio, as shown in equation (3.1):

$$k = \frac{W_a - W_b}{W_b} \quad (g/g) \ (3.1)$$

where W_a is the weight of the sponge in the oil-saturated state and W_b is the weight of the sponge in the initial state.

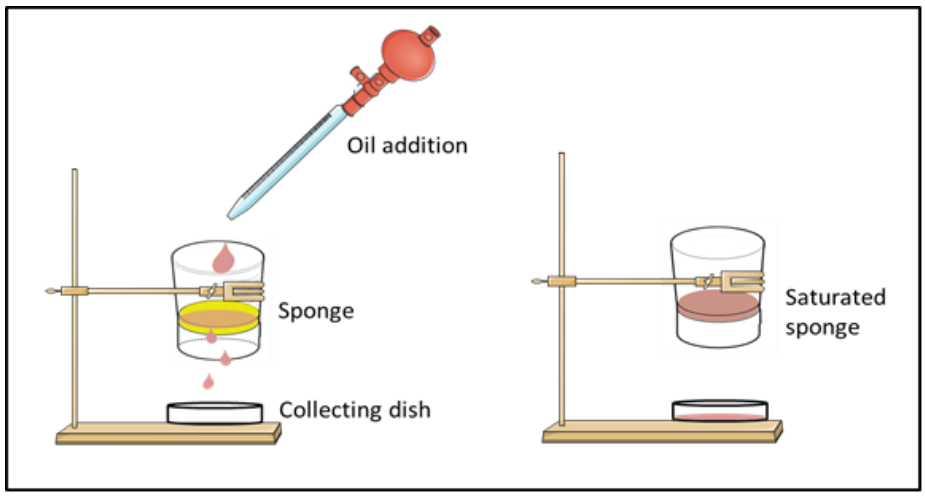

Fig.3.5. Experiment set up used to determine the sponge's maximum oil absorption capacity

For the separation efficiency analysis (Fig. 3.6), a mixture of oil and water (50 %, v/v) or emulsified oil in water in a beaker was poured directly into the sponge surface, and another beaker was placed underneath to collect the excess oil after saturation. The water was repelled from the sponge surface while the oil was absorbed into the sponge. Then, the excess oil after saturation fell into the collection beaker underneath. After the full volume of the oil-water mixture was poured onto the sponge, the remaining water layer (oil free as determined by UV-Vis spectroscopy) on the sponge surface was collected merely by pouring into another beaker for volume measurement. The repellent ratio of water or oil-water separation efficiency was determined according to equation (3.2):

$$\text{Separation efficiency} = \frac{V_a}{V_b} \times 100 \ \% \ (2)$$

where V_a is the volume of the collected water remaining on the sponge surface after pouring the oil-water mixture and V_b is the volume of water in the initial mixture with oil before the mixture was poured onto the sponge.

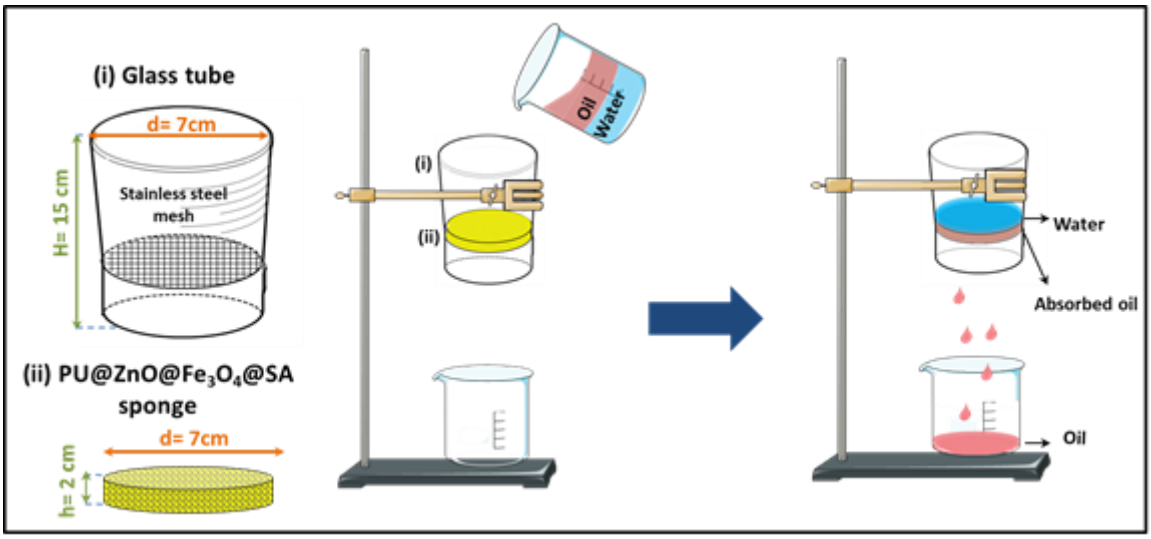

Fig.3.6. Oil-water separation experiment design

3.2.5. Stability and reusability tests

The mechanical stability of the material plays an important role in real applications. Thus, mechanical stability tests were carried out on the PU@ZnO@Fe_3O_4@SA sponge. An ultrasonic rinse test (D1), an abrasion test with 1000-grit mesh sandpaper (D2), a wringing out by hand test (D3) and a compression test with a stress level of 0.000600 MPa at 80 % strain (D4) were carried out to test the adhesion between the coated materials and the PU sponge. The details and digital images of these experiments are presented in Fig.3.7.

The recyclability of the PU@ZnO@Fe_3O_4@SA sponge was tested by a simple method. After oil-water separation, the contaminated sponge was squeezed and rinsed with alcohol and water to remove the absorbed oil. Subsequently, the cleaned sponge was oven dried at 50 °C for 12 h and then used for the next 100 cycles.

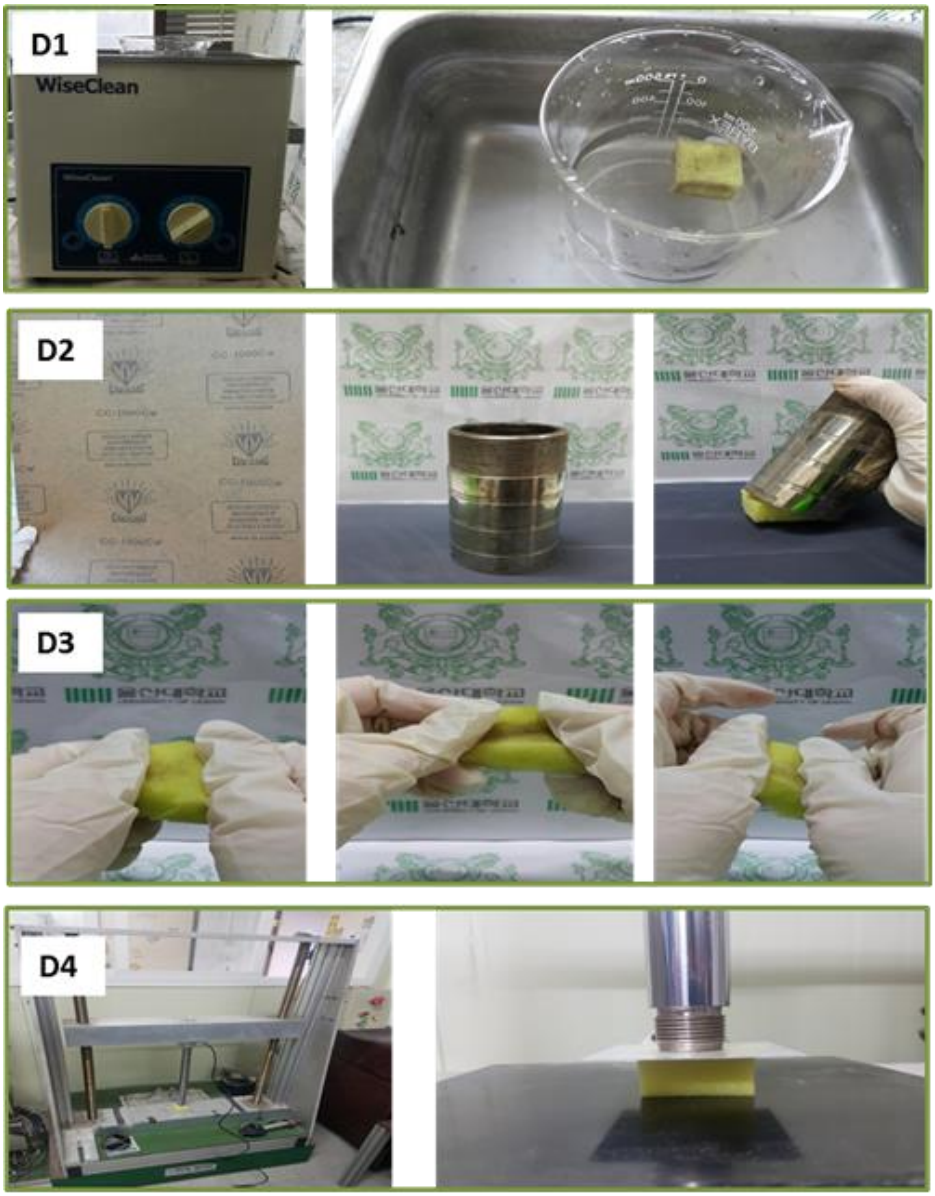

Fig.3.7. Mechanical stability tests for PU@ZnO@Fe_3O_4@SA sponge samples

3.3. Characterizations of superhydrophobic PU sponge

3.3.1. Surface morphology

The surface roughness is the first factor that should be considered in achieving a robust superhydrophobic state. Before modification, the PU substrate had a three-dimensional porous structure with a relatively smooth surface and an open cell structure (Fig.3.8 (a)). As described

above, in the first step of the modification process, ZnO was grown on the original PU sponge to afford a PU@ZnO sponge. In this step, high-density ZnO flakes were deposited on the PU substrate, which roughened the surface of the PU scaffold (Fig.3.8 (b)). This fabrication method, performed with a commercial microwave oven, was very useful for forming a relatively uniform ZnO structure on the PU surface. Furthermore, the use of a commercial microwave as the heating source to grow the structured ZnO shortened the fabrication time, reduced the specific equipment requirement and lowered the energy usage, thus rendering it an eco-friendly fabrication method.

In addition to the surface roughness, the chemical hydrophobicity of the material is an equally important factor. Our aim was to achieve a superhydrophobic material. Thus, SA was chosen to modify the sponge because it is a low surface energy material. After treatment with SA@Fe_3O_4-ethanol and SA-ethanol solutions, a PU@ZnO@Fe_3O_4@SA sponge was obtained (Fig.3.8 (c)). By adding Fe_3O_4 particles, the fabricated sponge was imparted with magnetically responsive properties, which is helpful for applications in floating oil absorption. The SA molecules formed a dense self-assembled monolayer on the ZnO surface as a result of the strong chelating bonds formed between the carboxylates and Zn atoms on the surface [82]. Therefore, the structure of the ZnO layer could no longer be clearly observed due to the fatty acid top-coating layer. Nevertheless, the achieved roughness of the PU@ZnO@Fe_3O_4@SA surface (Fig.3.8 (c)) was still much higher than that of the untreated PU sponge (Fig.3.8 (a)). This roughness was beneficial not only for imparting superhydrophobicity but also for increasing the surface area contact with oil, which improved the oil affinity of the material. The addition of Fe_3O_4 particles could not be observed in the SEM image due to their random deposition. However, the presence of the particles was confirmed by other analysis techniques, including mapping, XPS and XRD. The typical X-ray mapping results presented in Fig.3.8 (d) provided information about the elemental distributions in the samples. The distributions of carbon (original content of the PU sponge), oxygen, zinc and iron on the material surface were uniform, which further supports the presence of the desired components on the fabricated material.

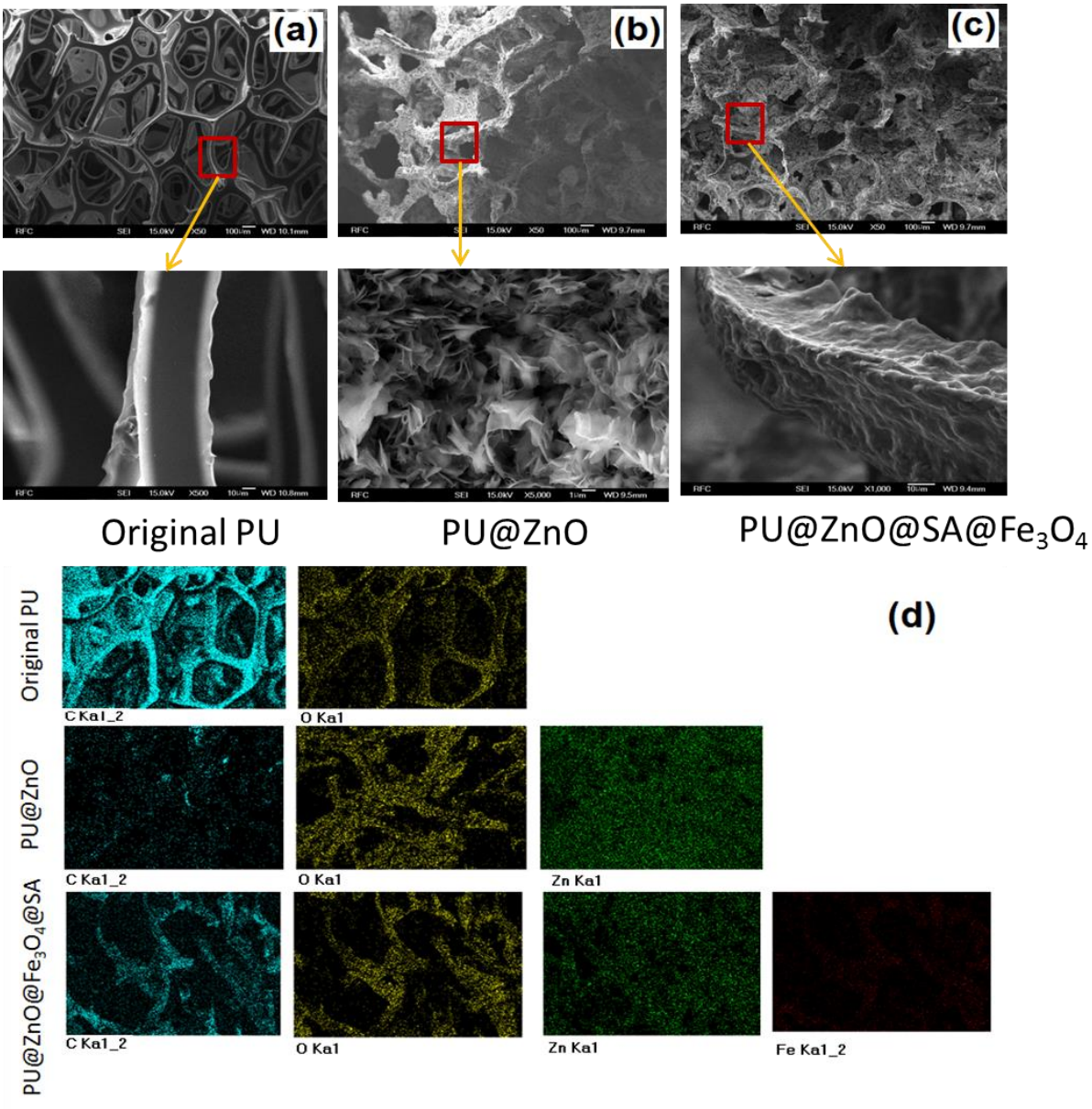

Fig.3.8. SEM images of (a) the original PU, (b) PU@ZnO, (c) PU@ZnO@Fe_3O_4@SA, and (d) mapping images of these sponges

The initial porosity of reticulated foams is critical when designing a custom component or product. The term "porosity" is evaluated by the pores per inch (PPI) value [83, 84], which is designated as the number of pores in one linear inch. The calculated PPI value of the original PU was approximately 60, corresponding to homogenous and uniform cells. The inspection of Fig.3.9 revealed that the pore sizes and PPI values of the sponges were not greatly changed after

modification compared with the initial values. This confirmed that the extra coating layers did not exert significant pore-blocking effects on the fabricated sponge.

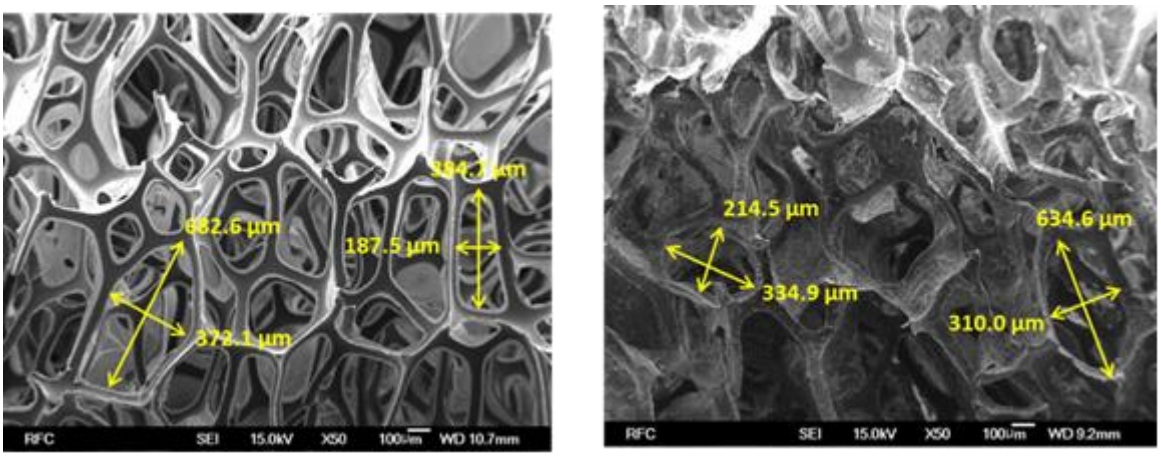

Fig.3.9. Pore sizes of original PU and PU@ZnO@Fe_3O_4@SA sponge

3.3.2. Crystalline structure and magnetic property

Fig.3.10 shows the XRD patterns of the original PU, PU@ZnO and PU@ZnO@Fe_3O_4@SA sponges. The broad peak detected in the XRD curves of all the samples indicates the low degree of crystallinity of PU. Compared to the XRD pattern of the original PU, the XRD patterns of PU@ZnO and PU@ZnO@Fe_3O_4@SA contain additional peaks at 2θ = 32.01°, 34.17°, 36.20°, 47.35°, 56.62°, 62.92°, 66.36°, 68.03° and 69.09°. These peaks correspond to the structure of ZnO according to the values of the Joint Committee on Powder Diffraction Standard (JCPDS) No. 36-1451 [73, 80, 81]. Characteristic peaks at 2θ = 30.1°, 43.1° and 53.5° are observed in the PU@ZnO@Fe_3O_4@SA sponge sample. These peaks fit well with the Fe_3O_4 patterns (JCPDS No.65-3107) reported in previous studies [85, 86]. The absence of any signals of impurities in the XRD patterns confirms the high purity level of the fabricated samples.

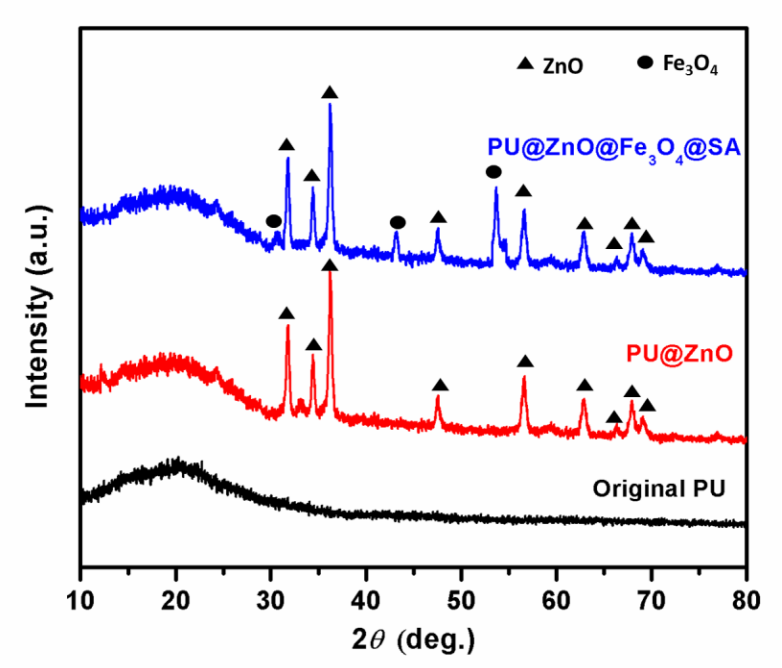

Fig.3.10. XRD pattern of sponges samples

Fig.3.11 shows the magnetic hysteresis loops of the fabricated sponge samples. The PU@ZnO@Fe_3O_4@SA sponge became magnetic with a saturation magnetization following the addition of Fe_3O_4 particles, and this magnetic property was still maintained even after 100 cycles. These results showed that the magnetic strength of the fabricated sponge was sufficient for it to be easily manipulated and guided by a magnet for the treatment of oil floating on the water surface.

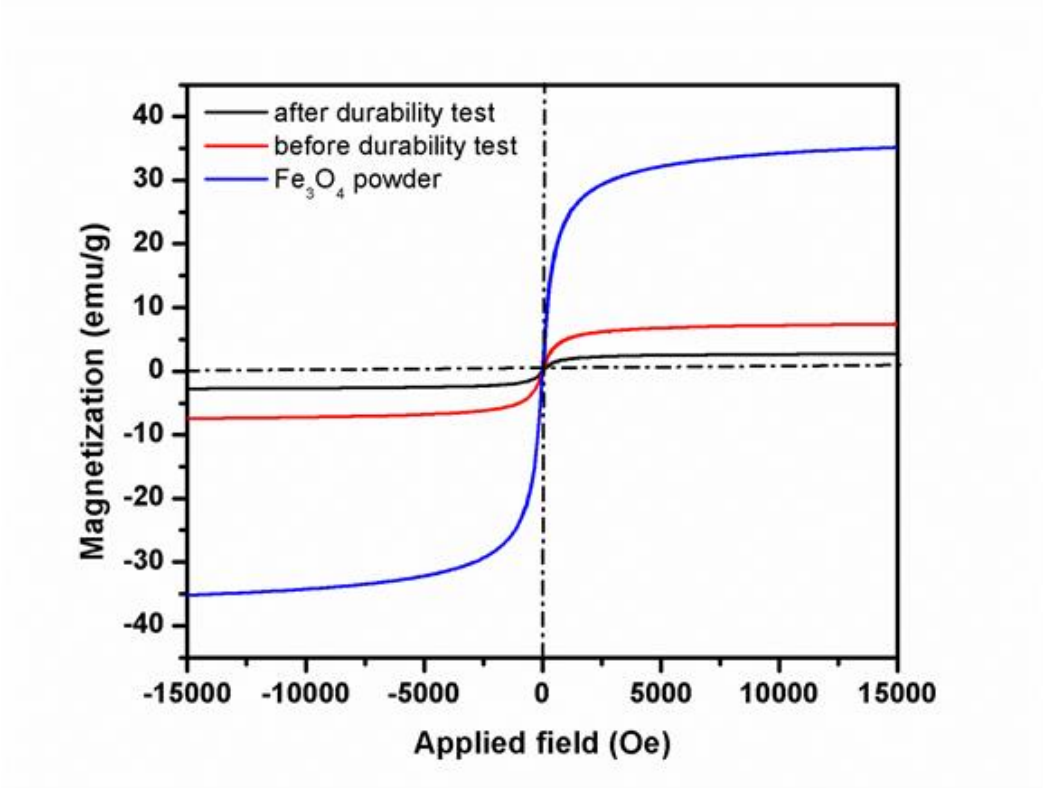

Fig.3.11. Magnetization curves of Fe_3O_4 and sponge samples

3.3.3. Elemental composition

FT-IR spectroscopy was used to investigate the possible interactions between the surface of the original sponge and the other functional groups. The FT-IR spectra of the original PU and PU@ZnO@Fe_3O_4@SA sponges are displayed in Fig.3.12. In the original PU sponge, the bands at 3340 cm^{-1} and 1541 cm^{-1} are consistent with the stretching of N-H bonds, which is consistent with the characteristic bands of urethane and urea groups [87]. The vibrations at 2970, 2931, and 2853 cm^{-1} are associated with the -CH_3 asymmetric stretching, -CH_2- symmetric stretching and -CH_2- asymmetric stretching, respectively [88]. The other characteristic bands of PU were also observed at 1718 cm-^{1}, corresponding to C=O stretching vibrations [88, 89], and 1092 cm^{-1}, corresponding to C-O-C symmetric stretching vibrations [90]. All of these characteristic peaks confirmed that the original sponge was a typical kind of PU. Compared with the original PU sponge, the peaks at 751 and 728 cm^{-1} observed for PU@ZnO@Fe_3O_4@SA were attributed to ZnO stretching modes [91-93]. In addition, the IR vibrations of -CH_3 and -CH_2- in the PU@ZnO@Fe_3O_4@SA sponge

exhibited an obvious increase in intensity and thus provide further evidence that SA was anchored on the surface of the original PU sponge.

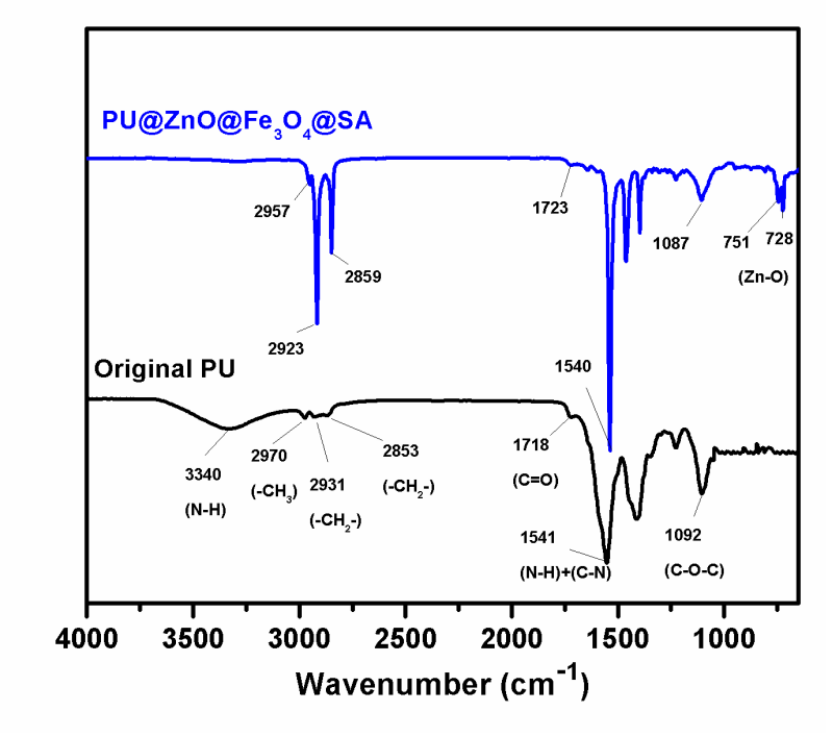

Fig.3.12. FT-IR spectra of the original PU and PU@ZnO@Fe_3O_4@SA sponges

Fig.3.13 depicts the XPS spectra of the original PU and PU@ZnO@Fe_3O_4@SA sponges. Compared with the original PU sponge, two new peaks of Zn 2p and Fe 2p appeared, and the peak intensity of C 1s clearly increased in the PU@ZnO@Fe_3O_4@SA sponge (Fig.3.13 (a)). Fig.3.13 (b) shows the corresponding C 1s XPS spectra of the sponges. The observed peaks correspond to the C-C/C-H bonds (284.23 eV), C-O/C-N bonds (285.08 eV) and O=C-O/O=C-N bonds (288.47 eV) present in both samples. The clear increase in the intensity of the C-C/C-H bonds in the modified sample is solid evidence for the presence of the long carbon chains of SA. The observation of Zn 2p and Fe 2p peaks (Fig.3.13 (c) and Fig.3.13 (d)) proves the formation of ZnO and Fe_3O_4 on the PU sponge surface. Combined with the XRD and FT-IR results, the XPS results further confirmed that the original PU sponge was thoroughly coated with a ZnO layer, a SA layer and Fe_3O_4 particles.

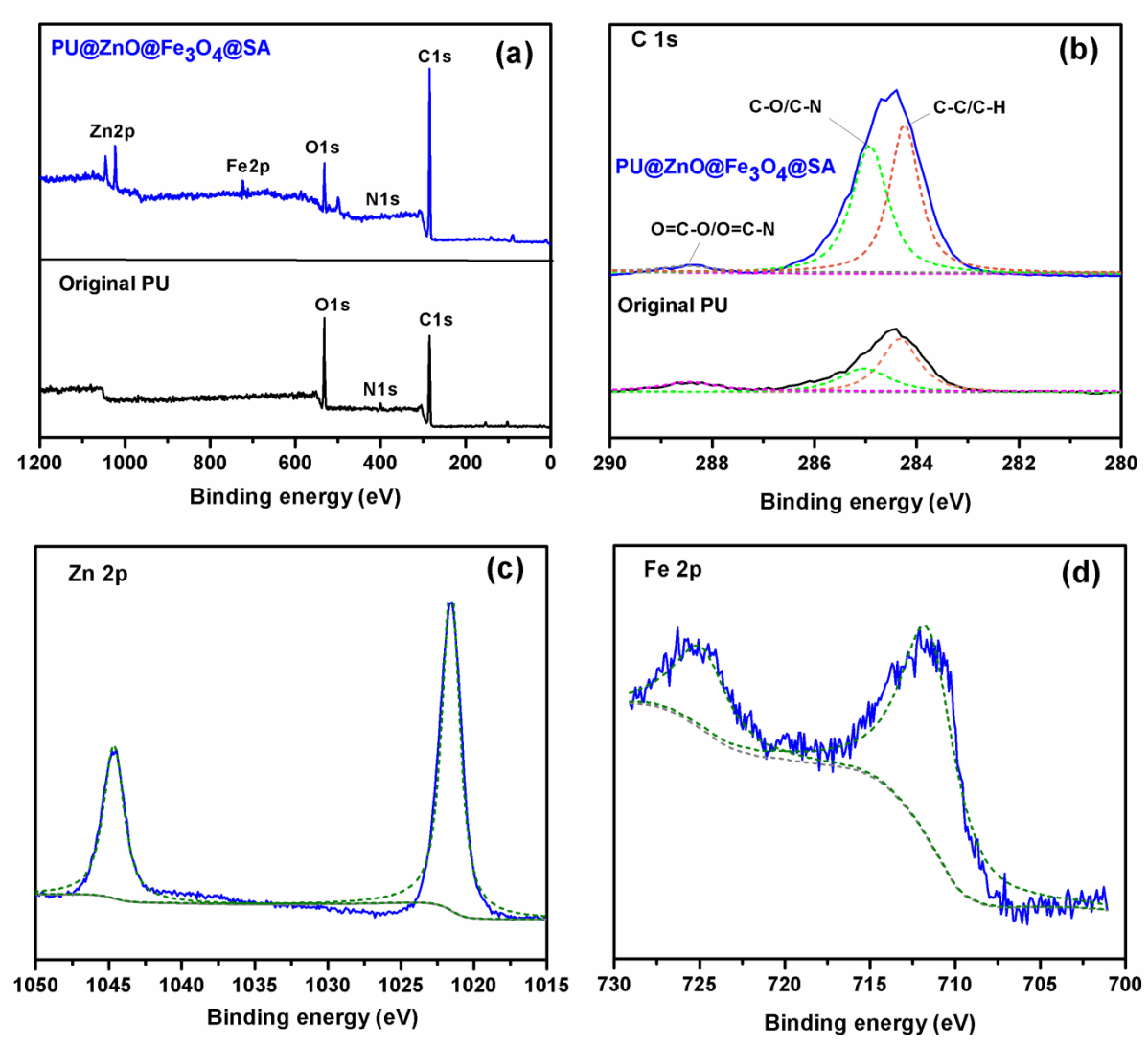

Fig.3.13. XPS data of the original PU and PU@ZnO@Fe_3O_4@SA sponges: (a) survey spectra, (b) C 1s spectra; and fitting peak of (c) Zn 2p and (d) Fe 2p spectra of the PU@ZnO@Fe_3O_4@SA sponge

3.3.4. Wettability measurement

For scientific analysis, the WCA measurement method was used to examine the surface wettability of the sponge. The static WCA measurement alone is does not provide a reliable evaluation due to the macroscopic nature of the sponge surfaces. Thus, the wettability of the sponge surface was also evaluated by dynamic WCA (including sliding WCA and shedding WCA)

measurements. Theoretically, a surface with a static WCA lower than 90° is termed a hydrophilic surface. In contrast, surfaces with static WCAs greater than 90° and 150° are called hydrophobic and superhydrophobic surfaces, respectively. Furthermore, a superhydrophobic surface also requires a dynamic WCA lower than 10°. The hydrophobicity of the surface can be attributed to two factors: the surface topography and the surface energy. We verified the role of these two factors on the wetting state of the synthesized PU@ZnO@Fe_3O_4@SA sponge by comparing the measurement results of the WCA of the following samples: (i) the original PU, (ii) PU@ZnO, (iii) PU@SA, (iv) PU@ZnO@SA and (v) PU@ZnO@Fe_3O_4@SA (Fig.3.14).

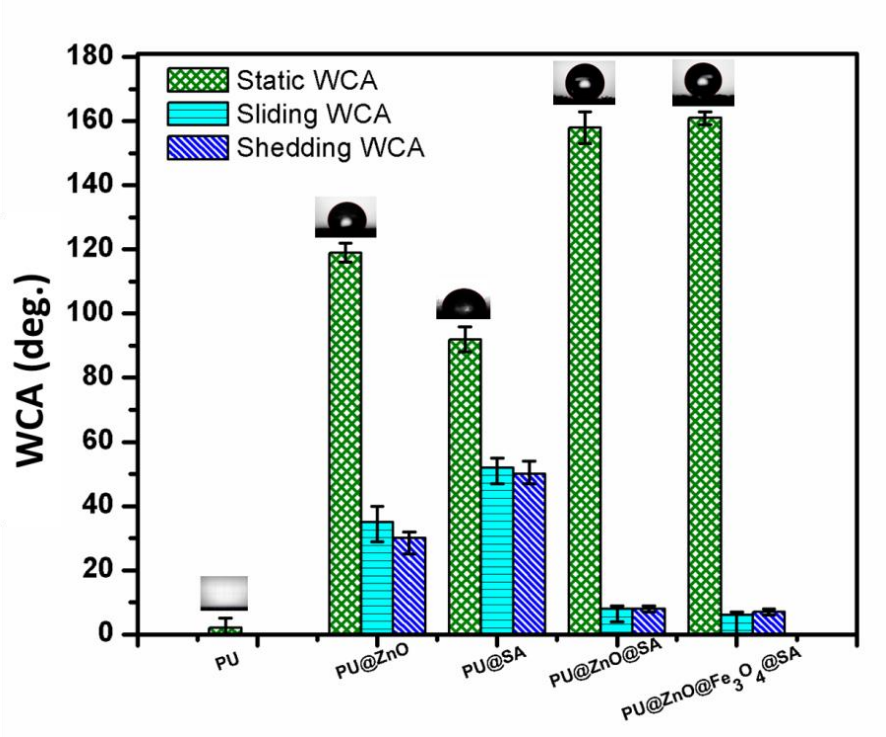

Fig.3.14. WCAs of the original PU, PU@ZnO, PU@SA, PU@ZnO@SA and PU@ZnO@Fe_3O_4@SA

The results showed that the static WCA increased from close to 0° on the original hydrophilic PU sponge surface to 119° for the PU@ZnO sponge. The Wenzel and Cassie-Baxter models, which are used to describe the wetting of a rough surface, can also be used to explain the improved static WCA for the PU@ZnO sponge. As mentioned before, after the first coating step, ZnO grew on the PU sponge surface in rough flake structures. Due to the high roughness of these structures,

air pockets are trapped in the rough cavities, which help to increase the surface hydrophobicity. On the other hand, a coating of steric acid can also increase the hydrophobicity of the PU@SA surface. The long-chain, hydrophobic alkyl groups of SA were introduced to achieve a low surface energy; thus, the static WCA of the PU@SA sample exhibited a value of 92°. However, the static WCA values of these two sponges indicated the achievement of a hydrophobic state, and a superhydrophobic state was still not attained.

The data shown in Fig.3.14 indicated that a superhydrophobic state was only attained when both ZnO and SA layers were introduced. The ZnO flakes first provided the necessary roughness features. After that, the polar, hydrophilic head of SA bound to ZnO, while the long, hydrophobic tail chain of SA was exposed outside, which induced superhydrophobicity [94-97]. The increased roughness and the lowered surface energy clearly exerted simultaneous effects on the superhydrophobic state of the sponge. The static WCAs of PU@ZnO@SA and PU@ZnO@Fe_3O_4@SA were 158° and 161°, respectively. The addition of Fe_3O_4 particles also had no significant effect on the wettability of the sponge surface. Furthermore, the dynamic WCAs of these two samples were lower than 10° (sliding WCA = 8° and shedding WCA = 7°), which strongly confirmed the excellent superhydrophobicity of the fabricated PU@ZnO@Fe_3O_4@SA sponge.

Interestingly, the fabricated PU@ZnO@Fe_3O_4@SA sponge showed both superhydrophobicity and oleophilicity properties. The wettability of the original PU sponge was completely transformed after modification. The original PU sponge was easily wetted by both water and oil drops. In contrast, water drops could not be absorbed by the PU@ZnO@Fe_3O_4@SA sponge, whereas oil could still penetrate. Based on this observation, the use of the fabricated PU@ZnO@Fe_3O_4@SA sponge for oil-water separation was proposed and is described in the next section.

3.4. Applications of superhydrophobic PU sponge

3.4.1. Anti-wetting

The wettability of the original PU was compared with that of the fabricated PU@ZnO@Fe_3O_4@SA sponges via a soaking test. The two sponges were immersed in an aqueous

solution of methylene blue dye with a concentration of 0.1 M. Fig.3.15 depicts photographs of the hydrophilic PU sponge, which quickly sank in the dye solution, while the superhydrophobic PU@ZnO@Fe_3O_4@SA sponge floated on the top of the same dye solution.

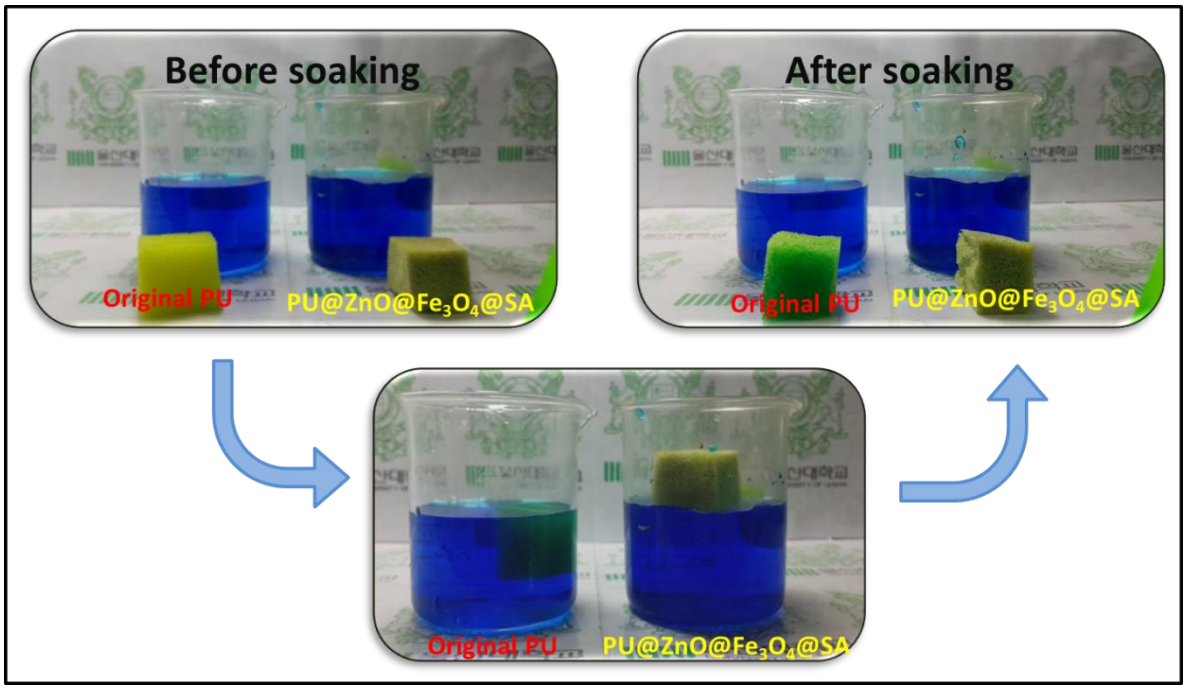

Fig.3.15. Soaking experiment with dye solution and different wetting behaviors of the original PU and PU@ZnO@Fe_3O_4@SA sponges

3.4.2. Floating oil absorption

The experiment was conducted on floating oil and is shown in Fig.3.4. By using an external magnet to place and control the direction of the fabricated sponge on the surface of the oil-water mixture, the floating oil in the polluted regions, shown in red color, was rapidly absorbed into the sponge, thereby purifying the water underneath. The sponge was removed from the solution when no sign of the dyed oil could be seen on the water surface (Fig.3.16). The absorbed oil was easily collected by squeezing due to the elasticity of the PU sponge. The proposed oil collection method is more environmentally friendly, faster and more cost efficient than other reported methods, such as burning off [65] or heat treatment [98] processes. Therefore, the fabricated sponge is applicable for oil spill cleanup.

Fig.3.16. Photographs of using PU@ZnO@Fe_3O_4@SA to remove floating oil

3.4.3. Oil-water separation

The experiments were conducted to determine the maximum oil absorption capacity, the PU@ZnO@Fe_3O_4@SA sponge showed superior performance in absorbing all seven types of oil. The maximum oil absorbency of the fabricated sponge depended mainly on the properties (density and viscosity) of the oil (Fig.3.17). For example, the absorbency of the sponge for hexane (density = 0.66 g/cm^3) was 32.01 g/g compared to 80.98 g/g for diesel (density = 0.87 g/cm^3). Furthermore, diesel has a much higher viscosity (103.90 mm^2/s) than hexane (13.10 mm^2/s), which can delay the wicking rate of oil from the sorbent surface and thus retain more oil in the porous structure of the sponge, leading to a higher k value. In the oil-water separation experiment, the oil solution was absorbed and penetrated into the sponge, whereas the water layer remained above the PU@ZnO@Fe_3O_4@SA sponge, resulting in complete oil-water separation. The separation efficiencies of the fabricated sponge were 99.89 %, 99.88 %, 99.87 %, 99.5 %, 99.2 %, 99.0 % and 98.21 % for hexane, toluene, dichloromethane, gasoline, soybean oil, diesel engine oil and vacuum pump oil, respectively (Fig.3.17). The oil absorption efficiency results, which ranged from 32.1 to 108.9, are much better than those previously reported for sponge materials (Table 3.2).

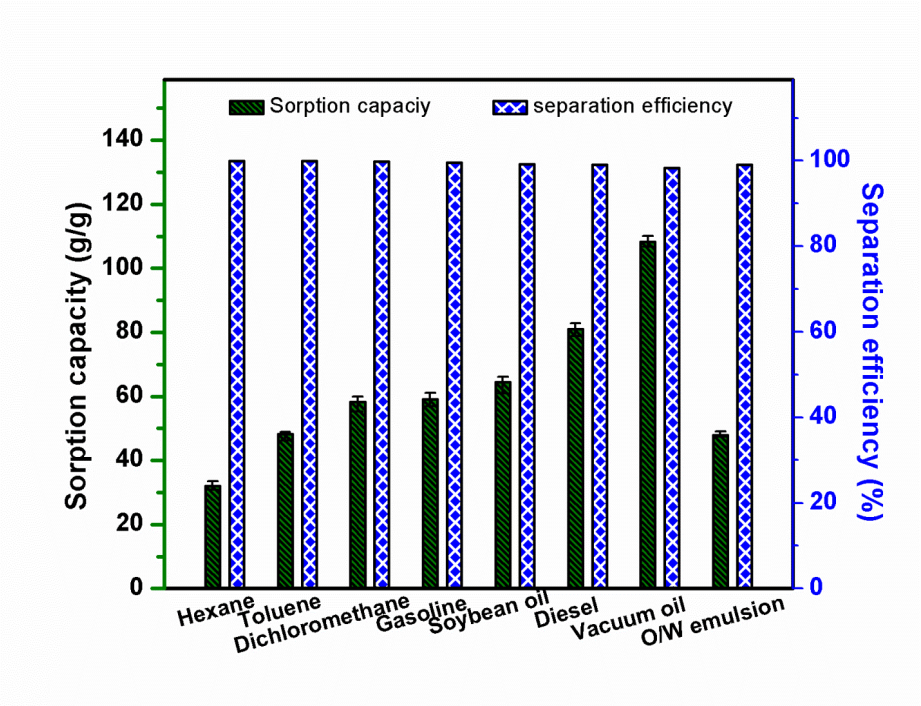

Fig.3.17. Oil absorption capacity and separation efficiency of the fabricated PU@ZnO@Fe_3O_4@SA sponge with different oils

Table 3.2. Comparison of the oil absorption capacity by sponge-based absorption materials between studies

Material	Fabrication method	Types of absorbed oil/organic solvent	Max. oil abs. cap.	Ref.
PU-IP-PA sponge	Interfacial polymerization and molecular self-assembly	Crude oil, soybean oil, dichloromethane, compressor oil, diesel oil, n-hexane	16.5 ~ 29.9	[79]
Copper-$C_{11}H_{23}COOAg$-modified PU sponge	Solution-immersion processes	Lubricating oil, octane, decane, dodecane	13 ~19	[99]
Alkyl-chain-capped TiO_2 with melamine sponge	Dipping	Methanol, ethanol, hexane, DMSO, DMF, acetone, chloroform, pump oil, motor oil	37.2 ~ 88.1	[100]
Lauryl methacrylate-modified PU sponge	Emulsifier-free emulsion polymerization and immersion	Diesel, kerosene	55.1 ~ 69.47	[101]
Mg–Al porous fiber/PU foam	Biotemplate method and foaming technology	Chloroform, soybean oil	25 ~ 43	[102]
CNT/PDMS-coated PU sponge.	Dip-coating	Soybean oil, motor oil, diesel, hexadecane, gasoline, hexane	15~25	[78]
Carbon soot-modified melamine sponge	Combustion flame process and dip coating	4-methyl-2-pentanone, cyclohexane, methanol, ethanol, hexane, toluene, crude oil, soybean oil, engine oil, pump oil	25 ~ 75	[103]
PU@PD@Ag@dodecyl mercaptan sponge	Immersion	Diesel, petrol, crude oil, soybean oil, alcohol, hexane, acetone, toluene	18~45	[104]
PU@Fe_3O_4@SiO_2@fluoropolymer sponge	Immersion	Petrol, toluene, chloroform	17~23	[27]
PU@ZnO@Fe_3O_4@SA sponge	**Microwave and dip-coating method**	**Hexane, vacuum pump oil, diesel engine oil, soybean oil**	**32.1 ~ 108.9**	**This study**

3.5. Stability and reusability of superhydrophobic PU sponge

To estimate the durability of the fabricated sponge, an ultrasonic rinse test (D1), an iterative abrasion test (D2) and a wringing out by hand test (D3) were performed. The results are shown in Fig. 3.18 (a). The superhydrophobic PU sponge retained the original shape after the durability test, and the WCA was not significantly changed after a 30 min ultrasonic rinse test and drying step (D1), an abrasion test with 2000 gr loading (D2), a wringing out by hand (D3) test and a compression test (D4). These results confirmed that the fabricated PU@ZnO@Fe_3O_4@SA sponge is robust and stable, which is advantageous for real applications.

After oil absorption, the contaminated sponge was cleaned and recycled (Fig.3.18 (b)). After 100 separation/recovery cycles, the fabricated sponge still exhibited good reusability. The sorption capacity was nearly stable after 100 cycles for hexane and after the first 50 cycles for the other oils. In the last 50 cycles, a decrease in the oil absorption capacity was unavoidable. This decrease was due to the presence of residual oil in the pores of the sponge that could not be totally removed by manual squeezing, particularly after many cycles.

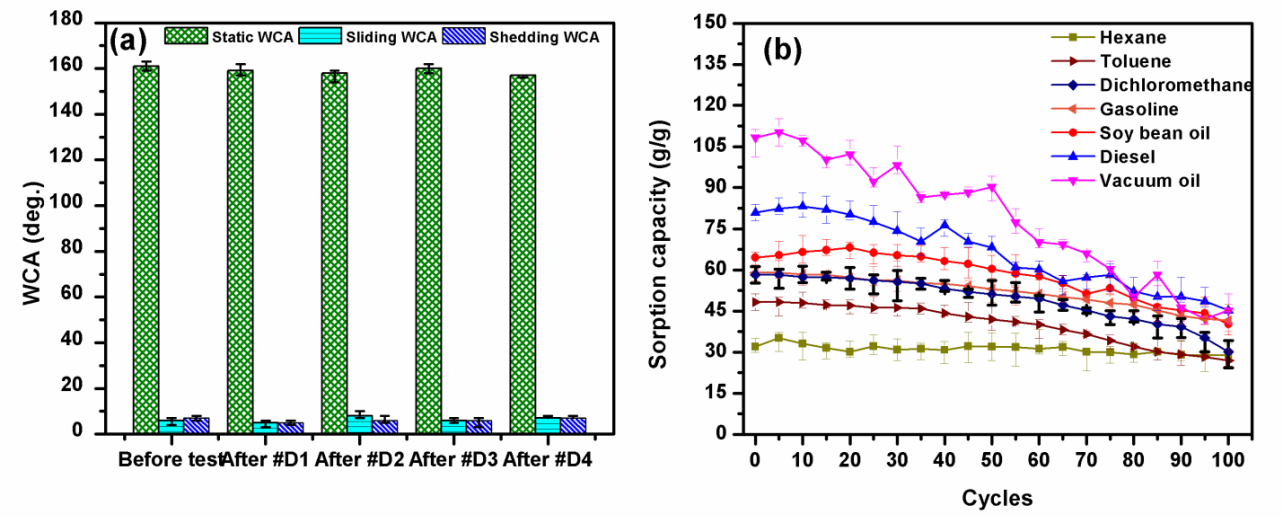

Fig.3.18. Stability and reusability of the PU@ZnO@Fe_3O_4@SA sponge for oil-water separation

3.6. Summary

In this work, we successfully fabricated a durable, magnetic and superhydrophobic PU@ZnO@Fe_3O_4@SA sponge by a novel, facile and environmentally friendly method. By mimicking nature, a PU sponge was modified with ZnO, SA and Fe_3O_4 to provide the necessary

high roughness, low surface energy and magnetic responsiveness, respectively. As a result, the fabricated sponge showed a very high static WCA (161°) and a very low dynamic WCA (sliding WCA = 7° and shedding WCA = 8°). The maximum sorption capacity of the fabricated sponge varied for the seven different oils examined (k = 32 ~ 108.9 g/g) due to the varying densities and viscosities of the oils, and these maximum sorption capacities were higher than those previously reported. The oil-water separation efficiency of the fabricated sponge exceeded 99 %, and the absorbed oil could be easily recovered by simple mechanical squeezing. In addition, the sponge could be magnetically guided to the oil-polluted area and then quickly absorb the floating oil for efficient removal. Furthermore, the superhydrophobicity and oil absorbency of the fabricated sponge were maintained after stretching, compression, cleaning and repeated sorption cycles. The novel and superior performance of PU@ZnO@Fe_3O_4@SA makes the proposed sponge a promising candidate for the separation of oily pollutants from water and the cleanup of oil spills.

CHAPTER 4

CHAPTER 4 - SUPERHYDROPHOBIC MELAMINE SPONGE

Abstract

Inspired by the nature phenomenon, novel superhydrophobic surfaces were prepared on melamine sponge (MS) base via the simple processes. In this work, MS was chosen as the substrate material to fabricate the superhydrophobic surface. We present a facile, cost effective and environmental friendly method to fabricate 3 types of robust superhydrophobic MS with excellent oil-water separation capacity and exceptional recyclabilityAfter the in-situ coating structured ZnO layer on MS surface to generate the surface roughness, the hydrophobization was conducted with the utilizations of (i) stearic acid (SA), (ii) 1H,1H,2H,2H-perfluorodecyltriethoxysilane (FDTS) and (iii) the mixture of SA@FDTS. It is confirmed that superhydrophilic MS has been easily turned to superhydrophobic due to two main factors: the surface roughness and the addition of the long carbon chain and/or perfluoroalkyl chain from the structure of SA and FDTES. As the results, the static water contact angle (WCA) of $159^o \pm 2^o$, $160^o \pm 2^o$ and $173^o \pm 2^o$ were exhibited for MS@ZnO@SA, MS@ZnO@FDTS and MS@ZnO@SA@FDTS samples, respectively. The novel MS@ZnO@SA, MS@ZnO@FDTS and MS@ZnO@SA@FDTS superhydrophobic sponges possessed many of the crucial properties of an ideal sorbent material for oil-water selective separation with extremely high separation capacity, stable under the mechanical tests, outstanding recyclability with sorption capacity retention after several cycles of sorption - squeezing process, being inexpensive, and wide availability. It is assert that such sponges are promising sorbent materials for oil spill containment and environmental remediation.

Keywords: melamine sponge, ZnO, stearic acid, 1H,1H,2H,2H-perfluorodecyltriethoxysilane,, superhydrophobic, separation

4.1. Introduction

As presented in previous chapters, control the wettability of solid surfaces, especially the conversion from hydrophilic to hydrophobic/superhydrophobic state, has recently considered as an interesting subject due to its importance in theoretical research and practical applications.

In this work, MS was chosen as the substrate material to fabricate the superhydrophobic surface. We present a facile, cost effective and environmental friendly method to fabricate 3 types of robust superhydrophobic MS with excellent oil-water separation capacity and exceptional recyclability. The pristine MS was first coated by ZnO layer in order to enhance the surface roughness. Subsequently, the superhydrophobic MS sponges were obtained after superhydrophobization step with the use of stearic acid (SA), 1H, 1H, 2H, 2H-perflourodecyltriethoxysilane (FDTS) and the mixture of SA@FDTS. The MS@ZnO@SA, MS@ZnO@FDTS and MS@ZnO@SA@FDTS sponges were obtained the superhydrophobic state with very high static water contact angle (WCA) and low sliding WCA. They could be used to selective separate oil and water effectively with extremely high separation efficiency. The fabricated superhydrophobic sponges were also carefully characterized in order to explain the mechanism of superhydrophobicity state and oil-water separation capacity. Moreover, the durability and recyclability of the fabricated sponge were also evaluated. Our novel materials may provide a facile but very effective strategy for separating oil-water mixtures in the real applications.

4.2. Materials and experiments

4.2.1. Materials

Commercial melamine sponge (MS) was purchased from a local store in Ulsan, Republic of Korea. Zinc acetate($Zn(CH_3COO)_2$), ammonium hydroxide solution 25% (NH_4OH) and stearic acid (SA) were supplied by Daejung Chemicals & Metals Co., Ltd., Korea. 1H, 1H, 2H, 2H-perflourodecyltriethoxysilane (FDTS) was obtained from Sigma-Aldrich Co. LLC. The information of organic solvents/oils used for separation experiment was summarized in the following table.

Table 4.1. List of the organic solvents and oils used in separation tests

Name	Manufacturer	Specification
Methanol	Daejung Co.Ltd., Korea	Pure 99.00 %
Hexane	Samchun Chemical, Korea	Pure 99.99%
Vacuum pumping oil	Moresco, Japan	NEOVAC MR-200
Gasoline	SK Energy, Korea	Commercial product
Canola oil	Ottogi Ltd, Korea	Canola extraction
Diesel	SK Energy, Korea	KIXX HD1 Cl-4/SL 15W-40

4.2.2. Fabrication of superhydrophobic MS

Pristine MS pretreatment: The pristine MS was cut into 3 × 3 × 3 cm blocks and cleaned with distilled water and ethanol for several times to remove impurities on the surface. After that, the sponge blocks were naturally dried in room condition at 25 ^{o}C.

Fabrication of ZnO layer on MS surface: MS@ZnO was fabricated via microwave method according to the previous work [105].A $Zn(CH_3COO)_2$ solution (0.2 M) was prepared, and NH_4OH droplets were dropped slowly in it with gentle stirring until the mixture solution become transparent. After that, the MS blocks were immersed into the prepared mixture solution of $Zn(CH_3COO)_2$ and NH_4OH for 30 min. The beaker containing MS blocks and mixture solution was then put onto a commercial microwave oven (Daewoo KR-G20EW, 1120 W, 2450 MHz) and heated for 3 times (each time include 60 s heating and 15 s stop). Subsequently, the beaker was cooled down in room temperature for 10 min, and the MS@ZnO sponge blocks were taken out from the solution, cleaned with water/ethanol and naturally dried. A possible formation mechanism of ZnO rods on MS surface was proposed (Eq. (4.1)-(4.4) [105].

$$Zn(NH_3)_4^{2+} + 2\ OH^- \rightarrow Zn(OH)_2 + 4\ NH_3 \quad (4.1)$$

$$Zn(NH_3)_4^{2+} + 2\ OH^- \rightarrow ZnO + 4\ NH_3 + H_2O \quad (4.2)$$

$$Zn(OH)_2 + 2\ OH^- \rightarrow Zn(OH)_4^{2-} \quad (4.3)$$

$$Zn(OH)_4^{2-} \rightarrow ZnO + H_2O + 2\ OH^- \quad (4.4)$$

Superhydrophobization of MS@ZnO: 100 mL of SA and FDTS in ethanol solutions were prepared in two different beakers at concentration of 10 mM and 5 mM, respectively. A mixture of 90 mL SA (10mM) and 10 mL FDTS (5mM) was also prepared in another beaker. Then, the MS@ZnO sponges were immersed in the beakers for 5 min and the derived MS@ZnO@SA, MS@ZnO@FDTS and MS@ZnO@SA@FDTS sponges were taken out and naturally dried. The SA, FDTS or their combination were grafted onto the ZnO rough layer to obtain the superhydrophobicity and the whole fabrication processes were illustrated in Fig.1.

4.2.3. Characterization methods

Scanning electron microscopy (SEM) characterizations were carried out in order to observe the morphology of materials. A JOEL JSM-7600F field emission scanning electron microscope apparatus was used at acceleration voltage of 10 kV. The crystalline phases in samples were determined by using an X-ray diffractometer (XRD Bruke AXS D8 ADVANCE). XRD data collection was performed using Cu-Kα (λ = 0.154060 nm) radiation (step size of 0.02°; 2θ angular range = 10°-80°). The chemical composition of sponge samples was investigated by using an X-ray photoelectron spectrometer (XPS K-alpha ThermoFisher) and Fourier-transform infrared spectroscopy (FT-IR Varian 670/620). The wettability of all samples was analyzed by using a contact angle meter (SmartDrop, Femtofab Co. Ltd., Korea). The static WCA and sliding WCA were measured three times for each sample using a 10 μL water droplet.

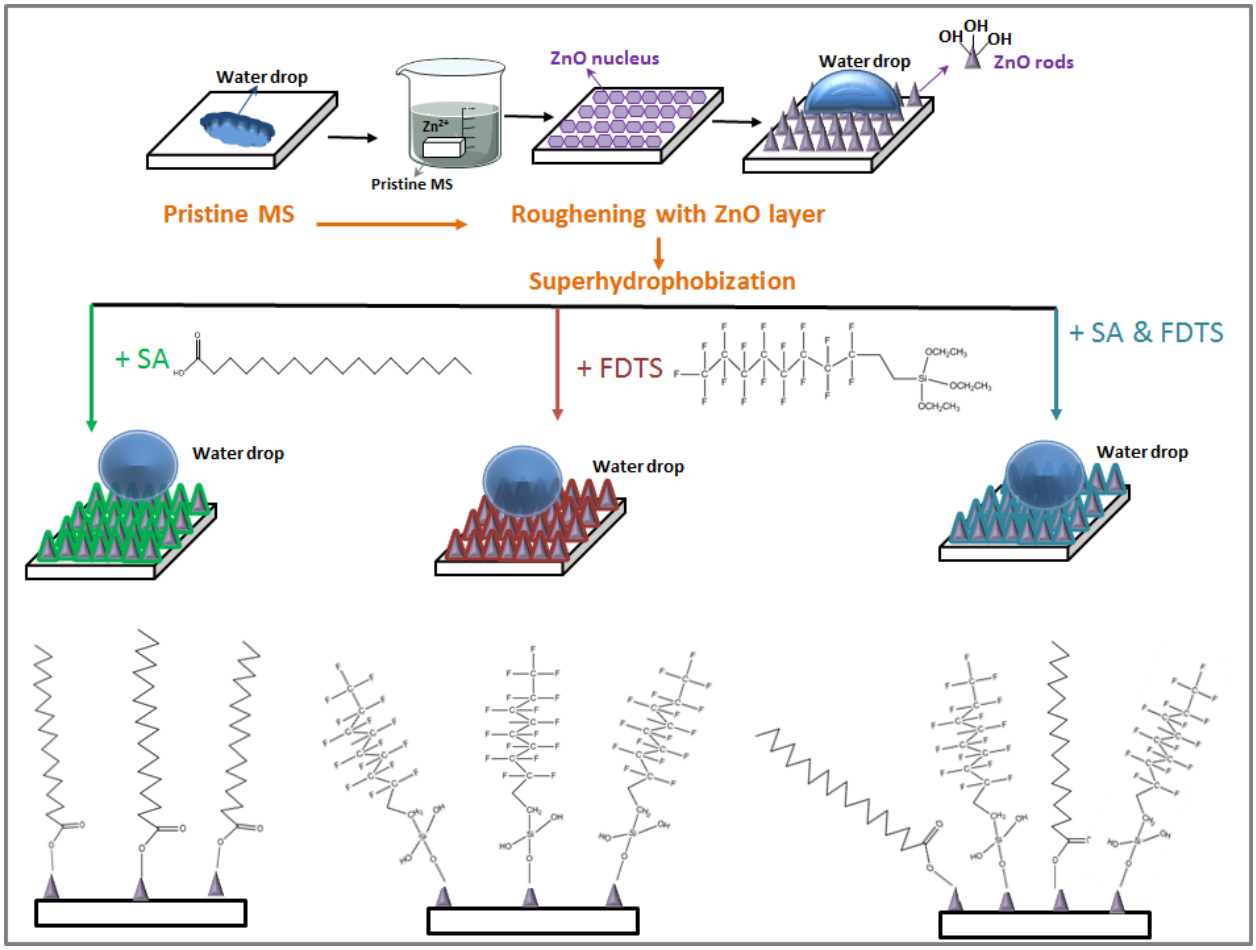

Fig.4.1. Fabrication processes for superhydrophobic MS@ZnO@SA, MS@ZnO@FDTS and MS@ZnO@SA@FDTS sponges

4.2.4. Oil-water separation experiment

The oil-water separation experiments were carried out with a home-made system which is illustrated in Fig.4.2. The sponge sample was put on the tubes with a diameter of 7 cm. A piece of stainless steel mesh, used as the stopper to keep the sponge sample, was fixed on the tube. The oil-water mixture (50%, v/v) was poured into the sponge. The oil would quickly penetrate through the sponge and drop to a cylinder placed at the bottom. The volume of water before and after the separation was measured as V_0 and V_1, and the separation efficiency (k) was calculated as the following equation (Eq. (4.5)):

$$k = V_1/V_0 \times 100\% \qquad (4.5)$$

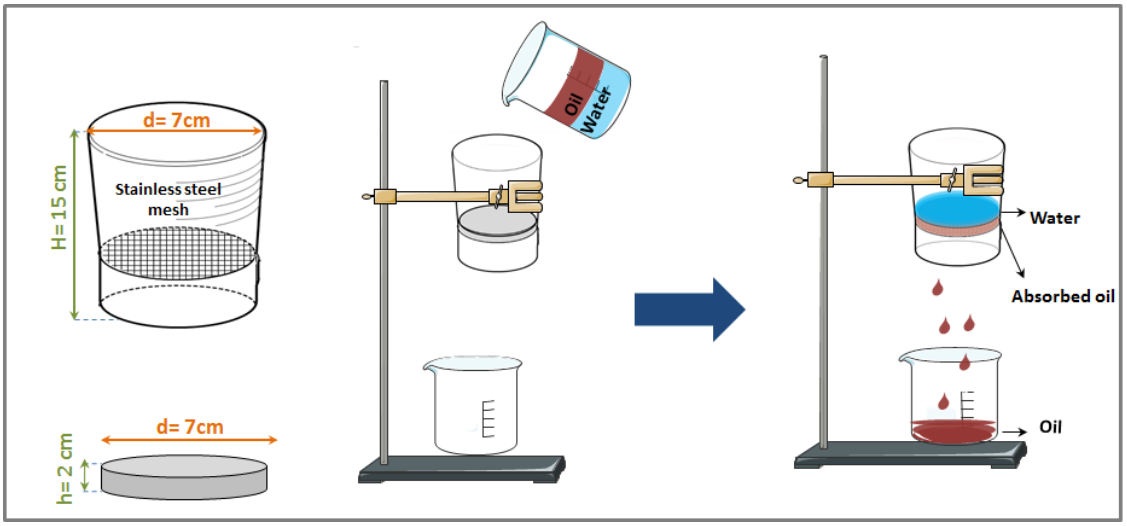

Fig.4.2. Set up for oil-water separation experiments

4.2.5. Stability and reusability tests

The mechanical stability of the material plays an important role in real applications. Thus, mechanical stability tests were carried out for the fabricated sponges. The mechanical testing equipment (Daekyung DTU-900MH300kN) was used to do the stability tests with the fabricated sponges. Due to the porous and spongy structure of the material, the compression test mode is chosen. The recyclable property of the fabricated sponges was also tested by a simple method. After the oil-water separation, the contaminated sponges were manual squeezed and then applied for the next cycles.

4.3. Characterizations of superhydrophobic MS

4.3.1. Surface morphology

The topography of surface is the first significant factor to the wettability of material. Thus, the morphological information of pristine and modified sponges were carefully investigated by SEM and illustrated in Fig. The starting material is commercially MS, which is widely used for various functions in daily life. The porous and 3Dtextures of MS can provide more contact area for the oil sorption. As shown in Fig.a, the pristine MS have three-dimensional (3D) interconnected network and the surface morphology of each skeleton fiber was smooth and even.

In contrast, MS@ZnO@SA, MS@ZnO@FDTS and MS@ZnO@SA@FDTS sponge samples with the coating layers showed a highly rough surface (Fig. b-d). In general view, the skeleton structure of the modified sponges was not changes as compared with the pristine MS. The biggest changes were the roughness of the sponge fibers - which was created by the ZnO rods. The uniform ZnO micro rods (with average length 5-7 µm of and diameter of 1-1.5 µm) were grown using a facile microwave method [73]. Compared to other synthesis methods, the microwave method was much simpler and quicker to operate [73, 105]. The changes on the surface roughness of MS was helpful for achieving the superhydrophobicity due to the air trapped among the rough structures [106].

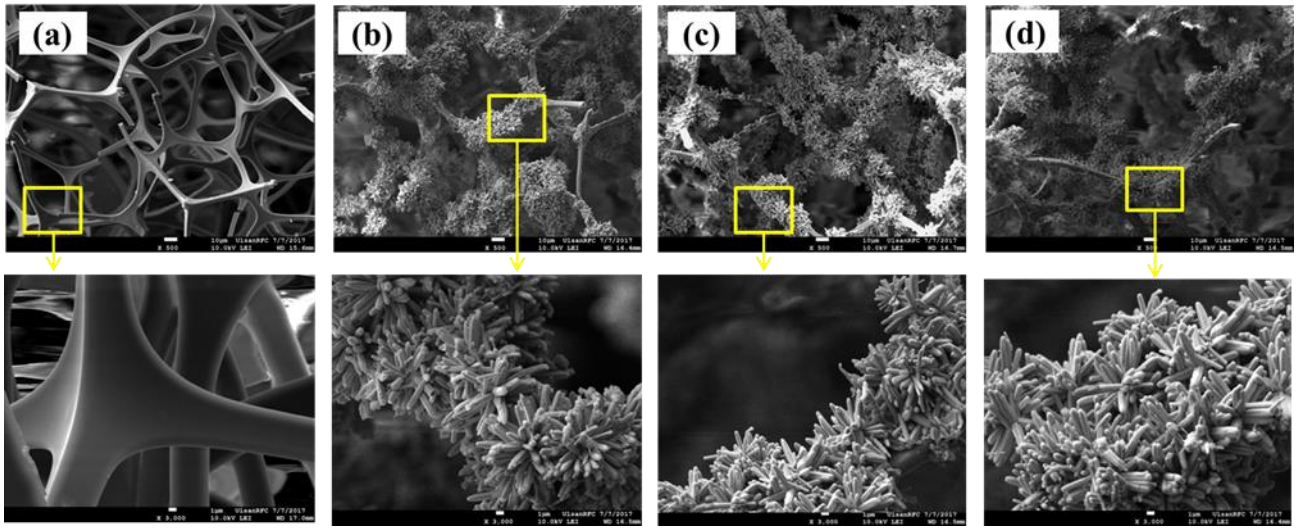

Fig.4.3. SEM images of (a) pristine MS, (b) MS@ZnO@SA, (c) MS@ZnO@FDTS and MS@ZnO@SA@FDTS sponges

4.3.2. Crystalline structure

The XRD patterns of the modified sponges were examined to gain more insight on the existence of ZnO component as shown in Fig. It is clearly seen that crystalline ZnO are present in all modified sponge samples with the sharp and strong characteristic peaks at 2θ = 32.00°, 34.15°, 36.13°, 47.48°, 56.61°, 62.93°, 68.20° and 69.03°. In the MS@ZnO@SA and MS@ZnO@SA@FDTS, the characteristic peaks of SA also deserved at 2θ = 11.01°, 20.48°, 21.55°, 23.98°. All these diffraction peaks of ZnO were indexed to the values of the Joint Committee on Powder Diffraction Standard (JCPDS) No. 36-1451 [105]. Combine with the

SEM results, the presence of these diffraction patterns are indications that the structured ZnO were successfully collated on the pristine MS.

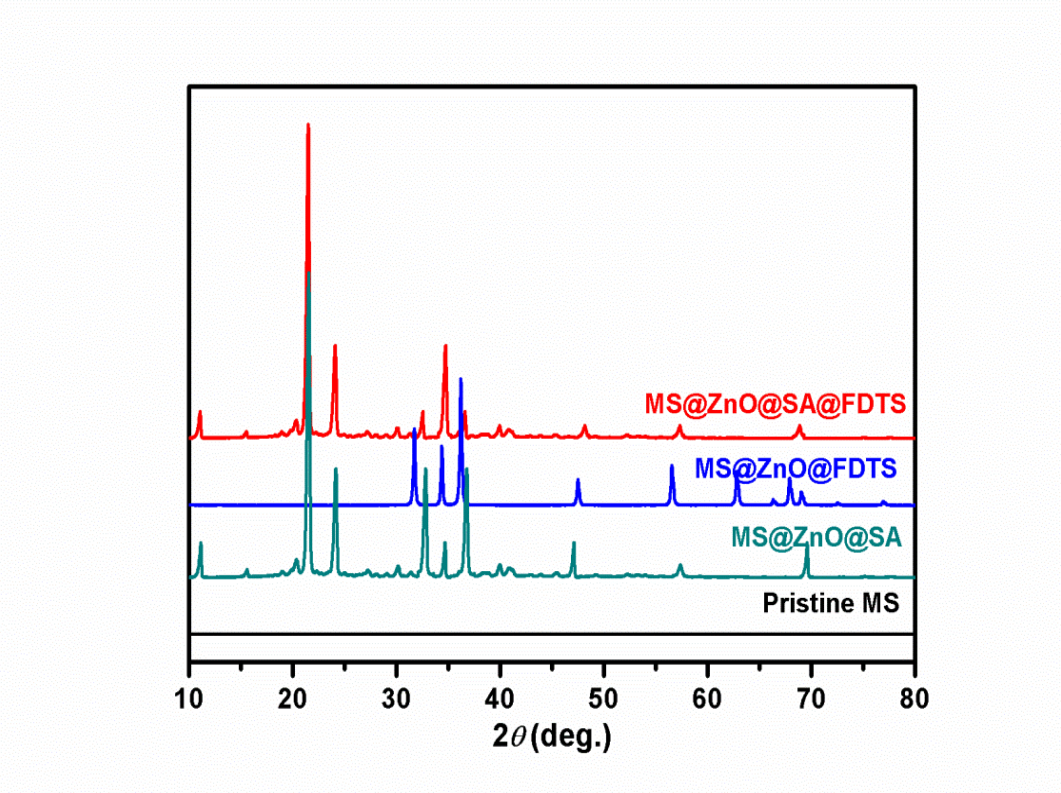

Fig.4.4. XRD patterns of pristine MS and MS@ZnO@SA, MS@ZnO@FDTS and MS@ZnO@SA@FDTS sponges

4.3.3. Elemental composition

The IR spectra of sponge samples are shown in Fig.4.5 (a) The main chemical structure of MS is aromatic ring containing three carbon atoms and three nitrogen atoms and each carbon atom is bonded with three high polar functional groups NH_2 [14]. Each aromatic ring is either connected by O-C or C-C bond. Thus, in all of the spectra, the absorption peaks at 3100-3400 cm^{-1} attributed to the stretching vibrations of secondary amine (N–H) on the surface of MS were observed. The absorbance at 1450-1650 cm^{-1}, 1330 cm^{-1} - 1400 cm^{-1}, 1120 cm^{-1} and 1066 cm^{-1} corresponding to the C=N, C-N, C-O-C and C-O stretching also presented in all of the spectra, respectively. These absorptions band are consisted with typical bond of pristine MS. After the superhydrophobization with SA and mixture of SA@FDTS, the vibrations at 2931, and 2853 associated with the $-CH_2-$ symmetric and asymmetric stretching were clearly observed. These IR vibrations of $-CH_3$ and $-CH_2-$ in the MS@ZnO@SA sponge exhibit an

obvious increase in intensity indicate the introduction of long-chain hydrocarbon in SA formula. Besides, C–F bond stretching could be observed in range of 1150-1250 cm^{-1} which confirmed the presence of silanol groups on the MS@ZnO@FDTS and MS@ZnO@SA@FDTS samples.

XPS analysis was further carried out to understand the chemical composition of sponge samples. Fig.4.5 (b) shows the XPS survey spectrum of the pristine MS sponge, which revealed the different peaks from different elements, including C, N and O. This was consistent with the composition of commercial foams containing the formaldehyde-melamine-sodium bisulfite copolymer. After the modifications, the formation of the ZnO layer on the sponge skeletons was confirmed by the peaks of Zn 2p on the spectrums. After the superhydrophobization with SA, the peak intensity of C 1s was increased in sample MS@ZnO@SA. Similarly, after the superhydrophobization with FDTS and SA@FDTS, the peaks of F 1s ans Si 2p were observed. These FTIR and XPS observations confirmed chemically that the as-described treatments were conducted successfully.

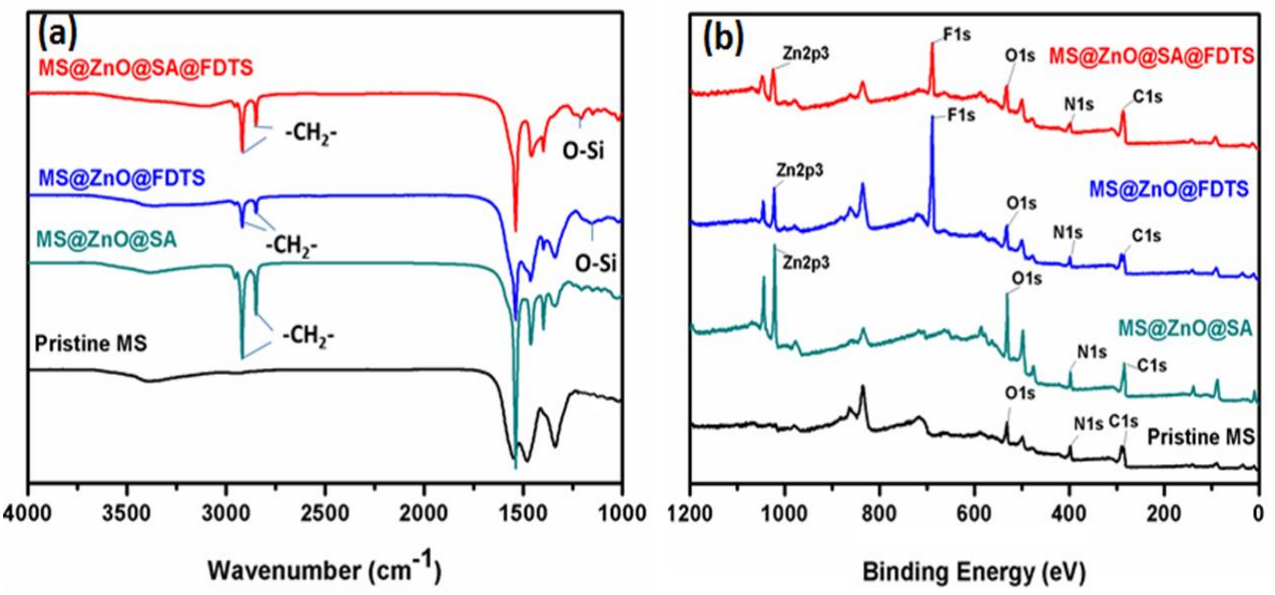

Fig.4.5. FTIR and XPS spectra of pristine MS and modified MS samples

4.3.4. Wettability measurement

Based on the described fabrication process, it is expected that the MS@ZnO@SA, MS@ZnO@FDTS and MS@ZnO@SA@FDTS sponges could own the superhydrophobic ability. As mentioned before, the successfully superhydrophobic surface was attributed to the

rough surface and chemical composition. After reaching the hydrophobic state with rough coating layer, the chemical coating would determine whether the sponge surface is "super"-hydrophobic or not. In the other words, the chemical composition could amplify the surface's hydrophobicity. Thus, after the superhydrophobization process with SA, FDTS and SA@FDTS, the water droplets on the surface of MS@ZnO@SA, MS@ZnO@FDTS and MS@ZnO@SA@FDTS sponges exhibited the spherical shape or even bounced (bouncing effect) from the surface, indicative the excellent superhydrophobicity. To verify the surface wettability, the WCA measurements were carried out in order to check the water wettability of sponge samples. After the MS@ZnO was treated with SA, FDTS and mixture of SA@FDTS, the static WCA was reached up to 159^o ± 2^o, 160^o± 2^o and 173^o± 2^o, respectively (Fig.4.6).

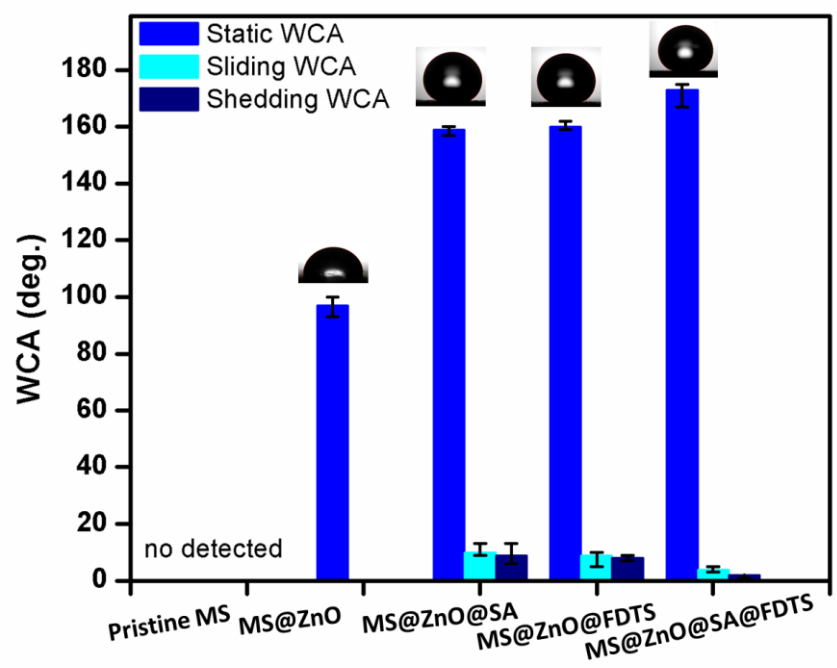

Fig.4.6. Static and dynamic WCA measurement data of sponge samples

Interestingly, the fabricated sponge not only showed the excellent water repellency behavior but also the great oil sorption ability. A feasibility test was carried out with drops of water and drops of oil on the surfaces of fabricated sponges (Fig.4.7). It can be seen that all the oil drops are quickly absorbed by the sponges when the water drops slide down from the surface of the superhydrophobic sponges. Based on these observed phenomena, the fabricated sponges was applied to separate oil and water in the mixture of them.

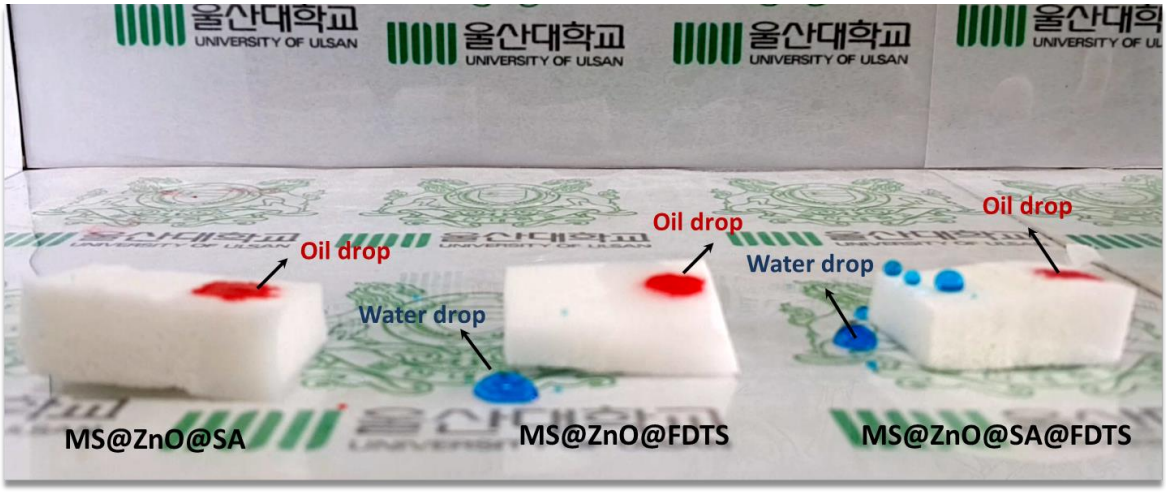

Fig.4.7. Different wetting behaviors between water and oil drops of fabricated sponges

4.4. Applications

4.4.1. Anti-wetting

The water was colored with methylene blue dye and then dropped to the sponge surfaces via a syringe. The pristine MS could easily absorb all the water drops. The surface modification with ZnO had an obvious influence in wettability of the sponge occurred. The water drops was not totally absorbed onto the sponge anymore and the shape of the water drops on the MS@ZnO surface was half-sphere shape. This phenomenon could be well explained according to the theory of Cassie-Baxter with the stable air molecules exist on the gap between the micro-nanostructures. The rough ZnO coating layer could trapped a lot quantity of air increased the water/air interface to amplify the hydrophobicity, resulting a higher WCA as compared with pristine MS sample (Fig.4.8).

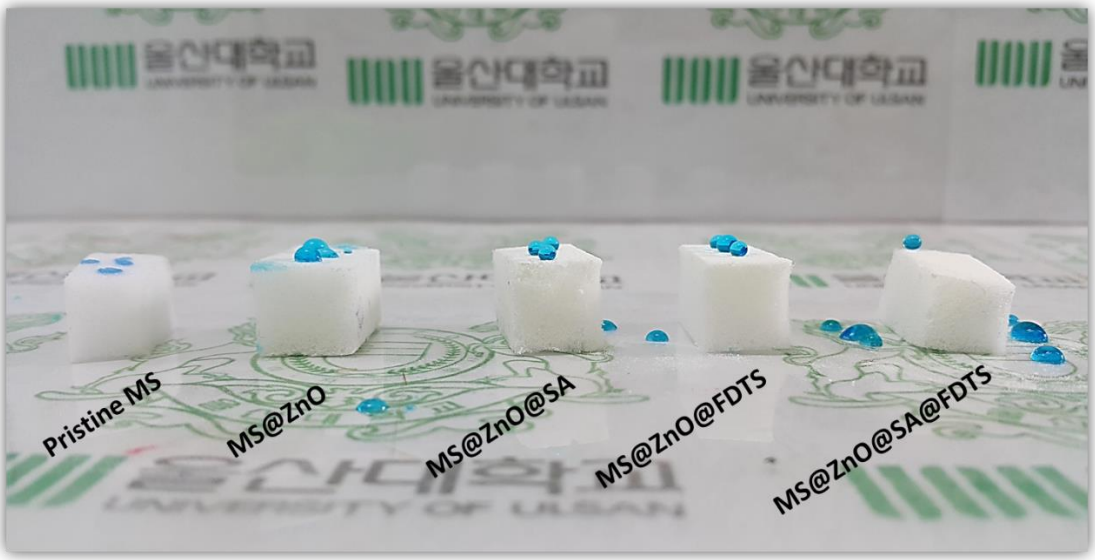

Fig.4.8. Water wettability of pristine MS and modified MS samples

4.4.2. Oil-water separation

According to the excellent properties as stated before, the supherhydrophobic MS sponges is very suitable for oil-water separation. When the oil-water mixture was poured, the surfaces of superhydrophobic MS sponges would stop the water permeation. On the contrary, the oil could quickly spread out and absorbed through the porous structure by capillary force. After the separation process, no oil scum could be seen in the collected water and the absorbed oil was easily recaptured by the squeezing process. These fabricated sponges may absorb various organic solvent-water mixtures and oil–water mixtures, including methanol, hexane, vacuum oil, gasoline, canola oil and diesel with efficiencies all exceeding over 99% for the 1st cycle. The separation capacity was presented in Fig.4.9, which is demonstrated that the fabricated MS@ZnO@SA, MS@ZnO@FDTS and MS@ZnO@SA@FDTS superhydrophobic sponges possessed very good selectivity oil-water separation behavior.

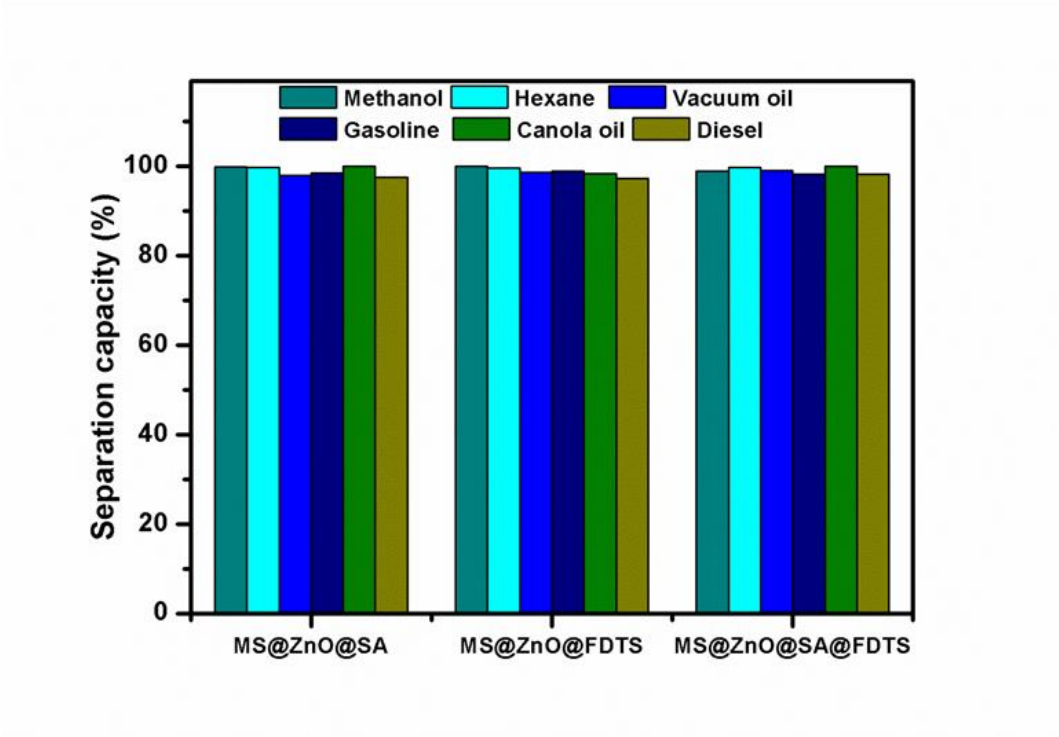

Fig.4.9. Oil-water separation capacity using superhydrophobic MS@ZnO@SA, MS@ZnO@FDTS and MS@ZnO@SA@FDTS sponges

4.5. Stability and reusability of superhydrophobic PU sponge

For practical applications, the durability and recyclability of the absorbent are key criteria for the clean-up of oils or organic solvent spills because of economic and ecological demands for sustainability.

For the recyclability test, the contaminated sponges were manual squeezed and recycled after the oil absorption (Fig.4.10 (a-c)). As mention before, the oil-water separation capacities of the fabricated sponges were extremely high for the 1st cycle. More importantly, the absorbed oil could be recovered by squeezing the oil absorbed sponges and the sponges could be applied for the next cycles. The sorption capacities were almost stable after first 30 cycles. However, the oil absorption capacity was a little bit decreased after that. It was unavoidable due to residual oils in the pores of sponge, which could not be totally removed by manual squeezing, particularly after many using cycles.

To verify the feasibility for practical applications, the durability tests were carried out (Fig.4.10 (d)). Due to the porous and spongy structure of the material, compression test is suitable for sponge material than tensile test. Commercial PU sponge is well known as material with good elasticity, so the sponge can against the highly compressible of the compression test at 50 and 70% strain. After the compression test, the sponge came back to the initial form. No fracture or collapse of the sponge was observed after the test. The robustness of the fabricated sponges was attributed to its elasticity, porosity and the strong adhesion of the coating to the sponge. The static WCA values of the sponge after the compression test were not significant changed, confirmed that the compress test did not effects to the wettability of the sponge.

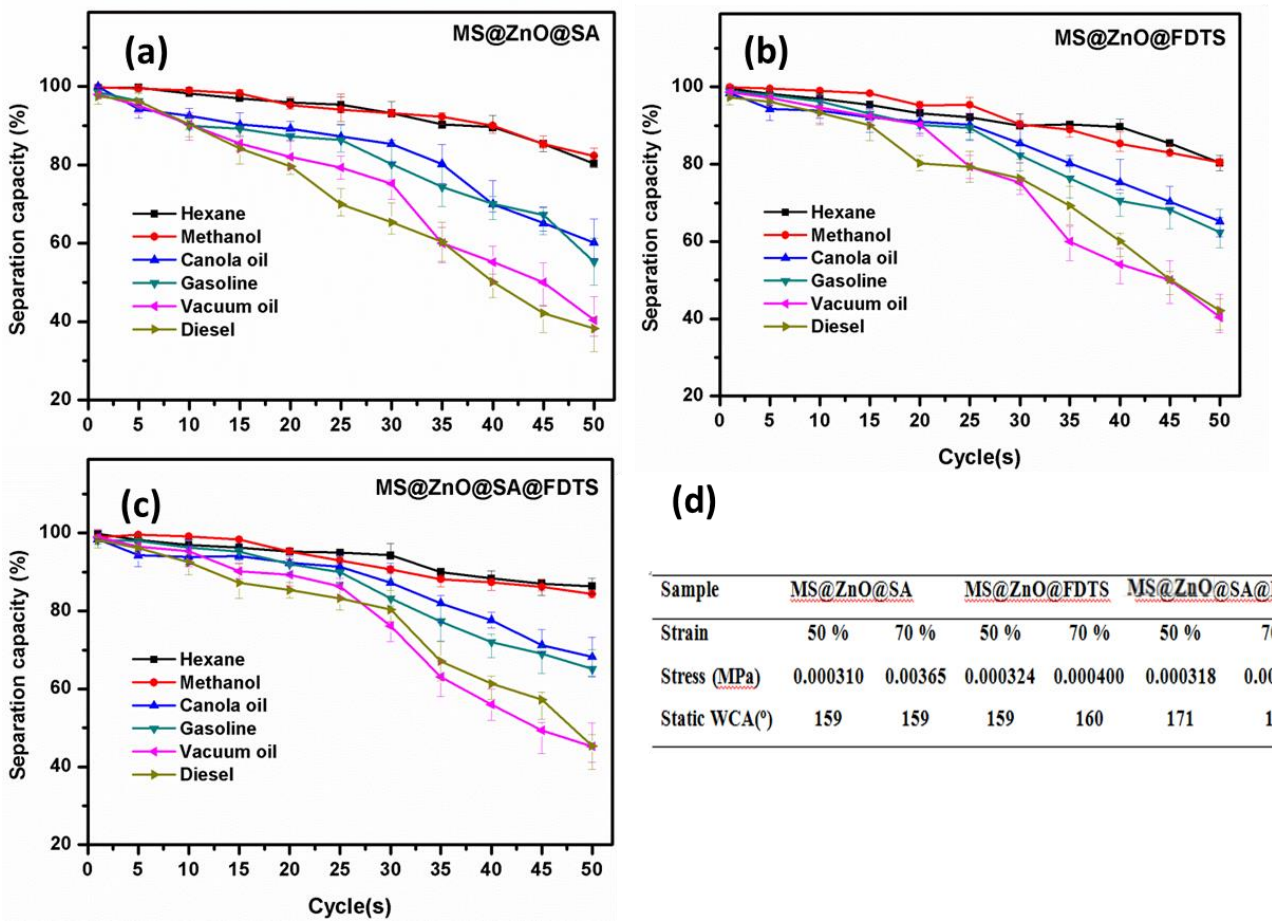

(d)

Sample	MS@ZnO@SA		MS@ZnO@FDTS		MS@ZnO@SA@FDTS	
Strain	50 %	70 %	50 %	70 %	50 %	70%
Stress (MPa)	0.000310	0.00365	0.000324	0.000400	0.000318	0.000410
Static WCA(°)	159	159	159	160	171	170

Fig.4.10. (a-c) Recyclability and (d) durability of the sponge samples for oil-water separation

4.6. Summary

In summary, a facile and cost-effective method was reported for the fabrication of three types

of robust superhydrophobic surfaces based on commercial melamine sponges, including MS@ZnO@SA, MS@ZnO@FDTS and MS@ZnO@SA@FDTS sponges. In the first step, structured ZnO was coated on the pristine MS surface in order to increase the roughness of the surface, then the wettability of the sponge was changed from hydrophilic to hydrophobic. In the second step, the SA, FDTS and mixture of SA@FDTS were used as the superhydrophobization materials in order to tune the characteristic of the sponge from hydrophobic to superhydrophobic state. The novel MS@ZnO@SA, MS@ZnO@FDTS and MS@ZnO@SA@FDTS superhydrophobic sponges possessed many of the crucial properties of an ideal sorbent material for oil-water selective separation with extremely high separation capacity, stable under the mechanical tests, outstanding recyclability with sorption capacity retention after several cycles of sorption - squeezing process, being inexpensive, and wide availability. It is assert that such sponges are promising sorbent materials for oil spill containment and environmental remediation

CHAPTER 5

CHAPTER 5- CONCLUSIONS AND FUTURE WORK

5.1. Conclusions

The outstanding non-wetting properties found on nature are direct result of their surface structure coupled with the hydrophobic chemistry. The features on these types of superhydrophobic phenomena are conducive to the formation of multiple tiny trapped air pockets underneath water droplets that minimize the real contact area and adhesion between the solid surface and liquid droplets. This results in very high water contact angles (> 150°) and very small water roll off or sliding angles (< 5°). Based on these observed phenomena in nature, the different artificial superhydrophobic surfaces were successfully fabricated in this dissertation.

All the base substrates used in this dissertation have common properties, which are soft, porous, flexible and good elasticity. Therefore, they are promising substrates for the preparation of a superhydrophobic material for oil-water separation and oil absorption applications. However, both cotton fabric and sponges are hydrophilic materials and they can easily absorb both oil and water. Therefore, several methods were developed in this dissertation to change the wettability of chosen base substrates.

The first reported superhydrophibic surface in this study was developed on cotton fabric surface. A stable and robust superhydrophobic composite of ZnO and commercial cotton fabric was successfully fabricated with a simple approach. ZnO layer was coated on the surface of cotton fabric via hydrothermal method. After the coating process, ZnO of high purity and uniform structure was grown on the cotton fabric surface. Superhydrophobicity was achieved with a WCA up to 151 ± 3^o mainly due to the ZnO coating layer on the original cotton fabric changed the surface roughness. The surface of the original cotton fabric was even and flat with R_a = 0.85, whereas the ZnO-CF surface was much rougher with R_a = 2.42. The enhanced C-H/C-C bonding and the decrease in C=O and C-O bonding also was another reason increased the water repulsion of ZnO-CF. ZnO-CF with soft and flexible properties exhibited an excellent hexane-water separation capacity and good stability in repeated applications. Therefore, ZnO-CF can be utilized for the selective separation of hexane and water in applications requiring self-cleaning ability.

The second superhydrophobic surface presented in this study was based on the commercial

polyurethane sponge. Durable, magnetic and superhydrophobic PU@ZnO@Fe_3O_4@SA sponge was successfully fabricated by a novel, facile and environmentally friendly method. Commercial PU sponge was modified with ZnO, SA and Fe_3O_4 to provide the necessary roughness, low surface energy and magnetic responsiveness, respectively. As a result, the fabricated sponge showed a very high static WCA (161°) and a very low dynamic WCA (sliding WCA = 7° and shedding WCA = 8°). The maximum sorption capacity of the fabricated sponge varied for the seven different oils examined (k = 32 ~ 108.9 g/g) due to the varying densities and viscosities of the oils, and these maximum sorption capacities were higher than those previously reported. The oil-water separation efficiency of the fabricated sponge exceeded 99 %, and the absorbed oil could be easily recovered by simple mechanical squeezing. In addition, the sponge could be magnetically guided to the oil-polluted area and then quickly absorb the floating oil for efficient removal. Furthermore, the superhydrophobicity and oil absorbency of the fabricated sponge were maintained after stretching, compression, cleaning and repeated sorption cycles.

The third superhydrophobic material was fabricated in the melamine sponge base via a similar mechanism with the second material, but the coating materials were changed. Three types of robust superhydrophobic surfaces based on commercial melamine sponges, including MS@ZnO@SA, MS@ZnO@FDTS and MS@ZnO@SA@FDTS sponges were successfully fabricated. For providing the roughness to the surface, in the first step, structured ZnO was also coated on the pristine MS surface, then the wettability of the sponge was changed from hydrophilic to hydrophobic. In the second step, besides SA, FDTS and mixture of SA@FDTS were used as the superhydrophobization materials in order to tune the characteristic of the sponge from hydrophobic to superhydrophobic state. The novel MS@ZnO@SA, MS@ZnO@FDTS and MS@ZnO@SA@FDTS superhydrophobic sponges possessed many of the crucial properties of an ideal sorbent material for oil-water selective separation with extremely high separation capacity, stable under the mechanical tests, outstanding recyclability with sorption capacity retention after several cycles of sorption - squeezing process, being inexpensive, and wide availability.

The results of these studies were further confirming the techniques to fabricate the superhydrophobic surface in different substrate. All the fabricated techniques are very simple, economic effective as well as environmental friendly. All the fabricated materials were characterized by various techniques to clearly explain their wettability behaviors.

Furthermore, the presented materials owned the excellent durability and reusability, thus they are promising sorbent materials for oil spill containment treatment, separation of oily pollutants from water and environmental remediation in real scales.

5.2. Future works

In this work, for superhydrophobic surface fabrication, two crucial factors must be available including hierarchical structure with the low surface energy. The obtained superhydrophobic surfaces could be used for the practical applications by investigating more effectiveness of their property in the provided potential applications. Moreover, several further researches could be found from this study. All the base substrates used in this dissertation have common properties, which are soft, porous, flexible and good elasticity. The surfaces with similar properties could be practically applied to fabricate the superhydrophobic surface well with the proper treatment process and mechanism. They are the very good candidates for environmental applications, especially oil/organic solvents separation applications.

Furthermore, the capability of creating different superhydrophobic surface may open the gate to apply in different applications. The soft surfaces are suitable for the oil-water separation, and the other surfaces might suitable for different applications. For example, the superhydrophobic developed on the hard substrates such as metal or ceramic… could be applied for anti-icing, anti-corrosion or anti-fogging etc…

It is hoped that new fabrication approaches and techniques for superhydrophobic surfaces accomplished in this work contribute to the advancement of materials and applications technology as well as broaden outlook for further research of practical applications in daily life.

LIST OF REFERENCES

[1] T.Y. S. Shibuichi, T. Onda, K. Tsujii, Super water- and oil-repellent surfaces resulting from fractal structure., Journal of Colloid and Interface Science, 208 (1998) 287-294.

[2] N.C. VInh, Fabrication of superhydrophobic metaalic surfaces with fast wettability transition using nanosecond laser ablation and heat treatment, in: School of Mechanical Engineering, University of Ulsan 2017, pp. 115.

[3] T.G.Y. Cha, J. W.; Moon, M. W.; Lee, K. R.; Kim, H. Y., Nanoscale paterning of microtextured surfaces to control superhydrophobic roughness, Langmuir, 26 (2010) 8319-8326.

[4] F.G. Thierry Darmanin, Superhydrophobic and superoleophobic properties in Nature, Materials Today, 18 (2015) 273-285.

[5] C.K. I. Ahmad, A Review on Development and Applications of Bio-Inspired Superhydrophobic Textiles, Materials, 9 (2016) 892.

[6] StoColorTM Lotusan®, in: S. Corporation (Ed.), 2017.

[7] J.W. Du, New Additive to Enhance Surface Cleanability, in: PCI Panit and Coating Industry, 2003.

[8] F. Tibu, An Interesting Geek Game: the Bandai Aqua Drop, in, 2008.

[9] C.-v.N. Do Man Chun, Kyong Min Lee, Fast fabrication of superhydrophobic metallic surface using nanosecond laser texturing and low-temperature annealing, CIRP Annals-Manufacturing Technology, 65 (2016) 519-522.

[10] J.H.X. M. Li, Q. H. Lu, Creating Superhydrophobic Surfaces with Flowery Structures on Nickel Substrates through a Wet-Chemical-Process, Journal of Materials Chemistry, 17 (2007) 4772-4776.

[11] H.D. L. Pan, P. Bi, Facile Preparation of Superhydrophobic Copper Surface by HNO3 Etching Technique with the Assistance of CTAB and Ultrasonication, Applied Surface Science, 257 (2010) 1707-1711.

[12] J.Z. C. Gu, J. Tu, A Strategy of Fast Reversible Wettability Changes of WO3 Surfaces

between Superhydrophilicity and Superhydrophobicity, Journal of Colloid and Interface Science, 352 (2010) 573-579.

[13] Z.S.C. B. Xu, Fabrication of a Superhydrophobic ZnO Nanorod Array Film on Cotton Fabrics via a Wet Chemical Route and Hydrophobic Modification, Applied Surface Science, 254 (2008) 5899-5904.

[14] J.N.W. Q. F. Xu, Superhydrophobic and Transparent Coatings Prepared by Selfassembly of Dual-Sized Silica Particles, Frontiers of Materials Science in China, 4 (2010) 180-188.

[15] M.Z. S. He, L. Yao, X. Yuan, M. Li, L. Ma, W. Shen, Preparation and Properties of ZnO Nanostructures by Electrochemical Anodization Method, Applied Surface Science, 256 (2010) 2257-2562.

[16] N.A. M. S. Islam, M. R. Karim, Preparation of Superhydrophobic Membranes by Electrospinning of Fluorinated Silane Functionalized Pullulan, Colloids and Surfaces A: Physicochemical and Engineering Aspects, 362 (2010) 117-120.

[17] R.J. M. Kang, H. S. Kim, H. J. Jin, Preparation of Superhydrophobic Polystyrene Membranes by Electrospinning,, Colloids and Surfaces A: Physicochemical and Engineering Aspects, 313-314 (2008) 411-414.

[18] X.F. M. Jin, J. Xin, J. Zhai, K. Cho, L. Feng, L. Jiang, Super-hydrophobic PDMS surface with ultra-low adhesive force, Macromole Rapid Communication, 26 (2005) 1805-1809.

[19] K.K. H. Yan, H. Mayama, K. Tsujii, Environmentally stable super water-repellent poly(alkylpyrrole) films, Angewandte Chemie International Edition, 44 (2005) 3453-3456.

[20] J.E.C. T. Baldacchini, M. Zhou, E. Mazur, Superhydrophobic surfaces prepared by microstructuring of silicon using a femtosecond laser, Langmuir, 22 (2006) 4917-4919.

[21] E.G. N. Verplanck, J. Camart, V. Thomy, Reversible electrowetting on superhydrophobic silicon nanowires, Nano Letters, 7 (2007) 813-817.

[22] J.L.S. A.B. Nordvik, K.R. Bitting, A. Lewis, T. Strøm-Kristiansen, Oil and water separation in marine oil spill clean-up operations, Spill Science & Technology Bulletin, 3 (1996) 107-122.

[23] P.A.T. K. Thomas Klasson, Joseph F. Walker Jr., Sandie A. Jones, Robert L. Cummins, Steve A. Richardson, Modification of a Centrifugal Separator for In-Well Oil-Water Separation, Separation Science and Technology, 40 (2005) 453-462.

[24] Y.T. J. Yang, J. Xu, B. Chen, H. Tang, C. Li, Durable superhydrophobic/superoleophilic epoxy/attapulgite nanocomposite coatings for oil/water separation, Surface and Coatings Technology, 272 (2015) 285-290.

[25] Z.G. Hai Zhu, Hybrid engineered materials with high water-collecting efficiency inspired by Namib Desert beetles, Chemical Communication, 52 (2016) 6809-6812.

[26] L.W. Bucheng Li, Lingxiao Li, Stefan Seeger, Junping Zhang, Aiqin Wang, Superwetting double-layer polyester materials for effective removal of both insoluble oils and soluble dyes in water, ACS Applied Materials and Interfaces, 6 (2014) 11581−11588.

[27] L.L. Lei Wu, Bucheng Li, Junping Zhang, Aiqin Wang, Magnetic, durable, and superhydrophobic polyurethane@Fe3O4@SiO2@Fluoropolymer sponges for selective oil absorption and oil/water separation, ACS Applied Materials and Interfaces, 7 (2015) 4936−4946.

[28] L.W. Junping Zhang, Yujie Zhang, Aiqin Wang, Mussel and fish scale-inspired underwater superoleophobic kapok membranes for continuous and simultaneous removal of insoluble oils and soluble dyes in water, Journal of Materials Chemistry A, 3 (2015) 18475–18482.

[29] M.M. Feng Liu, Deli Zang, Zhengxin Gao, Chengyu Wang, Fabrication of superhydrophobic/superoleophilic cotton for application in the field of water/oil separation, Carbohydrate Polymers, 103 (2014) 480– 487.

[30] C.H. Lee, Johnson, N., Drelich, J., & Yap, Y. K. , The performance of superhydrophobic and superoleophilic carbon nanotube meshes in water–oil filtration, Carbon, 49 (2011) 669-676.

[31] S.-W.G. Hui Liu, Jing-Sheng Cai, Cheng-Lin He, Jia-Jun Mao, Tian-Xue Zhu, Zhong Chen, Jian-Ying Huang, Kai Meng, Ke-Qin Zhang, Salem S. Al-Deyab , a.Y.-K. Lai, Recent Progress in Fabrication and Applications of Superhydrophobic Coating on Cellulose-Based Substrates, Materials and Design, 9 (2016) 124-161.

[32] X.L. Xiaogang Guo, Zhibo Wei, Xiaolin Li, Lidan Niu, Rapid fabrication and characterization of superhydrophobic tri-dimensional Ni/Al coatings, Applied Surface Science, 387 (2016) 8-15.

[33] W.L. Ben Wang, Zhiguang Guo, Weimin Liu, Biomimetic super-lyophobic and super-lyophilic materials applied for oil/water separation: a new strategy beyond nature, Chemical Society Reviews, 44 (2015) 336-361.

[34] T. Shenshen Ouyang, Xueying Jia, Yun Chen, Juming Yao, ShengWang, Self-indicating and recyclable superhydrophobicmembranes for effective oil/water separation in harsh conditions, Materials and Design, 96 (2016) 357-363.

[35] J.W. Chuan Du, Zhifu Chen, Darong Chen, Durable superhydrophobic and superoleophilic filter paper for oil–water separation prepared by a colloidal deposition method, Applied Surface Science, 313 (2014) 304-310.

[36] X.L. Na Liu, Weifeng Zhang, Yingze Cao, Yuning Chen, Lin Feng & Yen Wei, A Pure Inorganic ZnO-Co3O4 Overlapped Membrane for Efficient Oil/Water Emulsions Separation, in, Nature.com, 2015.

[37] M.R. Yangyang Zhang, Elias K. Stefanakos, D. Yogi Goswami, Synthesis, Characterization, and Applications of ZnO Nanowires, Journal of Nanomaterials, 2012 (2012).

[38] N.X. J. Zhou, and Z. L. Wang, Dissolving behavior and stability of ZnO wires in biofluids: a study on biodegradability and biocompatibility of ZnO nanostructures, Advanced Materials and Design, 18 (2006) 1047-1056.

[39] T.E. Volodymyr Khranovskyy, Rositsa Yakimova and Lars Hultman, Surface morphology effects on the light-controlled wettability of ZnO nanostructures, Applied Surface Science, 258 (1012) 8146-8152.

[40] J.C. Si Chen, Jianlin Liu, Jing Qi, Yuhua Wang, Enhanced field emission from ZnO nanowire arrays utilizing MgO buffer between seed layer and silicon substrate, Applied Surface Science, 387 (2016) 103-108.

[41] W.L. Ao, J.; Yang, H.; Zeng, X.; Ma, X., Mechanochemical synthesis of zinc oxide nanocrystalline, Powder Technology, 168 (2006) 128-151.

[42] K.M.M. Kumra, B.K.; Naidu, E.A.; Sinha, M.; Kumar, K.S.; Reddy, P.S., Synthesis and

characterization of flower shaped zinc oxide nanostructures and its antimicrobial activity, Spectrochimica Acta Part A: Molecular and Biomolecular Spectroscopy, 104 (2013) 171-174.

[43] Ö.A.D. Yildirim, C., Synthesis of zinc oxide nanoparticles elaborated by microemulsion method, Journal of Alloys and Compounds, 506 (2010) 944-949.

[44] A.K.-R.a.T. Jesionowski, Zinc Oxide—From Synthesis to Application: A Review, Materials, 7 (2014) 2833-2881.

[45] X.H. Xin Du, Xiaoyu Li, Xiangmin Meng, Lin Yao b, Junhui He, Hongwei Huang, Xueji Zhang Wettability behavior of special microscale ZnO nail-coated mesh films for oil–water separation, Journal of Colloid and Interface Science, 458 (2015) 79-86.

[46] C.N.C. Kyoung Ho Ha, Fabrication of an oil–water separation copper filter using laser beam machining, Journal of Micromechanics and Microengineering, 26 (2016).

[47] J.Z. Lei Wu, Bucheng Li, Aiqin Wang, Mimic nature, beyond nature: facile synthesis of durable superhydrophobic textiles using organosilanes, Journal of Materials Chemistry B, 1 (2013) 4756.

[48] J.Z. Lei Wu, Bucheng Li, Ling Fan, Lingxiao Li, Aiqin Wang, Facile preparation of super durable superhydrophobic materials, Journal of Colloid and Interface Science, 432 (2014) 31–42.

[49] S.S. Yao Lu, Jinlong Song, Colin R. Crick, Claire J. Carmal, Ivan P. Parkin, Robust self-cleaning surfaces that function when exposed to either air or oil, Science, 6 (2015) 1132-1135.

[50] T. Al-Harbi, Hydrothermal synthesis and optical properties of Ni doped ZnO hexagonal nanodiscs, Journal of Alloys and Compounds, 509 (2011) 87-390.

[51] X.W. Lihong Gong, Huibo Chen,Fengyu Qu, Maozhong An, Synthesis of Vertically Aligned Dense ZnO Nanowires, Journal of Nanomaterials, 2011 (2011).

[52] S.-Y.P. Myo Thuya Thein, Azizan Aziz & Mitsuru Itoh, The role of ammonia hydroxide in the formation of ZnO hexagonal nanodisks using sol–gel technique and their photocatalytic study, Journal of Experimental Nanoscience, 10 (2015) 1068-1081.

[53] K.S. Taehwan Jun, Youngmin Jeong, Kyoohee Woo, Dongjo Kim, Changdeuck Bae, Jooho Moon, High-performance low-temperature solution-processable ZnO thin film

transistors by microwave-assisted annealing, Journal of Materials Chemistry, 21 (2010) 1102-1108.

[54] T.P.L. Kevin M. McPeak, Nathan G. Britton, Zhorro S. Nickolov, Yossef A. Elabd, Jason B. Baxter, Chemical Bath Deposition of ZnO Nanowires at Near-Neutral pH Conditions without Hexamethylenetetramine (HMTA): Understanding the Role of HMTA in ZnO Nanowire Growth, Langmuir, 27 (2011) 3672-3677.

[55] Y.D. Benjamin Weintraub, Zhong L. Wang, Position-Controlled Seedless Growth of ZnO Nanorod Arrays on a Polymer Substrate via Wet Chemical Synthesis, The Journal of Physical Chemistry C, 111 (2007) 10162-10165.

[56] E.S. Naif Mohamed Al-Hada, A. H. Shaari, M.A.Kamarudin, Salahudeen A. Gene, The influence of calcination temperature on the formation of of zinc oxide nanparticles by thermal-treatment Applied Mechanics ans Materials, 446-447 (2014) 181-184.

[57] F.T.Z. Umair Manzoor, Sidra Rafique, Muhammad Tahir Moin, Mohammad Mujahid, Effect of Synthesis Temperature, Nucleation Time, and Postsynthesis Heat Treatment of ZnO Nanoparticles and Its Sensing Properties, Journal of Nanomaterials, 2015 (2015).

[58] D.S.B. K. Govender, P. B. Kenway, and P. O'Brien, Understanding the factors that govern the deposition and morphology of thin films of ZnO from aqueous solution, Journal of Materials Chemistry, 14 (2004) 2575-2591.

[59] R.G.U. Vincenzina Strano, Mario Scuderi, Kingsley O. Iwu, Francesca Simone, Enrico Ciliberto, Corrado Spinella, and Salvo Mirabella, Double Role of HMTA in ZnO Nanorods Grown by Chemical Bath Deposition, The Journal of Physical Chemistry C, 118 (2014) 28189−28195.

[60] K.C. Robertson Campbell, Gulf Spill Is the Largest of Its Kind, Scientists Say, The New York Times, (2010).

[61] L. Hampton, North Dakota spill sixth largest pipeline leak in 2016 - data, Reuters, (2016).

[62] A.S.K. Y. Yavuz, Ü.B. Öğütveren, Treatment of petroleum refinery wastewater by electrochemical methods, Desalination, 258 (2010) 201-205.

[63] K.A. B.K. Körbahti, Electrochemical oil/water demulsification and purification of bilge

water using Pt/Ir electrodes, Desalination, 258 (2010) 219-228.

[64] W.S. Srijan Aggarwal, Ian Buist, Jessica Garron, Robin Bullock, Robert Perkins, Steve Potter, David Cooper, Aerial application of herding agents to advance in-situ burning for oil spill response in the Arctic: A pilot study, Cold Regions Science and Technology, 135 (2017) 94-104.

[65] L.M.V.M. Laurens van Gelderen, Grunde Jomaas, Vaporization order and burning efficiency of crude oils during in-situ burning on water, Fuel, 191 (2017) 528-537.

[66] A.S. I. Noshadi, M. Hemmati, F. Rekabdar, T. Mohammadi, Experimental and ANFIS modeling for fouling analysis of oily wastewater treatment using ultrafiltration, Asia-Pacific Journal of Chemical Engineering, 8 (2013) 527-538.

[67] A.W.M. K. Karakulski, Recovery of process water from spent emulsions generated in copper cable factory, Journal of Hazardous Materials, 186 (2011) 1667-1671.

[68] L.Z. H. Song, L. Zhang, B. Gao, D. Wei, Y. Shen, Construction of a whole-cell catalyst displaying a fungal lipase for effective treatment of oily wastewaters, Journal of Molecular Catalysis B: Enzymatic, 71 (2011) 166-170.

[69] V.J.P.V. C.E. Santo, A. Bhatnagar, E. Kumar, C.M.S. Botelho, R.A.R. Boaventura, Biological treatment by activated sludge of petroleum refinery wastewaters, Desalination Water Treatment, 51 (2013) 6641-6654.

[70] B.L. Lingxiao Li, Junping Zhang, Dopamine-mediated fabrication of ultralight graphene aerogels with low volume shrinkage, Journal of Materials Chemistry A, 4 (2016) 512-518.

[71] F.Y.L. P.Zhang, A review of the recent advances in superhydrophobic surfaces and the emerging energy-related applications, Energy, 82 (2015) 1068-1087.

[72] T.D. Elena Celia, ElisabethTaffin de Givenchy, Sonia Amigoni, Frédéric Guittard, Recent advances in designing superhydrophobic surfaces, Journal of Colloid and Interface Science 402 (2013) 1-18.

[73] B.-K.L. Viet Ha Tran Thi, Chi-Vinh Ngo, Durable superhydrophobic cotton filter prepared at low temperature for highly efficient hexane and water separation, Journal of the Taiwan Institute of Chemical Engineers, 71 (2017) 527-536.

[74] L.Y. Jian Li, Weijun Li, Jianping Li, Fei Zha, Ziqiang Lei Superhydrophilic–underwater superoleophobic ZnO-based coated mesh for highly efficient oil and water separation, Materials Letters, 153 (2015) 62-65.

[75] X.Z. Dongliang Tian, Yu Tian, Yue Wu, Xiao Wang, Jin Zhai and Lei Jiang, Photo-induced water–oil separation based on switchable superhydrophobicity–superhydrophilicity and underwater superoleophobicity of the aligned ZnO nanorod array-coated mesh films, Journal of Materials Chemistry, 22 (2012) 19652.

[76] B.L. Lingxiao Li, Lei Wu, Xia Zhao, Junping Zhang, Magnetic, superhydrophobic and durable silicone sponges and their applications in removal of organic pollutants from water, Chemical Communication, 50 (2014) 7831-7833.

[77] Z.C. Xiaomeng Lü, Wei Wei, Jimin Xie, Liang Jiang, Jun Huang, Jun Liu, Constructing polyurethane sponge modified with silica/graphene oxide nanohybrids as a ternary sorbent, Chemical Engineering Journal, 284 (2016) 478-486.

[78] S.-J.L. Chih-Feng Wang, Robust Superhydrophobic/Superoleophilic Sponge for Effective Continuous Absorption and Expulsion of Oil Pollutants from Water, Applied Materials and Interfaces, 5 (2013) 8861-8864.

[79] L.X. Luhong Zhang, Yongli Sun, Na Yang, Robust and Durable Superhydrophobic Polyurethane Sponge for Oil/ Water Separation, Industrial and Engineering Chemistry Research, 55 (2016) 11260-11268.

[80] B.-K.L. Viet Ha Tran Thi, Development of multifunctional self-cleaning and UV blocking cotton fabric with modification of photoactive ZnO coating via microwave method, Journal of Photochemistry and Photobiology A: Chemistry, 338 (2017) 13-22.

[81] B.K.L. Viet Ha Tran Thi, Great improvement on tetracycline removal using ZnO rod-activated carbon fiber composite prepared with a facile microwave method, Journal of Hazardous Materials, 324 (2017) 329-339.

[82] E.K.M. Zana Hajdari Gretić, Vida Čadež, Suzana Šegota, Helena Otmačić Ćurković and Saman Hosseinpour, The influence of thickness of stearic acid self-assembled film on its protective properties, Journal of Electrochemistry Society, 163 (2016) 937-944.

[83] U. Technologies, Reticulated polyurethane foam Universal air filter (2017).

[84] U.A.f.F. Group, Why is Porosity important to air filters using foam media?, Universal Air Filter (2014).

[85] Q.H. Jiajia Ye, Binbin Liu, Yaping Li, Caixia Xu, Facile preparation of graphene nanosheets encapsulated Fe3O4 octahedra composite and its high lithium storage performances, Chemical Engineering Journal, 315 (2017) 115-123.

[86] H.W. Jing Hu, Fan Dong, Zhongbiao Wu, A new strategy for utilization of NIR from solar energy—Promotion effect generated from photothermal effect of Fe3O4@SiO2 for photocatalytic oxidation of NO, Applied Catalysis B: Environmental, 204 (2017) 584-592.

[87] P.M. Valeria Chiono, Monica Boffito, Susanna Sartori, Emilia Gioffredi, Antonella Silvestri, Alberto Rainer, Sara Maria Giannitelli, Marcella Trombetta,, Daria Nurzynska, Franca Di Meglio, Clotilde Castaldo, Rita Miraglia, Stefania Montagnani, Polyurethane-based scaffolds for myocardial tissue engineering, Interface Focus, 4 (2013).

[88] B.C.F. Craig A. Merlic, Table of IR Absorptions, in: T.R.o.U.o. California (Ed.) Web spectra, https://webspectra.chem.ucla.edu/index.html, 1997.

[89] Y.Z. Jintao Wang, Oil/water mixtures and emulsions separation of stearic acid-functionalized sponge fabricated via a facile one-step coating method, Separation and Purification Technology, 181 (2017) 181-191.

[90] A.M.G. Regina Coeli Moreira Dias, Rogéria Serakides, Eliane Ayres, Rodrigo Lambert Oréfice, Porous Biodegradable Polyurethane Nanocomposites: Preparation, Characterization, and Biocompatibility Tests, Materials Research, 13 (2010) 211-218.

[91] T.L. Yang Yang, Fabrication and characterization of graphene oxide/zinc oxide nanorods hybrid, Applied Surface Science 257 (2011) 8950-8954.

[92] N.V. Bhaskar Bhaduri, A zinc nanoparticles-dispersed multi-scale web of carbon micro-nanofibers for hydrogen production step of ZnO/Zn water splitting thermochemical cycle, Chemical Engineering Research and Design, 92 (2014) 1079-1090.

[93] L.M. A. Hernández, E. Sánchez-Mora and E. M. Sánchez, Sol-Gel Synthesis, Characterization and Photocatalytic Activity of Mixed Oxide ZnO-Fe2O3, Journal of Sol-Gel Science and Technology, 42 (2007) 71-78.

[94] X.L. Beibei Li, Xinying Zhang, Junchen Zou, Wenbo Chai and Yanyan Lou, Rapid

adsorption for oil using superhydrophobic and superoleophilic polyurethane sponge, Journal of Chemical Technology and Biotechnology, 90 (2015) 2106-2112.

[95] B.Z. Qi Wang, Mengnan Qu, Junyan Zhang, Deyan He, Fabrication of superhydrophobic surfaces on engineering material surfaces with stearic acid, Applied Surface Science, 254 (2008) 2009-2012.

[96] H.Z. Libang Feng, Pengzhi Mao, Yanping Wang, Yang Ge, Superhydrophobic alumina surface based on stearic acid modification, Applied Surface Science, 257 (2011) 3959-3963.

[97] M.F. R. Jafari, A simple method to create superhydrophobic aluminium surfaces, Materials Science Forum, 706-709 (2012) 2874-2879.

[98] H.H. Said Gharby, Bertrand Matthäus, Zakia Bouzoubaa, Zoubida Charrouf, The chemical parameters and oxidative resistance to heat treatment of refined and extra virgin Moroccan Picholine olive oil Journal of Taibah University for Science, 10 (2016) 100-106.

[99] Q.P. Qing Zhu, Fatang Liu, Facile removal and collection of oils from water surfaces through superhydrophobic and superoleophilic sponges, The Journal of Physical Chemistry, 116 (2011) 17464-17470.

[100] C.-W.C.-J. Er-Chieh Cho, Yu-Sheng Hsiao, Kuen-Chan Lee, Jen-Hsien Huang, Interfacial engineering of melamine sponges using hydrophobic TiO2 nanoparticles for effective oil/water separation, Journal of the Taiwan Institute of Chemical Engineers, 67 (2016) 476-483.

[101] L.L. Hua Li, Fenglin Yang, Hydrophobic modification of polyurethane foam for oil spill cleanup, Marine Poluution Bulletin, 64 (2012) 1648-1653.

[102] L.K. Tao Zhang, Muyang Zhang, Fengxian Qiu, Jian Rong, Jianming Pan, Synthesis and characterization of porous fibers/ polyurethane foam composites for selective removal of oils and organic solvents from water, RSC Advances, 6 (2016) 86510–86519.

[103] Y.S.Z. Yang Gao, Wei Xiong, Mengmeng Wang, Lisha Fan, Hossein Rabiee-Golgir, Lijia Jiang, Wenjia Hou, Xi Huang, Lan Jiang, Jean-Francois Silvain, Yong Feng Lu, Highly Efficient and Recyclable Carbon Soot Sponge for Oil Cleanup, ACS Applied Materials & Interfaces, 6 (2014) 5924−5929.

[104] L.L. Bucheng Li, Lei Wu, Junping Zhang, Aiqin Wang, Durable

superhydrophobic/superoleophilic polyurethane sponges inspired by mussel and lotus leaf for the selective removal of organic oollutants from water, Chempluschem, 79 (2014) 850-856.

[105] B.-K.L. Viet Ha Tran Thi, Great improvement on tetracycline removal using ZnO rod-activated carbon fiber composite prepared with a facile microwave method, Journal of Hazardous materials, 324 (2017) 329-339.

[106] B.C. Daniela Caschera, Alessio Mezzi, Marco Brucale, Gabriel Maria Ingo, Giuseppe Gigli, Giuseppina Padeletti, Ultra Hydrophobic/Superhydrophilic Modified Cotton Textiles through Functionalized Diamond-Like Carbon Coatings for SelfCleaning Applications, Langmuir, 29 (2013) 2775-2783.

APPENDIX 1

Response to the comments of Committee Members

1. Literature survey

Biomimetic surfaces and materials received great attention of scientists and engineers due to their unusual properties. Biologically inspired design, adaptation, or derivation from nature is referred to as "biomimetics" [1] Biological tiny structures have been observed on many kinds of surfaces such as lotus leaves, rice leaves, butterfly wings, mosquito eyes, moth eyes, cicada wings, red rose petals, gecko feet, desert beetle, spider silks, and fish scales which exhibit excellent hydrophobicity and/or superhydrophobicity [2-6]. Such natural structures offer new insights into the design of artificial superhydrophobic structures. A superhydrophobic surface is a surface on which a drop of water forms an almost perfect sphere and even a very slight tilting is sufficient to cause the water drop to roll off. In addition to high water contact angle and low sliding angle, the ability of a surface to bounce off water droplets constitutes the third property of a superhydrophobic surface that is important for both biological and technical applications [7]. These surfaces are of special interest, because properties such as anti-sticking, anti-contamination, and self-cleaning are expected. These properties are attractive for many industrial and biological applications such as anti-biofouling paints for boats, antisticking of snow for antennas and windows, self-cleaning windshields for automobiles, microfluidics, lab-on-a-chip devices, metal refining, stain resistant textiles, anti-soiling architectural coatings, dust-free coatings on building glasses and so on [8-12].

Recently, a research work has been devoted towards the preparation and theoretical modelling of superhydrophobic surfaces as observed by the large number of publications and diverse approaches. Many strategies to create superhydrophobic surfaces have been put forward. Many of the preparation techniques are simple, inexpensive; however, some of them involved multistep procedures and harsh conditions, or required specialized reagents and equipment. Up to now, procedures of roughening the surface followed by hydrophobization or transforming low-surface-energy materials into rough surfaces have been commonly used to produce superhydrophobic surfaces. The various methods for the preparation of biomimetic superhydrophobic surfaces since last two decades have been reported, such as phase separation [13], electrochemical deposition [14], template method [15,16], emulsion [17], plasma method

[18], crystallization control [19], chemical vapor deposition [20], wet chemical reaction [21], sol-gel processing [22-25], lithography so on [29-31]. Besides water repellency, other properties such as structure change, flexibility and reusability have also been incorporated into biomimetic superhydrophobic surfaces.

During the last few decades, many artificial self-cleaning surfaces were fabricated by different techniques. To fabricate superhydrophobic surfaces using a template-based approach there are two main requirements: 1) the surface must be sufficiently rough to allow for the formation of trapped air pockets underneath water droplets and 2) the surface should be a low surface energy material that is inherently hydrophobic. To date, a wide variety of physical and chemical methods have been explored to fabricate superhydrophobic surfaces through one of the following two approaches: (i) creating a rough surface on a hydrophobic material or (ii) modifying a rough surface with a hydrophobic coating.

(i) Roughening a hydrophobic material

Methods to make superhydrophobic surfaces by roughening low surface energy materials are mostly one-step processes and have the advantage of simplicity. There are many ways to make rough surfaces, including laser/mechanical treatment [31], chemical etching [32, 33], lithography, sol–gel and hydrothermal processing [34, 35], layer-by-layer and colloidal assembling [36], electrical/chemical deposition [37], electrospinning [38, 39]… For example, Jin et al. reported a laser etching method to make superhydrophobic polydimethylsiloxane (PDMS) surface, which contains micro-, submicro- and nano-composite structures [40]. Yan et al. fabricated superhydrophobic poly(alkylpyrrole) films by a electrochemical synthesis method. The film surface consists of thousands of ―needle‖-like microstructures in a perpendicular alignment [41].

As described by Cassie and Baxter, multi-level roughness enables trapping of air under the water droplet, enhancing the surface hydrophobicity. Microstructure pillar arrays fabricated by photolithography and soft lithography are often used to provide a predefined roughness. The major issues facing wide application of these techniques include high fabrication cost, limited applications to large scale coating, and reduced flexibility in modulation of surface morphologies. One of the low-cost alternatives is through surface deposition of nanoparticles. As silica nanoparticles are readily synthesized by a sol-gel process with uniform size, and as their surface chemistry is tunable via covalent modification, they are widely used in creating

surfaces with desirable properties.

(ii) Modifying a rough surface with a hydrophobic coating

Generally, the wettability behavior of rough surfaces is governed by the interface chemistry. There are also several methods commonly used to modify the chemistry of a surface. Although it is a relatively simple and one-step process to make superhydrophobic surfaces by using intrinsically hydrophobic materials, unfortunately, many materials do not possess a low enough surface free energy to be intrinsically hydrophobic. In order to make superhydrophobic surfaces on these intrinsically hydrophilic materials, a two-step process is usually required, i.e., making a rough surface first and then modifying it with chemicals, such as alkanethiols, organic silanes, and fatty acids, which can offer a low surface free energy after linked to the surface. For example, Baldacchini et al reported a way to create micro/nanoscale roughness on silicon wafers by using a femtosecond laser to etch the silicon wafers [42]. Verplanck et al. made silicon nanowires on Si/SiO_2 substrates through a vapor-liquid-solid mechanism. The resulting rough surfaces were modified with a fluoropolymer C_4F_8, and exhibited superhydrophobicity [43]. However, these current techniques deal with several toxic chemicals and processing time sometimes requires over than 1 day.

References

[1] B. Bhushan and Y. C. Jung, "Natural and Biomimetic Artificial Surfaces for Superhydrophobicity, Self-Cleaning, Low Adhesion, and Drag Reduction," Progress in Materials Science, Vol. 56, No. 1, 2011, pp. 1-108.

[2] T. Wagner, C. Neinhuis and W. Barthlott, "Wettability and Contaminability of Insect Wings as a Function of Their Surface Sculptures," Acta Zoologica, Vol. 77, No. 3, 1996, pp. 213-225.

[3] A. R. Parker and C. R. Lawrence, "Water Capture from Desert Fogs by a Namibian Beetle," Nature, Vol. 414, No. 6859, 2001, pp. 33-34

[4] X. Gao and L. Jiang, "Biophysics: Water-Repellent Legs of Water Striders," Nature, Vol. 432, No. 7013, 2004, p.36

[5] D. Byun, J. Hong, Saputra, J. H. Ko, Y. J. Lee, H. C. Park, B. K. Byun and J. R. Lukes, "Wetting Characteristics of Insect Wing Surfaces," Journal of Bionic Engineering, Vol. 6, No. 1, 2009, pp. 63-70.

[6] K. Koch, B. Bhushan and W. Barthlott, "Diversity of tructure, Morphology and Wetting of Plant Surfaces," Soft Matter, Vol. 4, No. 10, 2008, pp. 1943-1963.

[7] M. Nosonovsky and B. Bhushan, "Superhydrophobic Surfaces and Emerging Applications: Non-Adhesion, Energy, Green Engineering," Current Opinion in Colloid & Interface Science, Vol. 14, No. 4, 2009, pp. 270-280

[8] P. A. Levkin, F. Svec and J. J. M. Frechet, "Porous Polymer Coatings: A Versatile Approach to Superhydrophobic Surfaces," Advanced Functional Materials, Vol. 19, No. 12, 2009, pp. 1993-1998

[9] B. Bhushan, Y. C. Jung and K. Koch, "Self-Cleaning Efficiency of Artificial Superhydrophobic Surfaces," Langmuir, Vol. 25, No. 5, 2009, pp. 3240-3248

[10] X. Zhang, F. Shi, J. Niu, Y. G. Jiang and Z. Q. Wang, "Superhydrophobic Surfaces: From Structural Control to Functional Application," Journal of Materials Chemistry, Vol. 18, No. 6, 2008, pp. 621-633

[11] J. R. Dorvee, A. M. Derfus, S. N. Bhatia and M. J. Sailor, "Manipulation of Liquid Droplets Using Amphiphilic, Magnetic One-Dimensional Photonic Crystal Chaperones," Nature Materials, Vol. 3, No. 12, 2004, pp. 896-899

[12] K. Y. Suh, M. C. Park and P. Kim, "Capillary Force Lithography: A Versatile Tool for Structured Biomaterials Interface towards Cell and Tissue Engineering," Advanced Functional Materials, Vol. 19, No. 17, 2009, pp. 2699-2712

[13] J. T. Han, X. R. Xu and K. W. Cho, "Diverse Access to Artificial Superhydrophobic Surfaces Using Block Copolymers," Langmuir, Vol. 21, No. 15, 2005, pp. 6662-6665

[14] N. J. Shirtcliffe, G. McHale, M. I. Newton, G. Chabrol and C. C. Perry, "Dual-Scale Roughness Produces Unusually Water-Repellent Surfaces," Advanced Materials, Vol. 16, No. 21, 2004, pp. 1929-1932

[15] H. S. Hwang, S. B. Lee and I. Park, “Fabrication of Raspberry-Like Superhydrophobic Hollow Silica Particles,” Materials Letters, Vol. 64, No. 20, 2010, pp. 2159-2162

[16] Y. H. Huang, J. T. Wu and S. Y. Yang, “Direct Fabricating Patterns Using Stamping Transfer Process with PDMS Mold of Hydrophobic Nanostructures on Surface of Micro-Cavity,” Microelectronic Engineering, Vol. 88, No. 6, 2011, pp. 849-854

[17] T. Yang, H. Tian and Y. Chen, “Preparation of Superhydrophobic Silica Films with Honeycomb-Like Structure by Emulsion Method,” Journal of Sol-Gel Science and Technology, Vol. 49, No. 2, 2009, pp. 243-246

[18] H. Kinoshita, A. Ogasahara, Y. Fukuda and N. Ohmae, “Superhydrophobic/Superhydrophilic Micropatterning on a Carbon Nanotube Film Using a Laser Plasma-Type Hyperthermal Atom Beam Facility,” Carbon, Vol. 48, No. 15, 2010, pp. 4403-4408

[19] Z. G. Guo, J. Fang, J. C. Hao, Y. M. Liang and W. M. Liu, “A Novel Approach to Stable Superhydrophobic Surfaces,” ChemPhysChem, Vol. 7, No. 8, 2006, pp. 1674-1677

[20] K. K. Lau, J. Bico, K. B. K. Teo, M. Chhowalla, G. A. J.Amaratung, W. I. Milne, G. H. McKinley and K. K.Gleason, “Superhydrophobic Carbon Nanotube Forests,”, Nano Letters, Vol. 3, No. 12, 2003, pp. 1701-1705

[21] F. Mumm, A. T. J. van Helvoort and P. Sikoski, “An Easy Route to Superhydrophobic Copper Based Droplet Microfluidic Systems,” ACS Nano, Vol. 3, No. 9, 2009, pp. 2647-2652

[22] S. S. Latthe, H. Imai, V. Ganesan and A. V. Rao, “Superhydrophobic Silica Films by Sol-Gel Co-Precursor Method,” Applied Surface Science, Vol. 256, No. 1, 2009, pp. 217-222

[23] V. V. Ganbavle, U. K. H. Bangi, S. S. Latthe, S. A. Mahadik and A. V. Rao, “Self-Cleaning Silica Coatings on Glass by Single Step Sol-Gel Route,” Surface and Coatings Technology, Vol. 205, No. 23-24, 2011, pp. 5338-5344

[24] S. S. Latthe, H. Hirashima and A. V. Rao, “TEOS Based Water Repellent Silica Films Obtained by a Co-Precursor Sol-Gel Method,” Smart Materials & Structures, Vol. 18, No. 9, 2009, p. 095017

[25] A. V. Rao, S. S. Latthe, C. Kappenstein, V. Ganesan, M. C. Rath and S. N. Sawant, "Wetting Behavior of High Energy Electron Irradiated Porous Superhydrophobic Silica Films," Applied Surface Science, Vol. 257, No. 7, 2011, pp. 3027-3032

[26] R. Furstner, W. Barthlott, C. Neinhuis and P. Walzel,"Wetting and Self-Cleaning Properties of Artificial Superhydrophobic Surfaces," Langmuir, Vol. 21, No. 3, 2005, pp. 956-961

[27] M. Ma, Y. Mao, M. Gupta, K. K. Gleason and G. C. Rutledge, "Superhydrophobic Fabrics Produced by Electrospinning and Chemical Vapor Deposition," Macromolecules, Vol. 38, No. 23, 2005, pp. 9742-9748

[28] X. Zhang, Y. Guo, P. Zhang, Z. Wu and Z. Zhang, "Superhydrophobic CuO@Cu2S Nanoplate Vertical Arrays on Copper Surfaces," Materials Letters, Vol. 64, No. 10, 2010, pp. 1200-1203

[29] H. Liu, L. Feng, J. Zhai, L. Jiang and D. B. Zhu, "Reversible Wettability of a Chemical Vapor Deposition Prepared ZnO Film between Superhydrophobicity and Superhydrophilicity," Langmuir, Vol. 20, No. 14, 2004, pp. 5659-5661

[30] L. Huang, S. P. Lau, H. Y. Yang, E. S. P. Leong, S. F. Yu and S. Prawer, "Stable Superhydrophobic Surface via Carbon Nanotubes Coated with a ZnO Thin Film," The Journal of Physical Chemistry B, Vol. 109, No. 16, 2005, pp. 7746-7748

[31] C.-v.N. Do Man Chun, Kyong Min Lee, Fast fabrication of superhydrophobic metallic surface using nanosecond laser texturing and low-temperature annealing, CIRP Annals-Manufacturing Technology, 65 (2016) 519-522

[32] J.H.X. M. Li, Q. H. Lu, Creating Superhydrophobic Surfaces with Flowery Structures on Nickel Substrates through a Wet-Chemical-Process, Journal of Materials Chemistry, 17 (2007) 4772-4776

[33] H.D. L. Pan, P. Bi, Facile Preparation of Superhydrophobic Copper Surface by HNO3 Etching Technique with the Assistance of CTAB and Ultrasonication, Applied Surface Science, 257 (2010) 1707-1711

[34] J.Z. C. Gu, J. Tu, A Strategy of Fast Reversible Wettability Changes of WO3 Surfaces between Superhydrophilicity and Superhydrophobicity, Journal of Colloid and Interface Science, 352 (2010) 573-579

[35] Z.S.C. B. Xu, Fabrication of a Superhydrophobic ZnO Nanorod Array Film on Cotton Fabrics via a Wet Chemical Route and Hydrophobic Modification, Applied Surface Science, 254 (2008) 5899-5904

[36] J.N.W. Q. F. Xu, Superhydrophobic and Transparent Coatings Prepared by Selfassembly of Dual-Sized Silica Particles, Frontiers of Materials Science in China, 4 (2010) 180-188

[37] M.Z. S. He, L. Yao, X. Yuan, M. Li, L. Ma, W. Shen, Preparation and Properties of ZnO Nanostructures by Electrochemical Anodization Method, Applied Surface Science, 256 (2010) 2257-2562

[38] N.A. M. S. Islam, M. R. Karim, Preparation of Superhydrophobic Membranes by Electrospinning of Fluorinated Silane Functionalized Pullulan, Colloids and Surfaces A: Physicochemical and Engineering Aspects, 362 (2010) 117-120

[39] R.J. M. Kang, H. S. Kim, H. J. Jin, Preparation of Superhydrophobic Polystyrene Membranes by Electrospinning, Colloids and Surfaces A: Physicochemical and Engineering Aspects, 313-314 (2008) 411-414

[40] X.F. M. Jin, J. Xin, J. Zhai, K. Cho, L. Feng, L. Jiang, Super-hydrophobic PDMS surface with ultra-low adhesive force, Macromole Rapid Communication, 26 (2005) 1805-1809

[41] K.K. H. Yan, H. Mayama, K. Tsujii, Environmentally stable super water-repellent poly(alkylpyrrole) films, Angewandte Chemie International Edition, 44 (2005) 3453-3456

[42] J.E.C. T. Baldacchini, M. Zhou, E. Mazur, Superhydrophobic surfaces prepared by microstructuring of silicon using a femtosecond laser, Langmuir, 22 (2006) 4917-4919

[43] E.G. N. Verplanck, J. Camart, V. Thomy, Reversible electrowetting on superhydrophobic silicon nanowires, Nano Letters, 7 (2007) 813-817

2. Vision/novelty of the research

The presented techniques and materials in this dissertation can become a good candidate to apply in reality because:

- The technique is simple, economic.

- The current fabrication methods exist limitations, for example, aging post process requires long-time exposure, coating approach deals with toxic chemical and sometimes requires complex process. To shorten the time required for wettability transition from hydrophilicity to superhydrophobicity without requiring the use of any specific equipment, the simple fabrication process has been introduced. The fabrication time is very short as compared to other current laboratory techniques such as hydrothermal, printing or laser ablation processes. The process time was reduced from several weeks/months to few second with microwave treatment. The mechanism of wettability change was also explained. Several potential applications such as self-cleaning, anti-wetting and oil-water separation were proposed.

The fabrication method, performed with a commercial microwave oven, was very useful for forming a relatively uniform ZnO structure. The use of a commercial microwave as the heating source to grow the structured ZnO shortened the fabrication time, reduced the specific equipment requirement and lowered the energy usage, thus rendering it an eco-friendly fabrication method

- No need of complicated apparatuses, surfaces with micro structures show high static water contact angle and low dynamic water contact angle

- The coating quality is very good with uniform coating layer with good stability and excellent performance

- The obtained surfaces include anti-wetting, self-cleaning properties, which can be applied in industrial, aircraft, biological, and daily-life applications. For example, superhydrophobic surface with anti-wetting property can be applied in aircraft, ships, medical equipment, and air filters etc.,. Surrface with self-cleaning property can be used to prevent the harmful bacterial attachment to medical implant surfaces.

Additionally, this research can provide a useful guideline for other researchers as well as industrial engineers to choose an efficient fabrication method for superhydrophobic surface with various substrates. Furthermore, the capability of creating different superhydrophobic surfaces may open the gate to apply in different applications. The soft surfaces are suitable for the oil-water separation, and the other surfaces might suitable for different applications. For example, the superhydrophobic developed on the hard substrates such as metal or ceramic… could be applied for anti-icing, anti-corrosion or anti-fogging etc…

3. Explanation about coating materials

This dissertation presented the simple materials which fabricated base on different hydrophilic substrate. The chosen substrates included cotton fabric, PU sponge and MS sponge. Cotton fabric is well known as a porous, rough, flexible and hydrophilic surface with extremely high water absorption ability. PU and MS sponge are also the commercial materials which have high porosity, light weight and very good elasticity. These kinds of material also own the large number of hydroxyl groups on surfaces - which provide suitable active sites for chemical modification. As a result, they are the promising candidates to fabricate the superhydrophobic materials for environmental applications including oil-water separation. However, due to their superhydrophobicity, prudent chemical modifications are required to control the selectivity and wettability ofthem. Also, maintaining good stability of the cotton fabric-based material and coating with non-toxic chemicals are essential for large-scale practical application.

ZnO was selected as the 1st functional material/coating material due to its superior abilities. ZnO is expected to exhibit more advanced controllable wettability due to the ease with which the surface structure can be developed [1, 2]. ZnO has abundant structures: hexagonal, wurtzite, rod, pillar, wire, belt, flake, and flower-like [3 – 6]. The WCA can be enhanced by using ZnO's microstructure to change in the surface roughness.

Reducing the cost, simplifying the fabrication process, increasing the durability of the final products, and using nontoxic materials are a few of the barriers that need to be solved for large-scale manufacturing of superhydrophobic surfaces. SA and FDTS are also used as modifiers to tune the surface wettability from hydrophobic to superhydrophobic. Until now, to achieve a high contact angle, many superhydrophobic surfaces are processed with fluorine-containing

surfactants [7-9]. Thus, FDTS, a kind of fluorine material was used to fabricate the superhydrophobic surfaces in this dissertation. However, the biggest concerning in using this type material is the safety issue due to the fluorine component in it. So, the trend of recently research is using fluorine-free coating material to make superhydrohobic surfaces. SA is a kind of a long-chain saturated fatty acid with an 18-carbon chain and has the IUPAC name octadecanoic acid. Fatty acids are a kind of simple and cheap surfactants to be used to construct hydrophobic surfaces. The COOH groups in the fatty acid molecules can react with –OH functional group on fabric or sponge surfaces and the hydrocarbon chains with low surface energy can repulse water.

References

[1] T.E. Volodymyr Khranovskyy, Rositsa Yakimova and Lars Hultman, Surface morphology effects on the light-controlled wettability of ZnO nanostructures, Applied Surface Science, 258 (1012) 8146-8152.

[2] J.C. Si Chen, Jianlin Liu, Jing Qi, Yuhua Wang, Enhanced field emission from ZnO nanowire arrays utilizing MgO buffer between seed layer and silicon substrate, Applied Surface Science, 387 (2016) 103-108.

[3] W.L. Ao, J.; Yang, H.; Zeng, X.; Ma, X., Mechanochemical synthesis of zinc oxide nanocrystalline, Powder Technology, 168 (2006) 128-151.

[4] K.M.M. Kumra, B.K.; Naidu, E.A.; Sinha, M.; Kumar, K.S.; Reddy, P.S., Synthesis and characterization of flower shaped zinc oxide nanostructures and its antimicrobial activity, Spectrochimica Acta Part A: Molecular and Biomolecular Spectroscopy, 104 (2013) 171-174.

[5] Ö.A.D. Yildirim, C., Synthesis of zinc oxide nanoparticles elaborated by microemulsion method, Journal of Alloys and Compounds, 506 (2010) 944-949

[6] A.K.-R.a.T. Jesionowski, Zinc Oxide—From Synthesis to Application: A Review, Materials, 7 (2014) 2833-2881

[7] Xu, W. G.; Liu, H. Q.; Lu, S. X.; Xi, J. M.; Wang, Y. B. Fabrication of Superhydrophobic Surfaces with Hierarchical Structure through a Solution-Immersion Process on Copper and Galvanized Iron Substrates, Langmuir 2008, 24, 1089

[8] Kim, D.; Hwang, W.; Park, H. C.; Lee, K. H. Superhydrophobic Nanostructures Based on Porous AluminaCurr. Appl. Phys. 2008, 8, 770

[9] Goncalves, G.; Marques, P. A. A. P.; Trindade, T.; Pascoal, C.; Gandini, A. Superhydrophobic Cellulose Nanocomposites, Journal of Colloid Interface Science 2008

4. Pore-blocking issue and homogeneity of coating

In chapter 3 and 4, the sponge materials were chosen as the base substrates to fabricate the superhydrophobic surfaces. By coating with multi layers, the superhydrophilicity of the hydrophilic sponge tuned to superhydrophobicity, thus one of the biggest concerning is pore – blocking issue after the coating and homogenously of the coating layers. To clarify this issues, SEM and mapping analyses were carried out. For these characterizations, the small pieces of sponges were cut randomly with the size 0.5 x 0.5 x 0.2 cm from the initial sponge cubes.

- The pore-blocking issue

The initial porosity of reticulated foams is critical when designing a custom component or product. The inspection of Table 1 revealed that the diameter of original PU sponge and superhydrophobic PU sponge was in the range of 180 to 700 µm, and the diameter of original MS and superhydrophobic MS was in the range of 40 to 70 µm. It can be concluded that the pore sizes of the sponges were not greatly changed after modification compared with the initial values. This confirmed that the extra coating layers did not exert significant pore-blocking effects on the fabricated sponge.

- Homogeneity of coating

The uniformity of the coating layers were confirmed in the mapping analysis results. These results were presented in dissertation in surface morphology section of each chapter.

Table.1. Pore sizes of original sponge and modified sponge

<table>
<tr><td>Original PU</td><td>PU@ZnO@Fe_3O_4@SA</td></tr>
<tr><td> 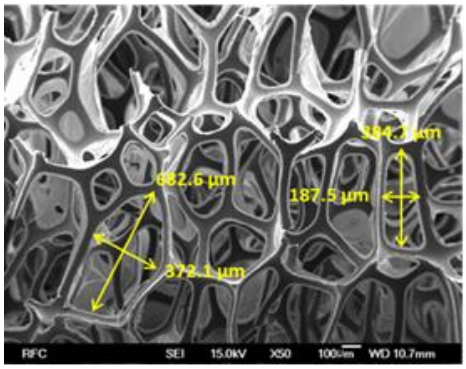
</td><td> 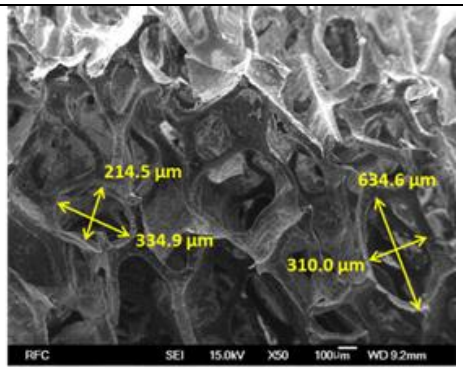
</td></tr>
<tr><td>Original MS</td><td>MS@ZnO@SA</td></tr>
<tr><td rowspan="3"> 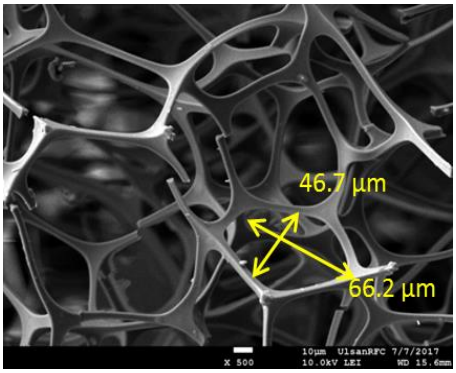
</td><td> 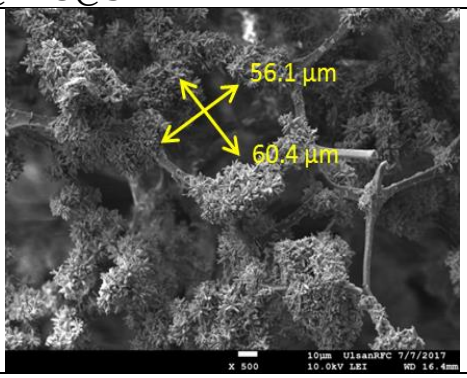
</td></tr>
<tr><td>MS@ZnO@FDTS</td></tr>
<tr><td> 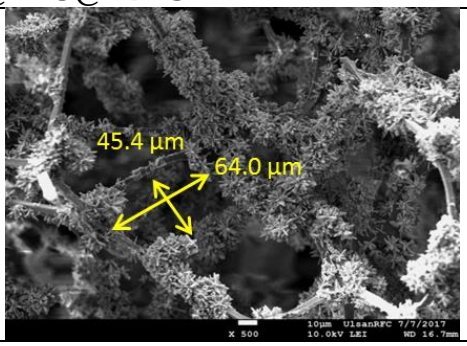
</td></tr>
<tr><td>MS@ZnO@SA@FDTS</td></tr>
<tr><td> 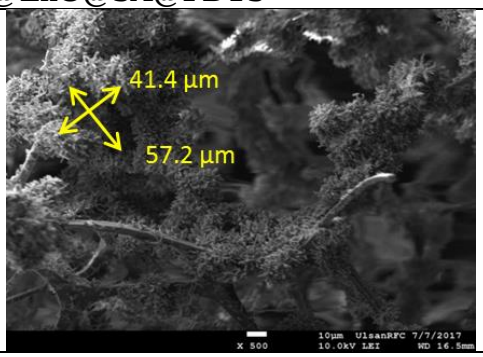
</td></tr>
</table>

5. Toxicity of materials

Metal oxide nanoparticles (NPs) like zinc oxide are being used in a large variety of applications such as textile materials, commercial sun-care products, lasers and light-emitting diodes, bioimaging agents, biosensors, in drug delivery vehicles, in ointments including coatings and pigments etc… Several published works have presented the versatile properties of ZnO which have a combination of physical properties (such as high electrical and thermal conductivity, optical absorption in the ultraviolet and very high temperature stability) and chemical characteristics (for instance stability at neutral pH values and mildly antibacterial action and UV blocking).

However, ZnO can be discharged into the environment in the using process. ZnO is an amphoteric oxide and can easily dissolve in both acids and bases. Like other oxides of metal, ZnO in the presence of water undergoes hydrolysis creating a hydroxide coating on its surface (≡M–OH). The hydroxide surface of these hydrolyzed ZnO particles may increase the chemical and physical adsorption of water molecules. This happens because of the amphoteric nature of the hydroxide surface that can react with both H^+ or OH^- ions:

$\equiv M–OH+H+ \leftrightarrow \equiv M–OH+_2$ with protons

$\equiv M–OH+OH- \leftrightarrow M–O- +H_2O$ with hydroxides

Thus, it is necessary to discuss about the toxicity when using ZnO in this study, especially in the acidic or alkaline condition. A piece of cotton sample (5 x 5 cm) and cube of sponge samples (3 x 3 x 3 cm) were prepared and then they were put in the aqueous at different pH value for 2h. After that, derived solutions were centrifuged and send to ICP-OES analysis in order to check the releasing level of ZnO to the aqueous solution. The results were presented in bellowing.

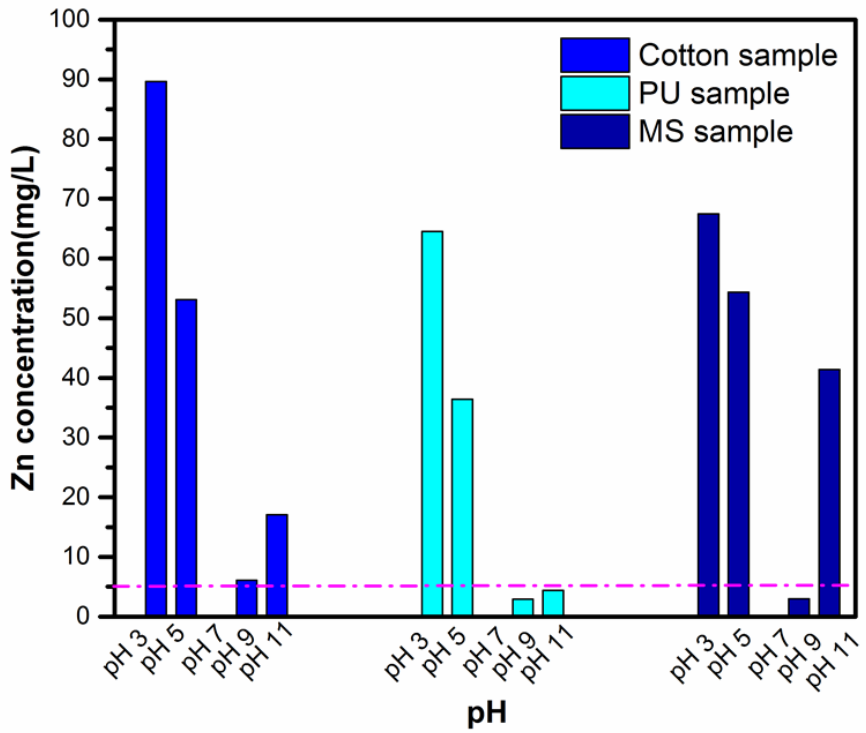

	pH=3	pH=5	pH=7	pH=9	pH=11
Cotton sample	89.6308	53.0933	0	6.10165	17.0544
PU sample	64.498	36.3893	0	2.95158	4.39112
MS sample	67.4487	54.3297	0	3.01094	41.4123

*Concentration [mg/L] of released Zn in different pH condition

It was showed that at neutral pH, the fabricated materials are stable and there was no releasing of ZnO to the environment. However, as mentioned before, at alkaline or acidic condition, ZnO would be released to the environment. As compared with Zn standard of United States Environmental Protection Agency, the limit level of Zn in water is 5 mg/L. Thus, the releasing of Zn from fabricated materials may cause some negative effects to the environment. It is recommend that before using the fabricated materials, the pH of solution should be maintained to the neutral pH. In the other hands, the chosen of safe coating materials is also a good way to have the environmental friendly materials.

APPENDIX 2

A - SCI Journal Publications

[5] **Viet Ha Tran Thi**, Byeong-Kyu Lee, 2017, Novel Fabrication of a Robust Superhydrophobic PU@ZnO@Fe3O4@SA Sponge and Tts Application in Oil-Water Separations, *Scientific Reports* 7:17520

[4] **Viet Ha Tran Thi**, Byeong-Kyu Lee, 2017, Effective Photocatalytic Degradation of Paracetamol Using La-doped ZnO Photocatalyst Under Visible Light Irradiation, *Material Research Bulletin* 96 (3), 171-182

[3] **Viet Ha Tran Thi**, Byeong-Kyu Lee, Chi-Vinh Ngo, 2017, Durable Superhydrophobic Cotton Filter Prepared at Low Temperature for Highly Efficient Hexane and Water Separation, *Journal of the Taiwan Institute of Chemical Engineers* 71, 527-536

[2] **Viet Ha Tran Thi**, Byeong-Kyu Lee, 2017, Development of Multifunctional Self-cleaning and UV Blocking Cotton Fabric with Modification of Photoactive ZnO Coating via Microwave Method, *Journal of Photochemistry and Photobiology A: Chemistry* 338, 13-22

[1**]** **Viet Ha Tran Thi**, Byeong-Kyu Lee, 2017, Great Improvement on Tetracycline Removal Using ZnO Rod - Activated Carbon Fiber Composite Prepared with a Facile Microwave Method, *Journal of Hazardous Materials* 324, 329-339

B- Attended International Conferences

[7] **Viet Ha Tran Thi,** Byeong-Kyu Lee, 2017, Durable Bio-inspired Superhydrophobic Polyurethane Sponge and Its Application in Oil-water Separation, International Colloids conference, Barcelona, Spain (Poster)

[6] **Viet Ha Tran Thi,** Byeong-Kyu Lee, 2016, Effective Photocatalytic Degradation of Paracetamol Using La-doped ZnO Photocatalyst Under Visible Light Irradiation, Advances in Functional Materials Conference, Jeju, Korea (Oral)

[5] **Viet Ha Tran Thi**, Byeong-Kyu Lee, 2016, Facile Microwave Synthesis of ZnO Rod-ACF Composite with Excellent Adsorption and Photocatalytic Performance for the Removal of Tetracycline Antibiotic, International Colloids conference, Berlin, Germany (Poster)

[4] **Viet Ha Tran Thi**, Byeong-Kyu Lee, 2015, Efficient Removal of MB Dye by Ag-ZnO/Graphene Oxide Nano Composite Under Visible Light Irradiation, International Water Nexus Conference, Deagu, Korea (Poster)

[3] **Viet Ha Tran Thi**, Byeong-Kyu Lee, 2015, High Photocatalytic Performance of Ag-ZnO/GO Nano Particle Under Visible Light Irradiation, 10th Asia Pacific Conference on Sustainable Energy and Environmental Technology, Seoul, Korea (Oral)

[2] Ajit Sharma, Byeong-Kyu Lee, **Viet Ha Tran Thi**, 2015, Characteristic Evaluation of Lime Incorporated Nanozeolite as Warm Mix Asphalt Additive to Reduce the Production Temperature, 3rd Global Conference on Environmental Studies, Izmir, Turkey (Oral)

[1] **Viet Ha Tran Thi**, Byeong-Kyu Lee, 2015, Synthesis of Ag-ZnO/GO Composite for Enhance Degradation of MB Under Visible Light, International Young Researcher Workshop, Hanoi, Vietnam (Poster)

C- Attended Domestic Conference

[1] Byeong-Kyu Lee, **Viet Ha-Tran Thi**, 2015, Efficient Removal of MB Dye by Ag-ZnO/Graphene Oxide Nano Composite Under Visible Light Irradiation, Korean Society for Atmospheric Environment (Poster)

D- Patents

✧ ***APPROVED PATENT***

[1] 이병규, **쩐 티 비엣 하,** 높은 가시광 활성을 갖는 광촉매 및 이를 이용한 수처리 방법 (출원번호: 10-2016-0051328, 발송일자: 2016.04.27)

✧ ***SUBMITTED PATENT***

[7] 이병규, **쩐 티 비엣 하**, 유기물과 물을 쉽게 분리하기 위한 금속산화물 코팅과 면섬유로 구성된 소수성 복합체의 개발 (울산대 관리번호: PA-20160396, 선행기술조사 의뢰일 2016.12.07)

[6] 이병규, **쩐 티 비엣 하**, 마이크로파와 산화아연 광촉매 코팅을 통한 자가 세척 및 자외선 차단용 섬유의 제조기법 (울산대 관리번호: PA-20160397, 선행기술조사 의뢰일 2016.12.07)

[5] 이병규, **쩐 티 비엣 하**, 스테아린산과 산화아연을 결합한 유수분리용 초소수성 폴리우레탄 스폰지 제조방법 (울산대 관리번호: PA-20170382, 선행기술조사 의뢰일 2017.10.10)

[4] 이병규, **쩐 티 비엣 하**, 초소수성과 자성을 띤 다기능 초소수성 폴리우렌탄 스폰지 제조방법과 해양오일유출사고 적용 및 수중 유기성 오염물 제거방법 (울산대 관리번호: PA-20170383, 선행기술조사 의뢰일 2017.10.10)

[3] 이병규, **<u>쩐 티 비엣 하</u>**, 유수분리용 멜라민수지-산화아연-스테아르산을 가진 초소수성 스펀지의 제조방법 (울산대 관리번호: PA-20170407, 선행기술조사 의뢰일 2017.11.01)

[2] 이병규, **<u>쩐 티 비엣 하</u>**, 유수분리용 멜라민수지-산화아연-할로겐계 실란을 가진 초소수성 스펀지의 제조방법 (울산대 관리번호: PA-20170408, 선행기술조사 의뢰일 2017.11.01)

[1] 이병규, **<u>쩐 티 비엣 하</u>**, 유수분리용 멜라민수지-산화아연-스테아르산-할로겐계 실란을 가진 초소수성 스펀지 제조 방법 (울산대 관리번호: PA-20170409, 선행기술조사 의뢰일 2017.11.01)